Characterization of ENTH domain proteins and their interaction with SNAREs in *S. cerevisiae*

Dissertation
zur Erlangung des Doktorgrades
der Mathematisch-Naturwissenschaftlichen Fakultäten
der Georg-August-Universität zu Göttingen

vorgelegt von
Subbulakshmi Chidambaram
aus Dharmapuri (Indien)

Göttingen 2005

D7

Referent:	Prof. Dr. Dr. h. c. Kurt von Figura
Korreferent:	PD Dr. Stefan Irniger
Tag der mündlichen Prüfung:	08.07.2005

Contents

Abbreviations

AA	Amino acid
ALP	Alkaline Phosphatase
Amp	Ampicillin
API	Aminopeptidase I
APNE	N-Acetyl-phenylalanin-β-naphtylester
APS	Ammonium peroxodi sulphate
ATP	Adenosine -Triphosphate
bp	Base pairs
BSA	*Bovine Serum Albumin*
cDNA	Complenmentary DNA
CPY	Carboxypeptidase Y
DAPI	4'-6-Diamino-2-phenylindol-dihydrochloride
ddH_2O	Double distilled water
DMP	Dimethyl-pimelinediimidat-dihydrochloride
DMSO	Dimethylsulfoxide
DNA	Deoxyribonucleicacid
dNTPs	Deoxynucleosidetriphosphate (dATP, dGTP, dCTP, dTTP)
ds	Double strand
DTT	Dithiothreitol
E. coli	*Escherichia coli*
EDTA	Ethylenediamintetraacetate-Disodium salt
ER	Endoplasmic Reticulum
EtOH	Ethanol
Fig	Figure
GFP	Green fluorescent protein
GST	Glutathione-S-Transferase
h	hours
HA	Haemagglutinin

HEPES	N-2-Hydroxyethylpiperazin-N'-2-ethanesulfonic acid
HPLC	High performance liquid chromatogryphy
HRP	Horseradish-Peroxidase
IgG	Immunglobulin G
IP	Immuno-precipitation
IPTG	Isopropyl-α-D-Thiogalactopyranoside
Kan	Kanamycin
kb	Kilobase
kDA	Kilodalton
l	Liter
LB	Luria Bertani
M	molar
mA	Milliampere
mg	Milligram
min	Minute
ml	Milliliter
mM	millimolar
MW	Molecular weight
nm	Nanometer
NSF	*N-Ethylmaleimid-Sensitive-Factor*
nt	Nucleotide
OD_{600}	Optical density at 600 nm
PAGE	Poly-acrylamide gel electrophoresis
pApe1	Precursor aminopeptidase I
PCR	Polymerase chain reaction
PEP4	A gene, which codes for vacuolar proteinase 1
Pfu	*Pyrococcus furiosus*
pH	Negative logrithm of Hydrogen ion concentration
PMSF	Phenylmethylsulfonylfluoride
RNA	Ribonucleic acid
rpm	revolutions per minute
RT	Room temperature

S. cerevisiae	*Saccharomyces cerevisiae*
SDS	*Sodium Dodecyl Sulphate*/*Lauryl Sulphzate*
sec	Seconds
SNAP	*Soluble-NSF-Attachment-Protein*
SNARE	Soluble N-ethylmalimide Sensitive factor Attachment protein receptor
ss	Single strand
Tab.	Table
TAE	Tris-Acetat-EDTA-buffer
Taq	*Thermus aquaticus*
TCA	Trichloroaceticacid
TE	Tris-EDTA-buffer
TEMED	N,N,N',N'-Tetramethylethylendiamine
TGN	Trans-Golgi network
Tm	Melting temperature
Tris	Tris-(hydroxymethyl)-aminomethane
ts	temperatursensitive
U	Unit
ON	Overnight
UV	Ultraviolet
V	Volt
v/v	volume/volume
w/v	weight/volume
WT	Wildtype
µ	Micro-

1 Introduction

1.1 The Membrane transport

All eukaryotic cells have within them functionally interrelated cellular membranes called "Endomembrane System". The various membranes involved, though interrelated, differ in structure and function. The endomembrane system consists of seven major compartments: the endoplasmic reticulum (ER), the Golgi complex, the *trans*-Golgi network (TGN), the vacuole (or lysosome in mammals), the plasma membrane (PM), the prevacuolar compartment (PVC), and the endosome (Fig.1) (Sanderfoot and Raikhel, 1999). The endomembrane system plays a very important role in moving materials around the cell, notably proteins and membranes with high fidelity. The movement of the cargo between different compartments is mediated primarily by coated vesicles that are detached from the donor membrane by a process commonly called "budding" and incorporated to the target membrane by docking and fusion. For every compartment, an organelle-specific mechanism exists to recruit and package a correct set of proteins and lipids into vesicles that are destined for transport to an acceptor membrane (Lippincott-Schwartz *et al.*, 2000; Schekman and Orci, 1996). The transport from the ER to either the cell surface or the vacuole is referred to as the 'anterograde pathway'. Some vesicles also carry proteins in the reverse direction which is called as the 'retrograde pathway', is essential for the recovery of proteins that may have escaped from other endomembrane compartments and also for the recycling of the machinery involved in anterograde transport. There are two major pathways for membrane or protein exchange, namely, the Secretory pathway and the Endocytic pathway.

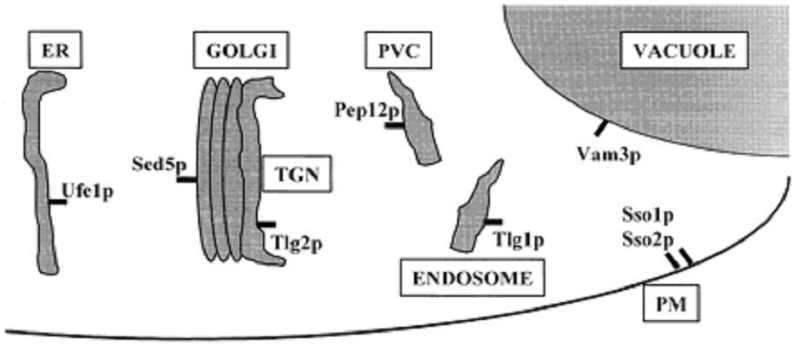

Fig.1. The Endomembrane System of Yeast Secretory pathway (Sanderfoot and Raikhel, 1999)

The secretory pathway is the biosynthetic path for the endomembrane system, which delivers the cargo to various compartments by anterograde pathway. This pathway was originally described in pancreatic exocrine cells (Palade, 1975). Secretion can be of two types, 'constitutive and regulated secretion'. In the constitutive secretion, the cargo is discharged to the cell exterior continuously and in unregulated manner. Most of the cells do it, to form the extracellular matrix and plasma membrane. But in the regulated secretion, the material to be secreted is held within secretory granules and released upon appropriate stimulation, for example, cells producing hormones, digestive enzymes and neurotransmitters (Traub and Kornfeld, 1997). The early secretory system consists of ER and the Golgi complex. Most of the proteins destined for secretion first enter at the ER. The sorting of proteins into specific vesicles are controlled by molecular markings such as signal sequences and glycosylation (Blobel, 1980). The ER-resident proteins carry a signal sequence called 'KDEL', the KDEL proteins which have escaped the ER, are recycled back from the Golgi to ER by COPI vesicles (Lippincott-Schwartz *et al.*, 2000). On the way through the Golgi, newly synthesized glycoproteins are subjected to several post-translational modifications such as ordered remodeling of their N-linked oligosaccharide side chains and biosynthesis of O-linked glycans.

The late secretory system starts at TGN, where the cellular sorting machineries and specific sorting signals in the cargo molecules are responsible for directing the cargo to the plasma membrane (PM), to regulated secretory granules, or to the endosomal/lysosomal system (Le Borgne and Hoflack, 1998). In higher eukaryotes, the proteins glycosylated with mannose-6-phosphate are targeted to the lysosome by the mannose-6-phosphate receptors present in the TGN through the late endosome (Kornfeld

and Mellman, 1989). In yeast, the Pre-vacuolar compartment (PVC) is the immediate target for the cargoes from the TGN though some proteins bypass the PVC and reach vacuole directly. Integral membrane proteins and secretory proteins are targeted to the plasma membrane and secreted out by exocytosis. In general, the secretory pathway links organelles together to provide a framework by which proteins undergo a series of post-translational modifications including proteolytic processing, folding and glycosylation (Storrie *et al.*, 2000).

1.1.1 Endocytosis

The endocytic pathway moves cargo or membrane surface into cell from outside to cytoplasmic compartments (endosomes, lysosomes etc.). Many critical functions of a cell are mediated by endocytic mechanisms, including the uptake of extra cellular nutrients, maintenance of cell polarity, regulation of cell-surface receptor expression and antigen presentation. Additionally, pathogens such as viruses, toxins and different micro-organisms utilize endocytic pathway to get inside the cell (Mukherjee *et al.*, 1997). In mammalian cells, at least five different pathways for endocytic internalization are known: the clathrin-dependent pathway, macropinocytosis, the caveolar pathway, a clathrin- and caveolin-independent pathway, and phagocytosis (Riezman *et al.*, 1997). The most common and best characterized endocytic pathway is receptor dependent clathrin-mediated endocytosis.

The pinched off vesicles rapidly lose their coats which leave them unstable, which in turn facilitate fusion of the vesicles with the sorting or early endosomes (EE), the first station of the endocytic pathway (Kornfeld and Mellman, 1989; Mellman, 1996). Early Endosomes are structurally seen as a network of tubules and vesicles throughout the cytoplasm, and their basic function includes the sorting of received molecules (Mellman, 1996). From the EEs the membrane-bound receptors are recycled efficiently back to the PM and the free ligands are further transported for degradation to the late endosomes (LE) or to the lysosomes (Mukherjee *et al.*, 1997). Late endosomes (LE) are responsible for the accumulation and concentration of the cargo after receiving it from the EEs. LEs contain hydrolytically active lysosomal hydrolases and they are considered to be a starting point for the degradative process of foreign material. Mannose 6-Phosphate Receptors (MPRs) concentrate in the LEs from there, they are recycled back to the TGN

(Mukherjee *et al.*, 1997). Delivery of endocytosed material from the LEs to the lysosomes is thought to occur by fusion of the LEs with the lysosomes, resulting in the digestion of cargo in the lysosomes by low pH and the lysosomal enzymes (Gruenberg and Howell, 1989; Mellman, 1996). The resulting degradation products are transferred out from the lysosomes to cytosol, where they can be utilized by the cell or alternatively transported out of the cell (Mellman, 1996). Clathrin-independent phagocytosis ("cell eating") refers to the internalization of large (> 0.5 μm diameter) particles. Micro-organisms are also internalised by phagocytosis (Mellman, 1996). In mammals, phagocytosis is seen preferentially in cells with specialized roles, such as e.g. macrophages and neutrophils (Mukherjee *et al.*, 1997). In contrast to phagocytosis, pinocytosis ("cell drinking") mediated by clathrin-coated pits is commonly seen in eukaryotic cells. It refers to a constitutive formation of smaller vesicles (< 0.2 μm) through which extracellular fluid and macromolecules bound to plasma membrane are internalized for further processing. The best characterized type of pinocytosis is receptor-mediated endocytosis which provides a selective uptake of specific macromolecules (Mellman, 1996).

1.1.2 Autophagy and Cvt pathway

Auto-phagy (self-eating) is an inducible, catabolic membrane transport pathway which transports bulk cytoplasm and sometimes entire organelles to the lysosome/vacuole for recycling in response to nutrient starvation or during specific physiological conditions (Klionsky and Emr, 2000). There are two major types of autophagy, viz, macroautophagy and microautophagy. The primary morphological difference between these pathways has to do with the site of sequestration and the origin of the sequestering membrane. In macroautophagy, a sequestering double membrane vesicle called 'autophagosome' is formed, *de novo* from the cytosol (Noda *et al.*, 2002). The outer membrane of the autophagosome fuse with the membrane of vacuole and releases the inner membrane bound 'autophagic body' in the lumen of the vacuole where the hydrolases digest the membrane and process the cargo. But in microautophagy, portions of cytosol or whole organelles are sequestered directly at the surface of the degradative organelle by invagination of the limiting membrane or by septation or protrusion of arm like structures and there is no intermediate transport vesicle.

Cytoplasmic to vacuole targeting (Cvt) pathway is an alternative biosynthetic pathway to the vacuole from the cytoplasm. This process has only been demonstrated in

Sacchromyces cerevisiae. Most of the vacuolar hydrolases in yeast, reach the vacuole by the secretory pathway except α-mannosidase and Aminopeptidase 1 (AP1) which uses the Cvt pathway. Autophagy and Cvt pathways share many components in common localized to a punctuate perivacuolar site, called the pre-autophagosomal structure (PAS), but they are two different distinct processes (Fig.2). Autophagy is catabolic, nonselective and is induced under various starvation conditions whereas Cvt pathway is biosynthetic, constitutive and active under growing conditions. The kinetics of the two pathways is also different. In 1992, studies on the transport process of Aminopeptidase I (AP1) by Klinsky *et.al*, confirmed the existence of Cvt pathway. The 61 kDa Aminopeptidase precursor (pApe1p) is synthesized in the cytosol and rapid oligomerization leads to homododecameric units as the major cytosolic form of pApe1p (Kim *et al.*, 1997). Multiple pApe1p dodecamers unite and form a 'Cvt complex' which finally matures into a double-membranous 'Cvt vesicel'. The Cvt vesicles are targeted to the vacuole where the outer membrane fuses with the vacuole and releases inner membrane bound 'Cvt body' inside the lumen of vacuole. The vacuolar hydrolases degrade the inner membrane and process the 61 kDa pApe1p into 51 kDa mature Ape1p (mApe1p). The maturation of pApe1p is a two step process where a 55 kDa intermediate form appears followed by a 51 kDa mApe1p by sequential action of two vacuolar proteinases PrA and PrB (Segui-Real *et al.*, 1995) coded by *PEP4* gene. Under starvation conditions, the Cvt complex containing pApe1p was found in the autophagosomes (Baba *et al.*, 1997) which showed that Ape1p is transported by two distinct (autophagy and Cvt) pathways, controlled by the nutrient conditions. Tor protein and phosphoinositide lipid mediated signaling are known to regulate the switch between the Cvt pathway and autophagy (Kamada *et al.*, 2000; Kihara *et al.*, 2001; Nice *et al.*, 2002). The processing of pApe1p is used as the best marker to study Cvt pathway.

Ape1p is recruited onto Cvt membranes and the Cvt vesicle is formed by homotypic membrane fusion which depends on the SNARE Tlg2p and Vps45p (Abeliovich *et al.*, 1999). For docking and fusion of Cvt vesicles with the vacuole, Vam3p (Darsow *et al.*, 1997) and Vps18p (Rieder and Emr, 1997) are thought to be required. The SNARE complex involved in the vacuolar fusion step is: Ykt6p, Nyv1p, Vti1p, Vam3p and Vamp7p along with the class C Vps protein complex also known as HOPS (Homotypic fusion and vacuole protein sorting) and a Rab family GTPase Ypt7p (Huang and

Klionsky, 2002). A protein called Ccz1p which is an interacting partner of Ypt7p is also required for the homotypic vacuolar fusion and conventional vacuolar hydrolase transport (Kucharczyk *et al.*, 2000).

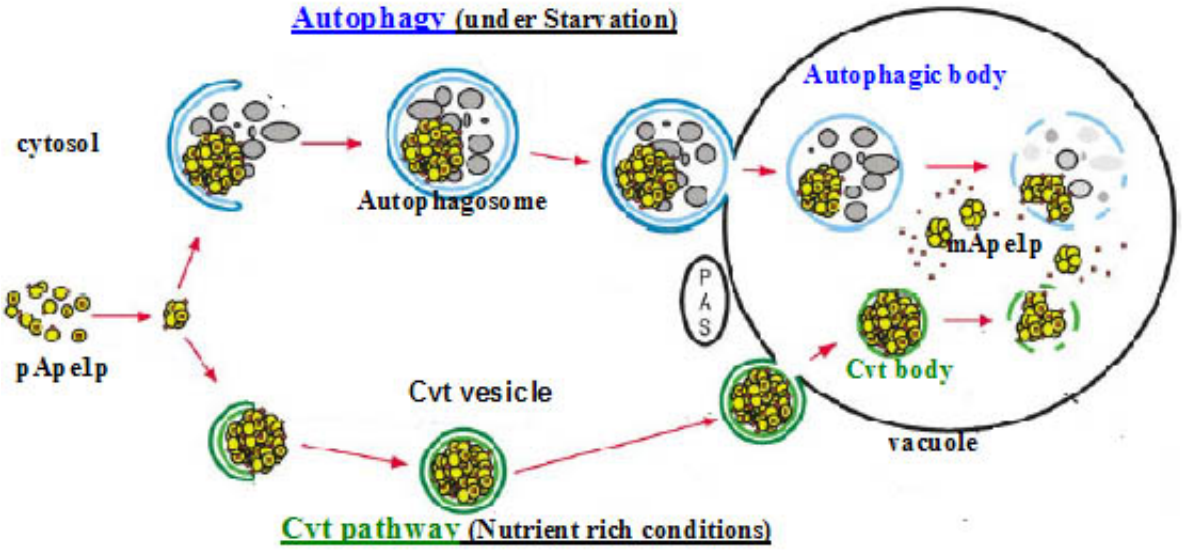

Fig.2. Autophagy and the Cvt pathway in yeast (Levine and Klionsky, 2004)

1.2 The process of membrane transport

The vesicle mediated transport is a multi-step process, consists of vesicle formation (budding), targeting, tethering and fusion. The vesicles, with their accompanying protein cargo, are released from the donor organelle in a process called budding (Rothman and Orci, 1996). After budding, interactions of v- and t-SNARE (SNAP receptor) proteins on the surface of the vesicle and acceptor organelle play a role in targeting the vesicle to the appropriate organelle (Rothman, 1994). Upon fusion, vesicle cargo is delivered to the target organelle (Fig.3).

1.2.1 Vesicle formation

Vesicle formation requires interaction of many proteins. Small GTPases of ARF (ADP-ribosylation factor) and Sar (Secretion-associated and Ras-related) families in their GTP bound form, recruit coat proteins like clathrin onto the membrane. Cargo proteins are concentrated at a specialized region called coated pits on the donor membrane and packed into a nascent vesicle. Clathrin assembles into a cage like lattice on membranes, even in the absence of vesicles, which during the process of vesicle formation, polymerizes into a

basket made out of hexagons and pentagons on vesicles. Vesicular transport within the early secretory pathway is mediated by two types of non-clathrin coated vesicles: COPI- and COPII-coated vesicles. COPII is a coat complex which forms a main structure of transport vesicles responsible for forward transport of cargo from the ER to the Golgi complex (Barlowe *et al.*, 1994). COPI vesicles in their turn carry cargo retrograde from the Golgi to the ER and are also involved in the intra-Golgi transport (Letourneur *et al.*, 1994; Orci *et al.*, 1997). Adaptor proteins are required to recruit cargo into coated vesicles. A group of cytosolic heterotetrameric adapter complexes (AP) is involved in the formation of clathrin coated vesicles both in the late secretory and the endocytic pathways. They recognize three distinct sorting signals, two tyrosine based signals (NPXY and YXXØ) and a dileucine sorting signal, for the selection of cargo into clathrin-coated vesicles. So far 4 Adaptor Proteins (APs) were identified in mammalian system (Boehm and Bonifacino, 2001; 2002; Kirchhausen, 1999; Robinson and Bonifacino, 2001). Yeast has only three adaptor complexes and lacks AP-4. In mammals, AP-1 is involved in the assortment and the clathrin dependent export of lysosomal enzymes and proteins bound to Mannose-6-Phosphate-Receptor (MPR) from the TGN to the lysosomes (Le Borgne and Hoflack, 1998). Now, AP1 is thought to be involved in the anterograde and retrograde transport between the TGN and the endosome and in traffic to the cell surface (Hinners and Tooze, 2003). In yeast, AP-1 seems to be involved in transport from the TGN to the early Endosome (Stepp *et al.*, 1995). The AP-2 is localized to PM and mediates clathrin dependent endocytosis (Schmid, 1997). AP-3 is involved in the clathrin independent transport from the TGN to the vacuole in yeast (Robinson and Bonifacino, 2001). In contrast to yeast, AP-3 in mammals binds clathrin (Dell'Angelica *et al.*, 1998) and transports proteins to the lysosomes, to some specialized compartments like the melanosomes and to the platlet granules. AP-4 also functions at the TGN and is involved in the basolateral sorting of proteins from the TGN (Dell'Angelica *et al.*, 1999; Simmen *et al.*, 2002).

There are three homologous monomeric clathrin adaptor proteins in yeast and in mammalian cells, GGA-1,-2,-3 (Golgi-localized, γ-adaptin homologue and ARF-binding) proteins (Boman *et al.*, 2000). They share functional similarities with APs. They are located in TGN and are involved in export of MPRs from TGN to endosome (Puertollano, 2001). In yeast, the double deletion of GGA1/GGA2 showed a defect in transport and

processing of Carboxypeptidase Y (CPY) (Dell'Angelica *et al.*, 2000; Hirst *et al.*, 2000). In addition, GGA proteins are also required for the sorting of the pre-vacuolar syntaxin Pep12p (Black and Pelham, 2000). AP-1 and GGA proteins co-operate in anterograde transport from the TGN to the vacuole (Costaguta *et al.*, 2001; Hirst *et al.*, 2001).

Thus, Clathrin Coated Vesicles (CCVs) with selected cargo are formed. A protein called dynamin, in its GTP-bound form, assembles into a collar around the neck of deeply invaginated pits. Hydrolysis of GTP bound to dynamin drives the closing of the collar´s neck, resulting in the dissociation of dynamin and pinching off of an isolated clathrin-coated vesicle (Hinshaw and Schmid, 1995). Amphiphysin recuits dynamin onto the membrane (Owen *et al.*, 1998) and endophillin helps in the final stages of vesicle budding. Synaptojanins and auxilins help in the uncoating of clathrin vesicles. COPI and COPII coats are removed after GTP hydrolysis of ARF and Sar1 respectively.

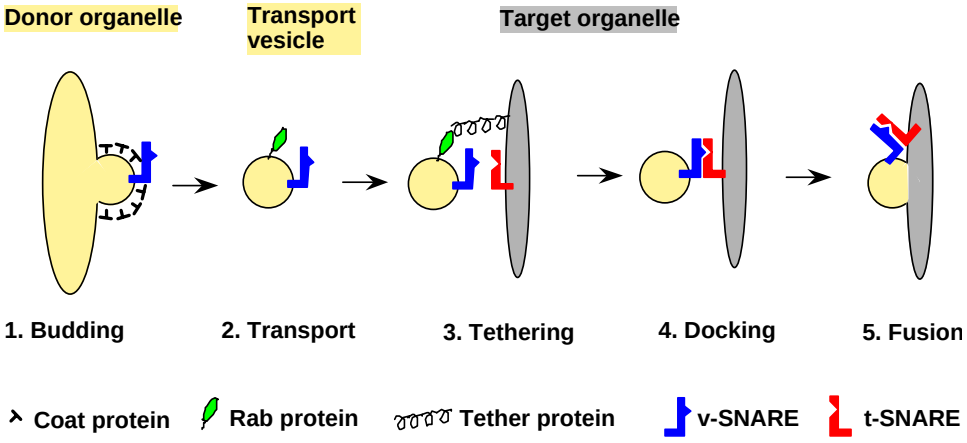

Fig.3. Molecular mechanisms of membrane trafficking

1.2.2 Vesicle tethering and docking

The uncoated vesicles may reach their destination by simple diffusion (e.g intra Golgi transport) but for long distances, the movement can be aided by cytoskeletal fibres or by motor proteins. As soon as the vesicle reaches the target membrane, a loose connection (physical contact) between the vesicle and the membrane is formed, which is called as 'Tethering'. Two broad classes of tethering proteins are proposed. A group of 'long coiled-coil proteins' like, Uso1p which is important for tethering ER-derived vesicles (Barlowe, 1997), endosomal EEA1/Vac1p protein (Dumas *et al.*, 2001) and Golgins may be attached to membrane by one end of the coil, using the other end it searches for the

vesicles passing by and may make a loose attachment with the membrane. Another group consists of 'multisubunit tethering complexes' like COG complex, the exocyst complex, GARP complex, TRAPP I and II, Class C Vps complex and Dsl 1p complex (Whyte and Munro, 2002). The small GTPase Ypt/Rab family proteins, present on the vesicle interacts with the tethering protein in a short time frame and further GTP hydrolysis dissociates the interaction (Cao *et al.*, 1998; Lazar *et al.*, 1997; Stahl *et al.*, 1996). Ypt/Rab proteins seem to be involved in all aspects of vesicle trafficking, localized to specific compartments and are key regulators of membrane trafficking. There are 11 Ypt proteins in yeast (Lazar *et al.*, 1997) and around 60 different Rab proteins in mammalian cells (Bock *et al.*, 2001). During the tethering process, the SNARE proteins (see chapter: 1.3.1) present both on the vesicle and the target membranes bind and form a firm link between the vesicle and the target membrane which is called as 'docking'. The time for the cognate-SNARE interaction is limited by the GTP hydrolysis rate of the Rab proteins (Clague, 1999). The interaction of tether proteins and rabs contributes to specificity.

1.3 Molecular mechanism of membrane fusion

1.3.1 SNARE hypothesis

In vesicular transport, the very fundamental question is how the vesicles recognize the correct target membrane. The SNARE hypothesis confers a widely accepted explanation of the mechanism of specificity in vesicle targeting (Söllner *et al.*, 1993). SNAREs (Soluble N-Ethylmaleimide-Sensitive factor Attachement Protein Receptors) are a superfamily of small membrane proteins found on both transport vesicles (v-SNARE) and target organelles (t-SNARE). The specific interactions between t- and v-SNAREs ensure that vesicles are targeted to the correct compartment and lead to membrane fusion. SNARE proteins were first implicated in membrane fusion by Rothman group in 1993, when they identified three previously known proteins (synaptobrevin, syntaxin and SNAP-25) as SNAP-receptors from bovine brain extract which are involved in Ca^{2+} mediated exocytosis of neurotransmitter at the nerve terminal (Söllner *et al.*, 1993). The role of SNAREs in membrane fusion was further confirmed by proteolysis of SNAREs with tetanus and botulinum toxin which blocked neurotransmission (Jahn and Niemann, 1994; Montecucco and Schiavo, 1995). SNARE proteins are type II integral membrane proteins of around 15-40 kDa in size. The original SNARE hypothesis postulates that

each target membrane contains t-SNAREs that interact with complementary v-SNAREs on the in-coming vesicle membrane, thus each fusion step would be mediated by a unique set of (cognate) SNAREs. This set of SNAREs would function only in one fusion step and the specificity for the interaction was offered by the intrinsic affinity of SNAREs (Rothman, 1994). But, later it has become very clear that at least some SNAREs can function in multiple trafficking steps such as the yeast proteins Sed5p which is involved in 3 different complexes by binding 7 different SNAREs (Nichols and Pelham, 1998) and Vti1p interacts with four different syntaxins (Fischer von Mollard *et al.*, 1997; Fischer von Mollard and Stevens, 1999; Holthuis *et al.*, 1998; Lupashin *et al.*, 1997). These proteins can pair with more than one set of partners and thus participate in the formation of several different SNARE complexes. In 1999, Reinhard Jahn's group showed that non-cognate SNARE complexes can be formed *in vitro* and are very similar to cognate SNARE complexes with respect to biophysical properties, assembly and disassembly. This disproved one of the aspects of original SNARE hypothesis, suggesting that the specificity of membrane fusion is not due to intrinsic specificity of SNARE pairing and (Fasshauer *et al.*, 1999). Studies on Ykt6p or Ykt6p and Vti1p on the transport vesicle showed that they are not sufficient to ensure specificity in membrane traffic (Dilcher *et al.*, 2001). This would support participation of additional proteins in vesicular targeting (Dilcher *et al.*, 2001; Fischer von Mollard *et al.*, 1997; Lazar *et al.*, 1997; Lupashin *et al.*, 1997).

SNAREs are distinguished by a functionally important, conserved stretch of approximately 60 amino acids near their membrane binding region, referred to as SNARE motif (Terrian and White, 1997; Weimbs *et al.*, 1997). Most of the SNAREs have only one SNARE motif with an N-terminal sequence followed by a C-terminal trans-membrane domain which anchors it on the membrane. SNARE motives contain sequences capable of forming α-helical coiled-coils near the C-terminus (Chapman *et al.*, 1994; Gerst, 1997). These putative coiled-coils are involved in interaction between various SNARE proteins. When the cognate sets of SNARE motives are mixed, a conformational change of the SNARE-motif from an unstructured form towards an α-helical bundle occurs spontaneously in a stoichiometric fashion which is a prerequisite for fusion (Sutton *et al.*, 1998). This mechanism docks vesicles to target membranes and the assembly is known as 'SNAREpins' (or trans-SNARE complex). Some SNARE motives

are constitutively active due to a binding of the N-terminus to the SNARE motif. Some SNAREs, for example SNAP-25 (Synaptosome associated protein of 25 kDa) have two SNARE motives, without a transmembrane domain. This SNARE is attached to membrane by palmytyl residues (by post translational modifications) present in the cyteine rich region which separates the two SNARE motives (Hess *et al.*, 1992). Others have two conformation, if the SNARE-motif is competent to bind with other SNARE proteins, the conformation is called as 'open conformation', if it is not able to interact, then it is named as 'closed conformation'.

1.3.2 Classification of SNARE proteins

In *S. cerevisiae*, so far, 24 SNARE proteins have been identified. In mammalian cells, more than 40 SNAREs were identified. By classical classification, SNAREs are classified on the basis of their localization either on a vesicle (v-SNARE) or on a target membrane (t-SNARE) (Söllner *et al.*, 1993). t-SNAREs were divided into Syntaxin- and SNAP-25-families and Synaptobrevins/VAMPs belonged to the v-SNAREs (Terrian and White, 1997; Weimbs *et al.*, 1997). But, the main disadvantage of this classification is that based on this it would be difficult to assign a function for a SNARE (Jahn and Sudhof, 1999). Also in the case of homotypic vacuolar fusion, there is no difference between the target and vesicle membrane and a single SNARE may be present on several membranes. So, v- and t-SNARE classification is incomplete. A further classification was done on the basis of the amino acid sequence similarity between different SNARE motives. When the four SNARE proteins form the complex, the amino acid side chains interact in 16 different layers. The amino acid composition of the 0-layer (ionic layer) at the centre of the SNARE complex is highly conserved with one arginine and three glutamines (Weimbs *et al.*, 1998). One arginine-residue (R) and three glutamine residues (Qa,b,c) form the central layer of each SNARE complex and contribute to the stability. Based on this, SNAREs were reclassified. R-SNAREs contribute Arginine to the ionic layer and Q-SNAREs contribute Glutamine to the 0-layer. The yeast SNARE, Bet1p, is an exception for this rule which provides serine to the 0-layer (Fasshauer *et al.*, 1998). Also the mouse and rat Vti1a has an aspartate residue in the 0-layer but it was shown that aspartate can functionally replace glutamine (Antonin *et al.*, 2000a). All t-SNAREs (syntaxins and SNAP-25) are Q-SNAREs and most of the v-SNAREs are R-SNAREs. Three families of Q-SNAREs can be distinguished due to sequence similarities. Among Q-SNAREs, the

conserved -3 layer has either a big amino acid like phenylalanine (Qa) or small amino acid residues like glycine or alanine (Qb or Qc). Syntaxin 1 related SNAREs are Qa-SNAREs, related to the N-terminal helix of SNAP-25 are Qb-SNAREs and Qc-SNAREs are similar to the C-terminal helix of SNAP-25 (Bock *et al.*, 2001). *S. cerevisiae* contains five R-SNAREs, seven Qa-SNAREs, Six Qb-SNAREs and seven Qc-SNAREs (Pelham, 2001).

1.3.3 Function of N-terminal domains of SNAREs

The N-terminal domains of many SNAREs have some independently folded domains which are not conserved and highly divergent in their amino acid sequences. The N-terminal domains of Qa-SNAREs and some Qb and Qc SNAREs such as vti1b and syntaxin8 consist of a three-helix bundle whereas the R-SNAREs Sec22p and Ykt6p form a mixed α-helical/β-sheet profilin-like fold. The N-terminal domains of SNAREs belonging to syntaxins or to Qa-SNAREs can bind proteins that regulate SNARE complex formation. Some R-SNAREs or Qa-SNAREs are recruited into budding vesicles by the binding partners of their N-terminal domain. The N-terminus of Vam7p contains a Phox domain which helps in membrane attachment (Cheever *et al.*, 2001; Lu *et al.*, 2002). The yeast syntaxins, Sed5p and Ufe1p bind to Sly1p (Sec1/Munc18 family protein which organizes membrane fusion) by a short peptide motif from the N-terminus (Yamaguchi *et al.*, 2002). In the same way, Munc-18 can bind to Syntaxin 1 in the closed comformation and is a negative regulator of SNARE complex formation (Dulubova *et al.*, 1999; Misura *et al.*, 2000). Sec20p through its N-terminus recruits Tip20 which is required for the retrograde transport to ER (Sweet and Pelham, 1993). The N-terminal domain of neuronal syntaxin 1 and its yeast plasma membrane homologue Sso1p, consists of a three-helix bundle which interacts with its own SNARE motif and can down regulate the capability to form SNARE complexes (Dulubova *et al.*, 1999; Munson *et al.*, 2000). But when the N-terminal domain of Sso1p was removed, formation of the SNARE complex assembly was accelerated (Nicholson *et al.*, 1998). VAMP-4 (Vaculor associated membrane protein) has a di-leucine motif in the cytoplasmic domain which interacts with AP-1 at the TGN (Peden *et al.*, 2001). The N-terminal extension of VAMP-4 contains a target signal for the TGN (Zeng *et al.*, 2003). From our lab, recently we showed that the N-terminus of vti1b interacts with the Epsin N-terminal homology domain (ENTH-domain) of Enthoprotin/CLINT/epsinR, and Vti1p with the ENTH-domain of Ent3p in yeast

(Chidambaram *et al.*, 2004). The ENTH domain proteins are needed for the formation of CCVs. The N-term of retrograde SNARE Use1p interacts with Frq1, which is a Ca2+ binding protein (Burri and Lithgow, 2004). It is believed that through Frq1p, Use1p might support Pik1p to dock and modify the phosophoinositide composition of membranes for retrograde transport. Syn8p, through its N-terminus interacts with Glc7p, a protein phosphatase which regulates vacuolar traffic by controlling final stages of vacuolar fusion (Burri and Lithgow, 2004). Thus, the N-terminal domains of SNAREs may serve as inhibitors of the adjacent SNARE motif and have regulatory functions.

1.3.3.1 Sorting sequences for SNAREs

The cytosolic domain of SNAREs can assist them to target and localize to some extent. But this is not well defined. For some SNAREs, the sorting sequences seem to be located within the region of the SNARE motif, ex. Bos1p, Bet1p and Sec22 and Vamp2p (Burri and Lithgow, 2004). In some SNAREs, sorting signal is present outside of the SNARE motif; for example, Ykt6p has a profilin-like domain proximal to the SNARE motif which is necessary and sufficient for sorting (Hasegawa *et al.*, 2003). In SNAP-25, the palmitoylated interhelical domain targets the protein to the PM (Gonzalo *et al.*, 1999; Loranger and Linder, 2002). For some SNAREs the N-terminal domain helps in the targeting and localization like Vamp4, as mentioned in chapter 1.3.3.

1.3.4 Crystal structure of SNARE complexes

So far only two SNARE complexes have been crystallized and the best characterized one is the exocytotic SNARE complex in synapses which releases neurotransmitter into the synaptic cleft. The crystal structure of this complex showed that one helix from Syntaxin1 and Synaptobrevin and two helices of SNAP-25 assembled to a parallel four helix bundle (Sutton *et al.*, 1998) (Fig.4a). When the SNARE motives of these SNAREs interact they form 16 layers, each layer containing four amino acids. The central 0-layer of this complex contains an arginine from Synaptobrevin and three glutamines one from syntaxin and two from SNAP-25. The stabilizing interaction is mainly mediated by hydrophobic interactions. The ionic interactions are shielded from the aqueous environment by neighboring leucin-zipper-motives and the peptide-backbone, which contribute to the stability of the complex. Apart from the ionic 0-layer, the amino acids which form the additional 15 layers in the centre of the bundle are hightly conserved. These other layers

were numbered positively towards the C-terminus and negatively towards the N-terminus (Fig.4b). An additional well characterized late endosomal SNARE-complex consists of the 4 SNAREs vti1b, Syntaxin 8, Syntaxin 7 and Endobrevin. Crystal structures as well as functional data supported the hypothesis, that all SNARE-complexes are similar in structure, despite of limited sequence homology (Antonin *et al.*, 2002b; Antonin *et al.*, 2000a). In yeast, a SNARE-complex which is involved in exocytosis and consists of the proteins Sec9p, Snc1/2p and Ssp1/2p shows a lot of similarities to the neuronal SNARE-complex (Gerst, 1997; Rice *et al.*, 1997). Therefore it seems that some features are common for all SNARE-complexes, for example, SNARE core complexes are extremely stable, most of them are resistant to SDS denaturation, heat stable, resistant to cleavage by toxins and for proteases digestion (Chen and Scheller, 2001). In contrary to the four helix bundle model of SNARE complexes, pentameric complexes was suggested to be formed by the SNAREs involved in homotypic vaculor fusion, Vti1p, Nyv1p, Ykt6p, Vam3p and Vam7p (Ungermann *et al.*, 1999). However, another group has disproven this by demonstrating that Nyv1p and Ykt6p compete for the same binding site in a complex with Vam3p, Vam7p and Vti1p and can form two different quarternary complexes (Fukuda *et al.*, 2000).

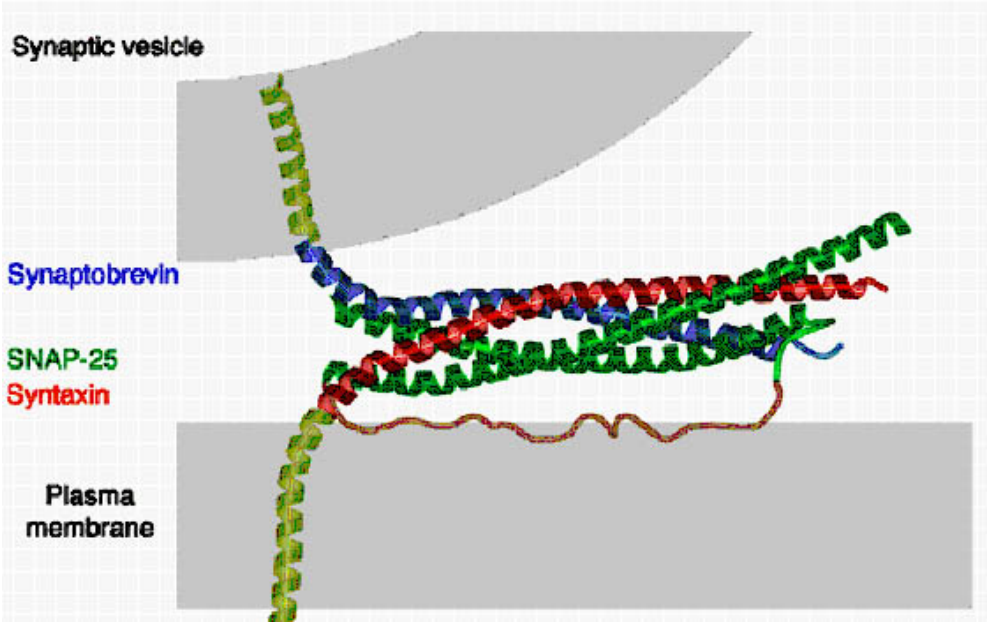

Fig.4a. Crytal structure of synaptic SNARE complex (Sutton *et al.*, 1998)

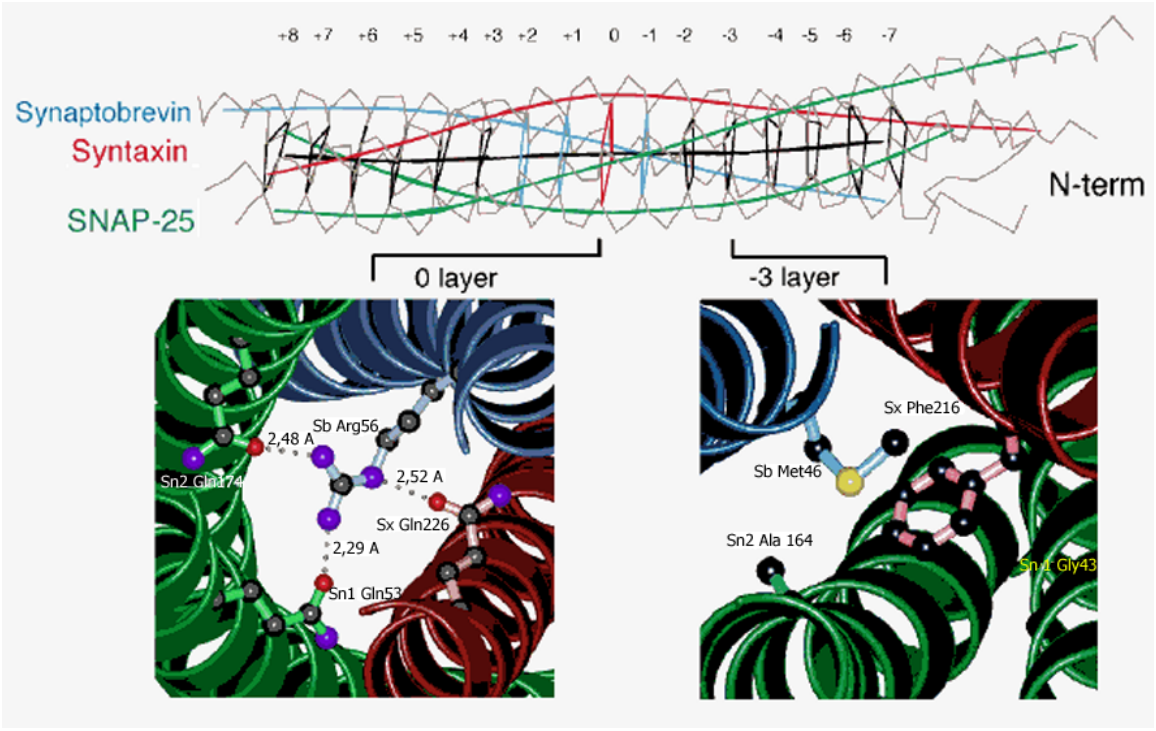

Fig.4b. Ionic layers of SNARE complexes (Sutton *et al.*, 1998)

1.3.5 Mechanics of membrane fusion

SNARE proteins are present in all intracellular compartments and mediate specific fusion reaction. A trans-SNARE complex is formed by the action of SM (Sec1/Munc18)-proteins which might link the Ypt/Rab effectors and tethering complexes to the SNARE complex (Jahn *et al.*, 2003). The SNARE complex formation is associated with release of energy which drives off the energy barrier and all the four SNARE proteins align on the same membrane, now it is called as cis-SNARE complex. After fusion, the SNARE complex is dissociated into individual SNARE proteins on the membranes, a step known as 'Priming' by the action of Sec17p and Sec18p by hydrolyzing ATP (Novick *et al.*, 1981) or by the mammalian chaperone-like ATPase NSF in conjunction with cofactors, thus re-activating the SNAREs for another round of membrane fusion (Hanson *et al.*, 1997). So, the SNARE proteins are ready for the next round of fusion. According to 'zipper' model of membrane fusion, once the amino termini of the SNARE motifs have found each other, they may 'zip' from the membrane-distal amino termini towards the membrane-proximal carboxyl termini of the SNARE motifs and the formation of the stable SNARE complex overcomes the energy barrier to drive fusion of the lipid bilayers (Hanson *et al.*, 1997; Lin and Scheller, 1997). SNARE proteins may partially zipper to

transfer the vesicle into a readily releasable state leading to 'hemi-fusion' or 'preassembled pore' between both membranes. In synaptic vesicle exocytosis, Ca^{2+} triggers the full zipping of the coiled-coil complex, which results in membrane fusion and release of vesicle contents. Further recruitment of NSF and α-SNAP dissociates the SNARE complex and free SNARE proteins are ready for next round of fusion. In viral protein mediated membrane fusion, coiled-coil helical bundles are the main structural component of the fusion protein, and a conformational change of the protein promotes fusion (Jahn and Sudhof, 1999; Skehel and Wiley, 1998). In viral fusions, a helix bundle bends and brings two membranes together, which is called as 'jack-knife' mechanism (Hughson, 1997). Studies on yeast homotypic vacuolar fusion, showed that membrane fusion is promoted by a proteinaceous pore (Peters *et al.*, 1999). It was proposed that V0-subunits, the membrane integral sector of the H+-ATPase, is a target of calmodulin in yeast and assemble into gap-junction-like channels that connect the fusing membranes.
Various SNARE (SNAP receptor) proteins critical to intracellular membrane fusion is believed to operate by similar mechanisms in eukaryotic organelles (Götte and von Mollard, 1998; Rossi *et al.*, 1997; Rothman and Wieland, 1996). Operation by a similar mechanism would imply structural similarity, regardless of a lack of sequence conservation among evolutionarily distant members of the SNARE family. This structural similarity has been observed between mammalian SNARE proteins and some yeast homologues. Structural similarity between yeast v-SNARE Vti1p and its human homologue is suggested by the recent result that the human homologue can functionally replace Vti1p in two vesicle transport pathways (Fischer von Mollard and Stevens, 1998).

1.4 Biosynthetic transport to the yeast vacuole

At the trans-Golgi Network, the vacuolar proteins are sorted due to the presence of vacuolar sorting signals (Bryant and Stevens, 1998). Different routes have been identified from the TGN to the vacuole. They are the carboxypeptidase Y (CPY) pathway, the alkaline phosphatase (ALP) pathway and the multivesicular body (CPS-1) pathway. Vacuolar proteins are usually synthesized as precursors, modified during the transport in different ways, processed into the mature form in the vacuole by proteinase A encoded by *PEP4* and thus used as marker proteins to study the different pathways. After translocation into the ER and transport through the Golgi-complex most of the soluble

proteins and integral membrane proteins of the yeast vacuole are transported in the biosynthetic-secretory pathway through the pre-vacuolar compartment (late endosome) towards the vacuole. The soluble vacuolar hydrolase carboxypeptidase Y (CPY) serves as a marker protein for this transport route. Therefore this pathway is also called as the CPY-pathway (Bryant and Stevens, 1998; Conibear and Stevens, 1998). The inactive precursor-form of CPY (prepro-CPY) is transported into the lumen of the ER after synthesis. After removal of the signal sequence, the proteins receive a core-glycosylation by which the 67 kDa p1CPY-form is generated. This is then transported to the Golgi-apparatus, where further oligosaccharide-modifications take place which leads to the 69 kDa p2CPY-form. In the TGN p2CPY binds the CPY-transport receptor Vps10p (Marcusson *et al.*, 1994). This complex is then transported in transport vesicles towards the pre-vacuolar compartment. Here the complex dissociates. p2CPY is further transported to the vacuole and Vps10p recycles back to the Golgi-apparatus (Cereghino *et al.*, 1995; Cooper and Stevens, 1996; Piper *et al.*, 1995). In the vacuole p2CPY is processed to the mature 61 kDa mCPY-form by the action of proteinase A. These different forms of CPY can be analyzed by separating them on a SDS-gel.

Apart from the CPY-pathway there exists a second, direct transport pathway from the TGN to the vacuole, without the detour through the pre-vacuolar compartment. This pathway is called as ALP-pathway, the vacuolar membrane protein alkaline phosphatase (ALP) serves as a marker protein (Piper *et al.*, 1997). After translocation into the ER ALP is glycosylated to the 76 kDa proform (pALP), which does not change in size through out the transport within the Golgi-apparatus. It was shown that the adapter-complex AP-3 is involved in the transport of ALP from the TGN to the vacuole. In addition pALP accumulates in AP-3 deficient strains (Cowles *et al.*, 1997a). In the TGN pALP is sorted into transport vesicles via interaction of its N-terminal dileucine-signal with AP-3. In the vacuole pALP is processed to the mature 72 kDa mALP-form. Apart from ALP, the vacuolar SNAREs Vam3p and Nyv1p are also transported via this direct pathway (Cowles *et al.*, 1997b; Reggiori *et al.*, 2000). The specific marker of multivesicular body (MVB) pathway is CPS1, a type II integral membrane protein, is synthesized as an inactive precursor (proCPS) that is transported through the secretory pathway to the TGN and delivered to the prevacuolar compartment (PVC). In the PVC, proCPS is sorted to the forming internal vesicles of the multivesicular bodies (MVB), and these vesicles are then

delivered to the vacuole where the vesicles are degraded and CPS1 proteolytic maturation yields the active mature form of CPS1 (mCPS) (Cowles *et al.*, 1997b). The fourth biosynthetic pathway to the yeast vacuole is used by the soluble vacuolar hydrolase aminopeptidase I (API) (Klionsky *et al.*, 1992). This route is called as the API-pathway or the Cvt-pathway (cytoplasm-to-vacuole-targeting) and described in chapter 1.1.3.

1.5 SNARE protein Vti1p

The yeast-v-SNARE-protein Vti1p (Vps10- tail-interacting) was discovered in a 2-hybrid-screen in search for binding partners of the cytosolic domain of Vps10p (CPY-transport receptor) (Fischer von Mollard *et al.*, 1997). But a specific biochemical interaction between Vti1p and Vps10p could not be shown. The *VTI1*-gene encodes a 217-amino acid protein with a C-terminal transmembrane domain, which is followd by a luminal part of 4 amino acids. *VTI1* is an essential gene and Vti1p was shown to be localized to Golgi and pre-vacuolar membrane by sub cellular fractionation and immunofluorescence microscopy (Fischer von Mollard *et al.*, 1997; Fischer von Mollard and Stevens, 1999). The SNARE-motif is located next to the transmembrane domain which contains a glutamine in the 0-layer. Therefore Vti1p belongs to the Q-SNARE-family and sequence comparisons showed that the SNARE-motif of Vti1p is related to the N-terminal helix of SNAP-25 (Qb-SNARE). Functional studies showed that Vti1p is involved in several transport steps, from Golgi to late endosomes, retrograde transport to the cis-Golgi, biosynthetic transport to the vacuole and in TGN homotypic fusion (Fig.5). Vti1p interacts with the Syntaxin (Qa-SNARE) Sed5p in the retrograde transport to the cis-Golgi, (Lupashin *et al.*, 1997) with the Qa-SNARE Pep12 in the transport from the Golgi to the prevacuole (Fischer von Mollard *et al.*, 1997) and with the vacuolar Syntaxin Vam3p in the biosynthetic transport of CPY, ALP and API to the vacuole (Fischer von Mollard and Stevens, 1999). In addition Vti1p is involved in the homotypic vacuolar fusion by interaction with Vam3p (Ungermann *et al.*, 1999). It was also shown, that Vti1p interacts biochemically with the Syntaxin Tlg2p (TGN) (Holthuis *et al.*, 1998). Snc1/2, Tlg2p, Tlg1p and Vti1p are involved in the homotypic TGN fusion and the retrograde transport from the early endosome to the TGN transport (Brickner *et al.*, 2001). The N-terminus of Vti1p interacts with ENTH domain of Ent3p which is involved in endocytosis (Chidambaram *et al.*, 2004).

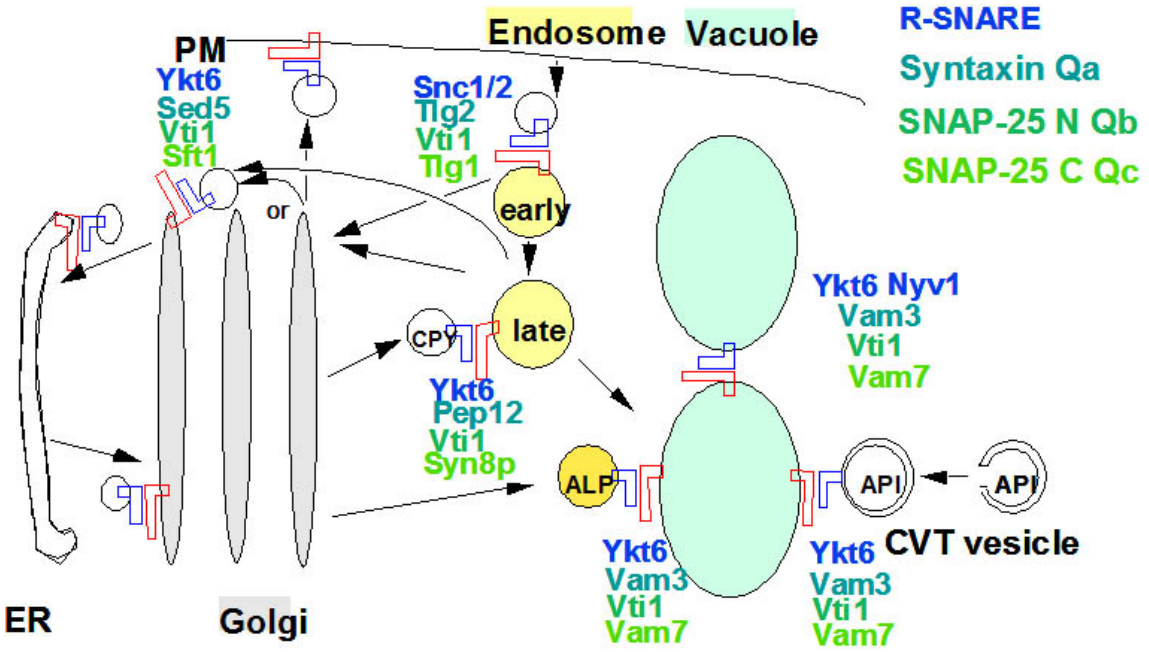

Fig.5. SNARE complexes with Vti1p

1.5.1 Vti1p homologues

Vti1p-homologuous proteins were found in *C. elegans*, *Drosophila*, *Arabidopsis* and mammals. In *Arabidopsis* so far 3 Vti1-homologues were identified (Sanderfoot *et al.*, 2000; Zheng *et al.*, 1999). In mammals two Vti1-proteins exist, Vti1a (27 kDa) which shares 33% identity with Vti1p and Vti1b (29 kDa), which only shares 27 % identity (Fischer von Mollard and Stevens, 1998; Lupashin *et al.*, 1997). Mouse Vti1a and Vti1b share only 30% amino acid identity. In addition a brain specific splice-variant of Vti1a, Vti1a-ß (29 kDa) was identified, which contains an insertion of 7 amino acids (Antonin *et al.*, 2000c). As already mentioned, mouse-, rat- and human-Vti1a contain an aspartate instead of the glutamine in the 0-layer-position (Antonin *et al.*, 2000c). It seems that the two mammalian and the 3 plant-homologues of Vti1p do not possess redundant functions, but that they are specialized to different transport-pathways, which is also supported by their different subcellular localization. In the indirect immunofluorescence Vti1a was localized to Golgi and TGN-structure, whereas Vti1b seems to be associated to early and late endosomes (Kreykenbohm *et al.*, 2002). During homotypic fusion of late endosomes, Vti1b forms a complex with the SNARE-proteins Syntaxin 7, Syntaxin 8 and Endobrevin/Vamp-8 of which the crystal-structure has been solved (Antonin *et al.*, 2000a;

Antonin *et al.*, 2000b). Vti1b-knock-out-mice are viable, but show phenotypic heterogeneity. The protein level of the SNARE partner Syntaxin 8 is decreased in these mice. Hepatocytes of small knock-out-mice show a decreased level of the lysosomal degradation of endocytosed material (Atlashkin *et al.*, 2003). The N-terminus of Vti1b interacted with ENTH domain of Epsin-R, a protein involved in transport between the TGN and the endosomes (reference: chapter 1.7) (Chidambaram *et al.*, 2004) and Epsin-R is an adaptor for Vti1b (Hirst *et al.*, 2004). Vti1a forms a SNARE-complex with VAMP-4, Syntaxin 6 and Syntaxin 16, which is involved in the fusion of early endosomes and in the retrograde transport from the early endosome to the TGN (Kreykenbohm *et al.*, 2002; Mallard *et al.*, 2002). Vti1a-ß functions in a SNARE complex during recycling or biogenesis of synaptic vesicles but not in exocytosis (Antonin *et al.*, 2000c). It has been shown, that human Vti1b could functionally replace the yeast-Vti1p in the transport to the cis-Golgi as well as in the transport from the Golgi to the prevacuolar compartment, but not in the ALP-pathway (Fischer von Mollard and Stevens, 1998). In activated macrophages, Vti1b and syntaxin 6 forms a novel SNARE complex which is up regulated to secrete increased level of cytokines (Murray *et al.*, 2005).

1.5.2 Temperature sensitive mutants of Vti1p

Since *VTI1* is an essential gene, temperature sensitive *vti1* mutants were generated to study the function of Vti1p. Different temperature sensitive alleles of *vti1* cause blocks at different stages in the secretory pathway. Via random mutagenesis of the *VTI1* gene and analysis of cells, which showed an impaired growth at higher temperatures, or defects in the protein transport, 3 different temperature-sensitive (ts) *VTI1*-mutants were identified: *vti1-1*, *vti1-2* and *vti1-11* (Fischer von Mollard *et al.*, 1997) (Fig.6). *vti1-1* mutants were obtained by shuttle mutagenesis with hydroxylamine treated *VTI1* on a *CEN*-based plasmid. The other two alleles, *vti1-2* and *vti1-11* were generated by PCR mutagenesis. It turned out, that the mutations in all *vti1*-ts-mutants affected amino acids in the SNARE-motif, especially conserved amino acids in the interaction points (layers) with which Vti1p forms SNARE-complexes with other SNARE-proteins. The mutants *vti1-1, vti1-2* and *vti1-11* all show defects in CPY-transport from the Golgi to the prevacuolar compartment after temperature shift. *vti1-11* cells display in addition a block in the retrograde transport to the cis-Golgi, which leads to an acculumation of the ER-modified p1CPY-form because of an indirect effect on the ER to Golgi transport. *vti1-2* cells are

defective both in CPY and ALP pathway whereas *vti1-1* cells are defective only in CPY pathway (Fischer von Mollard and Stevens, 1999). *vti1-1* cells show slight defects in API-transport to the vacuole, whereas this pathway is completely blocked in *vti1-11* cells after temperature-shift. Also *vti1-2* cells show a partial defect in API transport step. *vti1-1* and *vti1-2* mutants also cause a defect in homotypic vacuolar fusion *in vitro* (Ungermann *et al.*, 1999). *vti1-1* cells grow at 37°C nearly like wild type cells, whereas *vti1-2* and *vti1-11*-cells exhibit a growth defect at 37°C (Fischer von Mollard *et al.*, 1997). Apart from these SNARE motif mutants, few N-terminal mutants of Vti1p were also obtained by random mutagenesis (unpublished data, Fishcer von Mollard). vtiQ29RW79Rp is an interesting N-terminus mutant with two point mutations, replacing glutamine (at 29) and tryptophan (at 79) by arginine.

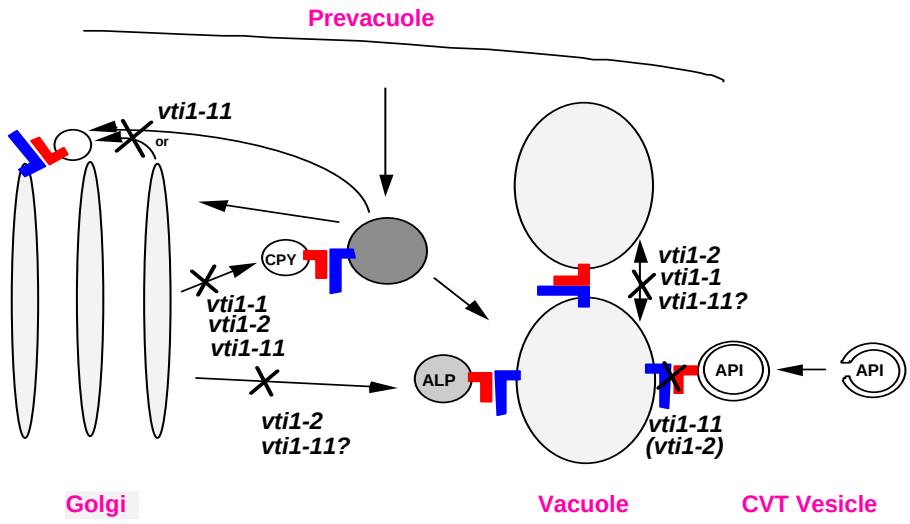

Fig.6. Temperature sensitive mutants of Vti1p

1.6 Role of SNARE Pep12p

The endosomal syntaxin, Pep12p is required for the delivery of proteins to the vacuole of the *S. cerevisiae*. It is a multifunctional SNARE which controls all the known membrane fusion events in pre-vacuolar endosomes (PVC) since the deletion of Pep12p results in the block of all the trafficking pathways to PVC (Gerrard *et al.*, 2000a). Pep12p forms SNARE complexes with Vti1p (Fischer von Mollard *et al.*, 1997), Ykt6p and Syn8p. Pep12p is localized to pre-vacuolar (late) endosomes. Syntaxin 7 is the mammalian homolog of Pep12p (Becherer *et al.*, 1996). In the absence of Tlg1p, Syn8p is required for Pep12p function. But when Tlg1p is present, Syn8p can be removed without loss of

function of Pep12p (Lewis and Pelham, 2002). Pep12p localization requires clathrin and GGA coat proteins and also it contains a FSD motif which directs it to the late endosome (Black and Pelham, 2000). The TMDs from SNAREs on each membrane is needed to transfer the 'zipping' force to form the core complex. In the vacuole only Vti1p and Vam3p contribute the TMDs. In the PVC, Syn8p, Vti1p and Pep12p provide the TMDs. Pep12p requires its transmembrane domain (TMD) for its proper localization but not for its role in vesicle fusion. Overexpression of Pep12p can compensate for loss of Vam3p and vice versa which indicates that Vam3p and Pep12p are interchangeable in the endosomal as well as the vacuolar SNARE complexes. But the TMD of Pep12p is required for participation in this complex. Thus the TMD of Pep12p plays different role in the pre-vacuolar and the vacuolar SNARE complexes (Darsow *et al.*, 1997; Gerrard *et al.*, 2000b). Vti1p uses the retrograde transport to achieve its proper steady-state localization. Loss of Pep12p may alter the localization of Vti1p but it could not be shown clearly because of the diffuse and punctuate localization of Vti1p (Gerrard *et al.*, 2000a).

1.7 ENTH domain proteins

Membrane recruitment of cytosolic proteins is mediated by a growing number of modular membrane targeting modules like, PH, FYVE, PX, ENTH, ANTH, BAR and FERM domains that recognize specific lipid molecules in the membrane. Epsin N-terminal homology domain (ENTH) is a highly conserved domain of around 140 amino acids shared by variety of proteins implicated in the regulation of endocytosis or cytoskeletal machinery in budding and fission yeast, in nematodes, rat, mouse, oat and man (Kay *et al.*, 1999). There is a homologous domain for ENTH domain which is called as ANTH domain (AP180 N-terminal homology) present in AP180/CALM and HIP1/HIP1R protein families. Both ANTH and ENTH domains bind $PI(4,5)P_2$ with high specificity which is essential for endocytosis, mediated by clathrin-coated pits (Itoh *et al.*, 2001). ENTH proteins have binding sites for adaptor proteins, clathrin and some multidomain proteins like Eps15. Phylogenetic analysis of ENTH domains suggested two ENTH domain families, namely the epsin family (contains epsins 1-3, Ent1p and Ent2p), which interacts through NPF motifs with EH domains and functions at the cell surface; and the enthoprotin family (contains enthoprotin/clint/EpsinR and Ent3p), which contains sequences for binding to GGAs and γ-adaptin and functions on internal membranes

(Legendre-Guillemin *et al.*, 2004). The ENTH and ANTH domain proteins in mammals and yeast are summarized in the Fig.7.

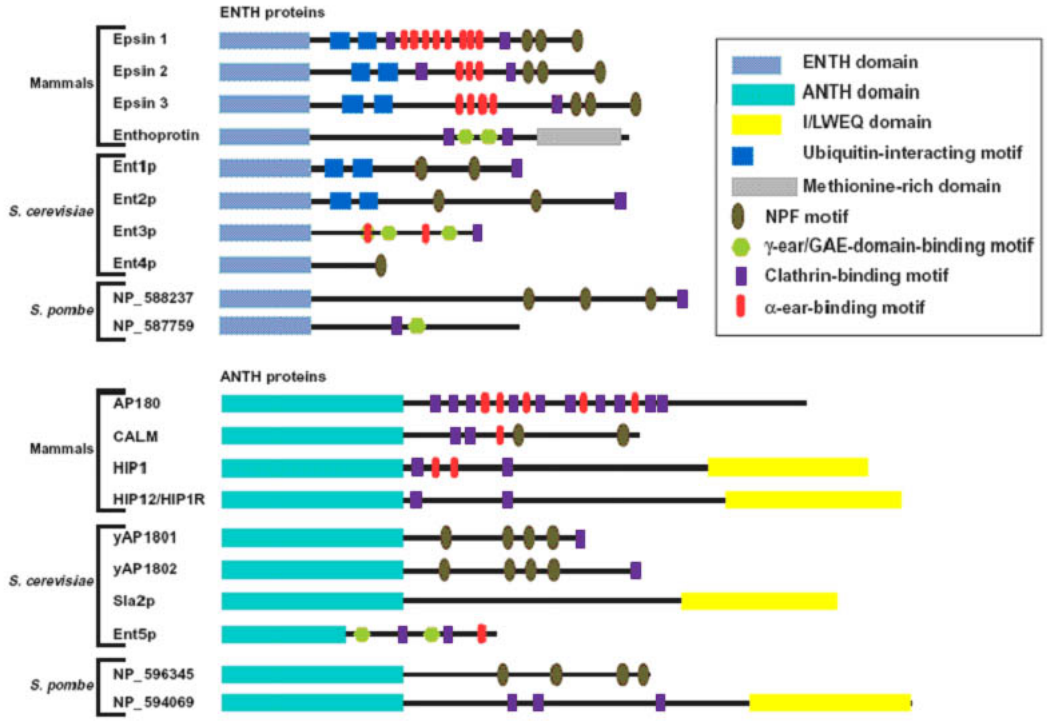

Fig.7. A/ENTH domain proteins in yeast and mammals (Legendre-Guillemin, 2004)

1.7.1 Ent proteins in yeast

There are five Ent proteins in *S. cerevisiae*, from Ent1p through Ent5p. Ent1p and Ent2p were identified by a two hybrid screen in a search for interacting factors for EH domains of Pan1p (Wendland *et al.*, 1999). ENTH domains of Ent1p and Ent2p are 76.9% identical, while their identities with the ENTH domains of Ent3p and Ent4p range from 24 to 34%. The ENTH domain is required for the essential functions of Ent1p and Ent2p and single deletions of these two proteins did not show any phenotype but the double mutant was inviable, suggesting that Ent1p and Ent2p are redundant in function. At least one ENTH domain was required for the viability. Ent1p is localized to the cell periphery and internal compartments and both the proteins are required for endocytosis and organization of actin cytoskeleton. The ENTH domain of Ent1p interacts with phospholipids, whereas the ubiquitin-interaction motifs (UIMs) in the C-terminal region bind to ubiquitylated proteins at the membrane (Wendland *et al.*, 1999). These events promote interactions between NPF motifs in Ent1p and EH-domain proteins (Aguilar *et*

al., 2003). Ent3p and Ent4p are functionally non redundant with Ent1p or Ent2p. Ent3p and Ent5p localized to TGN and early endosomes (Duncan *et al.*, 2003). ENTH domain of Ent5p resembles lysine-rich ANTH domain, so the ENTH domains of Ent3p and Ent5p may be functionally different and Ent5p is unlikely to promote membrane curvature. Ent3p and Ent5p interact with Gga2p and localized to clathrin coats at the TGN and endosomes. Ent5p binds with AP1 and clathrin. Ent3p and Ent5p are required together for clathrin recruitment but they differ in clathrin-binding properties. Single deletions of *ENT3* and *ENT5* did not lead to defects in clathrin-mediated protein transport but the double mutant caused a defect in clathrin localization, but Ent3p lacks a clathrin binding motif. All these points provide evidence for overlapping functions of ENTH and ANTH domains in clathrin assembly and CCV mediated transport in the yeast. Ent3p and Ent5p seem to be functional accessory factors for CCV formation and function at TGN/endosomes (Duncan *et al.*, 2003). Ent3p has been shown as a specific effector of $PI(3,5)P_2$ localized to endosomes and is required for protein sorting into the MVB (Friant *et al.*, 2003). Ent5p binds $PI(3,5)P_2$ specifically, associates with Vps27p and together with Ent3p is required for ubiquitin-dependent protein sorting into the multivesicular body (Eugster *et al.*, 2004). In *Schizosaccharomyces pombe*, Ent1p is an essential component of endocytosis, required for actin organization and cell morphology. $PI(4,5)\ P_2$ may not be needed for the proper localization of Ent1p to endocytic sites (Sakamoto *et al.*, 2004).

1.7.2 Epsin family proteins in mammals

The best characterized among the epsin proteins is epsin 1 which consists of an ENTH domain in the N-terminus which is highly conserved in yeast, plant, frogs and human (Kay *et al.*, 1999; Rosenthal *et al.*, 1999) and the C-terminus contains multiple short peptide motifs that mediate interaction with endocytic proteins. These short peptides are eight copies of DPW tripeptide that mediate binding to α-ear of AP-2 (Owen, 1999; Traub *et al.*, 1999), two distinct clathrin binding motifs (Drake and Traub, 2001; Hussain *et al.*, 1999; Rosenthal *et al.*, 1999), three NPF motifs which bind to the EH domain of Eps15 and intersectin (Chen *et al.*, 1998; Hussain *et al.*, 1999). Epsin1 is localized to clathrin coated pits and participates in clathrin-dependent endocytosis, including endocytosis at synapses (Chen *et al.*, 1998). Itoh et al showed that in cultured mammalian cells, overexpression of epsin1 containing a mutation in the ENTH domain prevented epsin1 from binding to PIP2 which blocked clathrin dependent endocytosis (Itoh *et al.*, 2001).

Epsin1 interacts with promyelocytic leukemia zinc finger protein (PLZF), a transcription factor which can target epsin 1 to the nucleus (Hyman *et al.*, 2000). Enthoprotin was independently discovered (Wasiak *et al.*, 2002) and referred also as Clint (Kalthoff *et al.*, 2002) and epsinR (Hirst *et al.*, 2003). It contains two clathrin binding domains in its C-terminal region and binds directly to clathrin. It also binds to AP-1 and GGA2 through its C-terminal domain at the TGN. The γ-ear (of AP1) and GAE domain (of GGA2) both bind to two conserved motifs in the C-term of enthoprotin (Duncan and Payne, 2003; Miller *et al.*, 2003; Mills *et al.*, 2003; Wasiak *et al.*, 2003). Enthoprotin is localized primarily to the TGN and in endosomal membranes (Wasiak *et al.*, 2003). Constructs of enthoprotin lacking ENTH domain concentrate on clathrin-enriched membrane fractions (Wasiak *et al.*, 2002) thus C-terminal domain of the protein seems to contain membrane-targeting sequences. However, ENTH-domain mutants unable to bind phospholipids relocalize from the TGN to large perinuclear puncta (Mills *et al.*, 2003) which suggested that ENTH domain contributes to the specificity of membrane localization. Enthoprotin/EpsinR specifically binds to PI4P (Hirst *et al.*, 2003; Mills *et al.*, 2003). EpsinR is functionally equivalent to epsin 1 in CCV budding but in a different transport step, namely in budding from the TGN/endosomes rather than from the plasma membrane (Fig.8) (Mills *et al.*, 2003). *Drosophila* epsin, Liquid facets (Lqf), was shown to be important for internalization of the Delta (D1) transmembrane ligand in the developing eye. Also, when Lqf was divided into two pieces, one with ENTH domain and one without ENTH, surprisingly each part retain significant ability in D1 internalization and eye patterning (Overstreet *et al.*, 2003).

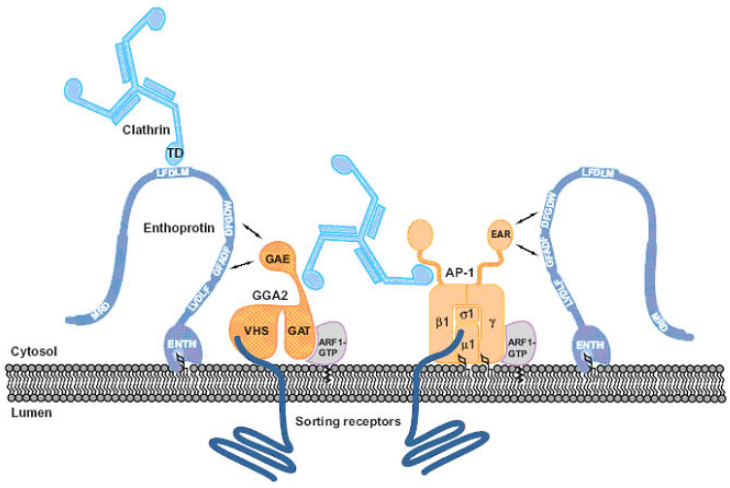

Fig.8. Enthoprotin interaction at the TGN (Legendre-Guillemin, 2004)

1.7.3 Membrane curvature by ENTH domain

ENTH proteins are anchored to the membrane by PI(4,5) P_2 through ENTH domain, leaving their C-terminal region available to recruit coat components and catalyze clathrin assembly (Kalthoff *et al.*, 2002). Epsins are recruited to biological membranes by multiple independent interactions instead of being targeted to the membrane by the ENTH domain alone. The ENTH domain is made up of a superhelix of 8 α-helices (Lohi *et al.*, 2002) whereas ANTH domain is extended by one or more α-helices compared to ENTH domain, which has in total nine α-helices (Ford *et al.*, 2001). When the ENTH domain binds PI(4,5) P_2, the structure shifts from eight α-helices to nine, the additional helix termed as 'helix 0' (Ford *et al.*, 2001). Structurally the ENTH domain is similar to another N-terminal domain called, VHS [Vps27p, Hrs (hepatocyte growth-regulated tyrosine kinase substrate), STAM (signal-transducing adaptor molecule)] domain, (Hyman *et al.*, 2000) present in the proteins involved in membrane trafficking. The binding site for PI(4,5) P_2 in ENTH consists of a pocket of basic amino acids conserved in all ENTH domains (Ford *et al.*, 2002) and that in ANTH domain consists of a cluster of lysine amino acids (Ford *et al.*, 2001). Though both domains bind PI(4,5) P_2, they have different modes of membrane interaction (Stahelin *et al.*, 2003b). The ENTH domain of epsin by itself caused liposome tubulation while the ANTH domain could not do it (Ford *et al.*, 2002). In the monolayer analysis, PI(4,5) P_2 specifically triggers the penetration of the ENTH domain but not the ANTH domain (Stahelin *et al.*, 2003b) which is similar to specific membrane penetration of FYVE domains and PX domain by PI3P (Stahelin *et al.*, 2003a; Stahelin *et al.*, 2002). The ENTH domain lacks a well-defined ligand binding pocket, but when PI(4,5) P_2 binds, it triggers the formation of the binding pocket, also aligns the hydrophobic residues toward the membrane surface and inserts the residues (helix 0, an amphipathic helix) into the cytoplasmic leaflet of the membrane by electrostatic switch mechanism. This membrane insertion initiates the membrane deformation by pushing surrounding lipids aside, producing a more curved surface. The energy cost for this process could be obtained by increasing the surface pressure on one side of the membrane, creating an imbalance and lowering the curvation energy. If epsin is only involved in the initial budding process, dozens of epsin molecules might be enough to shift the balance to favor the curved state (Hurley and Wendland, 2002). There are two possible models for the formation of the curvature. Insertion of the ENTH domain

could function synergistically with the clathrin assembly to drive the membrane curvature or ENTH domain itself is enough to bend the membrane with the assembled clathrin stabilizing the deformed membrane (reviewed in: Legendre-Guillemin *et al.*, 2004).

Since PI(4,5) P_2 is a central player in the formation of membrane curvature, regulation of its synthesis and turnover are great importance for endocytic vesicle trafficking. Synaptojanin dephosphorylates PI(4,5) P_2, converting it into PI4P which could weaken the association of ENTH proteins and other coat components with the membrane, resulting in the uncoating of clathrin-coated vesicles (Cremona, 1999).

1.7.4 Functions of ENTH proteins

Apart from the membrane attachment of proteins by phsopholipid binding, ENTH domain proteins stimulate clathrin assembly (Kalthoff *et al.*, 2002; Morgan *et al.*, 2000). In addition to recruiting coat components to membranes, ENTH proteins contribute to the formation of ordered clathrin coats. Also ENTH proteins act as cargo specific adaptors, for example, EpsinR acts as a cargo adaptor for Vti1b (Hirst *et al.*, 2004). Mammalian and yeast epsins carry UIMs and are likely to accumulate ubiquitylated membrane proteins (Aguilar *et al.*, 2003; Polo *et al.*, 2002) thus act as adaptors for a wide range of ubiquitylated cargo. Epsin 1 may function as a transcriptional regulator by binding PLZF (Legendre-Guillemin *et al.*, 2004). E/ANTH domains, isolated from various species bind tubulin and microtubules (de Camili *et al.*, 2002; Hussain *et al.*, 2003). So, ENTH domain proteins may link clathrin-coated membranes to microtubules. Two ANTH domain containing proteins HIP1 and HIP1R were shown to localize to clathrin coated pits, also contains a putative actin binding motif (ILWEQ) in the C-terminus shows evidence for the elusive link between the actin cytoskeleton and endocytosis (Senetar *et al.*, 2004). A/ENTH domains play multiple roles as lipid and protein binding modules.

1.7.5 ENTH domains interact with SNARE proteins

To identify interacting partners for the N-terminal domain of Vti1b, a two hybrid screen was done in our lab. Interestingly, an ENTH domain containing protein, EpsinR/enthoprotin/Clint was identified as a binding partner (Fig. 9(i) a). To check whether this interaction was conserved in yeast also, two hybrid interactions were done with N-terminal domain of Vti1p and yeast A/ENTH domains (Fig. 9(ii) a). A specific interaction between ENTH domain of Ent3p and Vti1p was observed. These interactions

were confirmed further by in vitro binding assays with bacterially expressed Strep tagged ENTH domains of Ent3p/EpsinR and His-Vti1p/Vti1b (Fig. 9(i) and (ii) b).

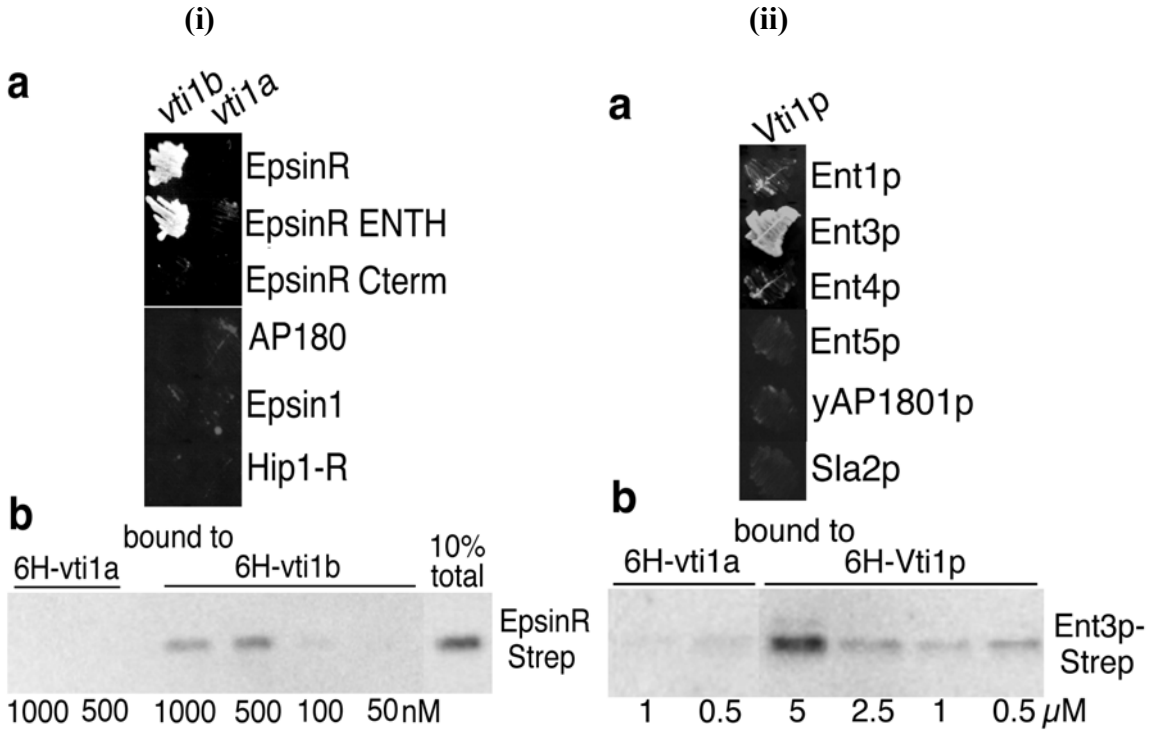

Fig.9. Two hybrid (a) and *in vitro* binding assay (b) for the interaction of vti1b/EpsinR (i) and Vti1p/Ent3p (ii)

1.8 Aim

Project 1: Function of the N-terminus of Vti1p

The precise function of the SNARE complex, its individual components, and of its accessory proteins remains to be characterized. The extent to which SNAREs are responsible for the initial recognition and specificity of interactions between vesicles has, however, been controversial. Many questions have arisen because some SNAREs, can act at more than one transport step (Clague, 1999). Some individual SNAREs are promiscuous in their partnerships, for example the yeast v-SNARE Vti1p has been shown to pair with four of the seven yeast syntaxin related t-SNAREs. The ability of Vti1p to mediate multiple fusion steps requires additional proteins to ensure specificity in membrane traffic. In addition, the activity of Vti1p has to be tightly regulated and it has to be transported to the correct organelles. While interaction with SNAREs, requires the SNARE motif, the function of the N-terminus is poorly understood. It is proposed that the N-terminal domains of SNAREs may have some regulatory functions. So, we would like to unravel the functions of the N-terminus of Vti1p, a versatile SNARE protein which deserves intensive investigation. Using an N-terminal mutant vtiQ29RW79R, the stability, localization, function and the turn over of mutant Vti1p should be studied to get further insight.

Project 2: Characterization of Ent proteins in yeast

The preliminary data from our lab showed that ENTH domain proteins EpsinR/Ent3p interacted with the N-term domain of SNARE proteins Vti1b/Vti1p. Further studies should be conducted to investigate the functional interaction between Vti1p and Ent proteins. Also, the function of Ent3p and Ent5p should be studied by generation and characterization of deletion mutants.

2 Materials and Methods

2.1 Materials

2.1.1 Laboratory Equipments

All Glasswares	Schütt, Göttingen
Autoclave bags	Sarstedt, Nümbrecht
Autoclave type Tecnoclav 50	Tecnomara, Zürich
Bottle top filters	Sarstedt Inc., Newton, USA
Corex® tubes 15ml	Corning Inc., NY
Cuvetts for Electroporation	Invitrogen, Leek
DNA-Sequencer Type 310	ABI, PE Biosystems
Electroporator 1000	Stratagene, USA
Eppendorf- Tabletop centrifuge 5415C	Schütt, Göttingen
Fluorescence microscope IX50	Olympus, Hamburg
French® Pressure Cell Press, SLM-Minco®	Spectronic Instruments
Gene quant II, RNA/DNA calculator	Pharmacia Biotech, UK
Ice machine	Ziegra, Isernhagen
Incubators Innova 4230 and 4330	New Brunswick Scintific, Edison
Intelligent Dark Box II, LAS-1000	Fuji, Japan
Phosphoimager Fujix BAS1000	Fuji, Japan
Ultra turrax T8	IKA Labortechnik, Staufen
Supersignal Chemiluminiscent Substrate	Pierce, Illinois/ USA
Syringes	Sarstedt, Braunschweig
Tabletop Ultracentrifuge TLA-100.3	Beckmann, Münich
Thermocycler GeneAmp PCR system 9600	Perkin-Elmer Cetus, Norwalk
Mastercycler gradient	Eppendorf, Hamburg
JA-10 and JA-20 Polypropylene tube	Nalgene, München
Culture flasks for bacteria	Schott, Mainz
Glass pipettes	Schütt, Göttingen

Microscope slides	Menzel-Glaser
Needles for syringes	B.Braun Melsungen AG, Melsungen
Liquid Scintillation counter 1900R	Packard, Frankfurt
Parafilm	American National Can™ Chicago
Pasteur pipettes	Schütt, Göttingen
Pipette tips	Sarstedt, Nümbrecht
Plastic tubes 10, 15 and 50 ml	Sarstedt, Nümbrecht
Nitrocellulose membrane 0.2 µM	Schleicher and Schüll, Dassel
Whatman GB002 paper	Schleicher and Schüll, Dassel
Whatman GB003 paper extra thick	Schleicher and Schüll, Dassel
X-ray films XAR-5	Kodak, Stuttgart
X-ray film developing machine	Agfa-Gevaert, Leverkusen

2.1.2 Chemicals

All the chemicals are of Analysis grade.

Aminoacids	Biomol, Serva, Sigma, ICN	Hamburg, Heidelberg, München, Meckenheim
APNE (N-Acetyl-Phenylalanin-β-Naphtylester)	Sigma	Münich
Bacto-Agar	DIFCO	Detroid (USA)
Bacto-Pepton	DIFCO	Detroid (USA)
Bacto-Trypton	DIFCO	Detroid (USA)
Coomassie Brilliant Blue	Serva	Heidelberg
DAPI (4'-6-Diamino-2-phenylindoldihydrochlorid)	Sigma	Münich
Dimethyl-pimelinediimidat-dihydrochlorid (DMP)	Fluka	Buchs
dNTPs	Amersham	Braunschweig
Fast Carnet GBC Salt	Sigma	Münich
Liquid Scintillation Lumasafe Plus	Packard	Groningen
Yeast Extract	DIFCO	Detroid (USA)
Isopropyl-α-D-Thiogalactopyranosid (IPTG)	BTS	St. Leon-Rot
Pansorbin® Cells, Standardised	Calbiochem	Bad Soden
Phenol:Chloroform:Isoamylalkohol (25:24:1)	Fluka	Buchs (Schweiz)
Poly-L-Lysin Hydrobromide	Sigma	Münich
Ponceau-S	Serva	Heidelberg
Protein-A-Sepharose / Protein-G-Sepharose	Pharmacia	Freiburg
Bovine Serum Albumin (Albumin bovine Fraction V, BSA)	Serva	Heidelberg
Triton X-100	Serva	Heidelberg

Tween-20	Serva	Heidelberg
Water, HPLC-purified	Baker	Deventer
Yeast-Nitrogene-Base	DIFCO	Detroid (USA)
30% (w/v) Acrylamid/0.8% (w/v) Bisacrylamid	Roth	Karlsruhe

2.1.3 Proteaseinhibitors

Leupeptin	Biomol, Hamburg
Pepstatin A	Biomol, Hamburg
Phenylmethylsulfonylfluorid (PMSF)	Serva, Heidelberg

100 µl 100x Proteaseinhibitor-Mix

50 µl 100 mM PMSF (17.4 mg/ml in Ethanol)

10 µl Pepstatin (1 mg/ml in Methanol)

39 µl Methanol

1 µl Leupeptin (10 mg/ml in H_2O)

2.1.4 Antibodies

Primary Antibody	Molecular weight (kDa)	Immunized species	Dilution for western blot	Dilution for Immunofluorecence	Source
Vti1p	29	Rabbit	1:3000	1:50	FvMollard
Ape1p	60(p),51(M)	Rabbit	1:5000		Thumm
Vph1p	100	Mouse	1:100		T. Stevens
Vps10p	190	Rabbit	1:1000		T. Stevens
Pep12p	33	Rabbit	1:1000	1:50	FvMollard Molecular probes
GFP	45	Mouse	1:2000		MBL
Use1p	33	Rabbit	1:1000		FvMollard
ALP	72	Mouse	1:100		T. Stevens
Bip/Kar2p	75	Rabbit	1:1000		H.D. Schmitt
ENT3p	48	Rabbit	1:500		FvMollard

HA	-	Mouse	1:1000		BabCo, Richmond
CPY	69	Mouse	1:100		T. Stevens
Secondary antibodies					
Cy2		anti Mouse		1:100	Dianova
Cy2		anti Rabbit		1:100	Dianova
Cy3		anti Mouse		1:100	Dianova
Cy3		anti Rabbit		1:100	Dianova
Goat anti-mouse Horseradish peroxidase			1:10000		Sigma
Goat anti-rabbit Horseradish peroxidase			1:10000		Sigma

2.1.5 Enzymes, Nucleotides and Standards

1 kb-DNA-Ladder	Gibco BRL, Eggenstein
Alkaline Phosphatase (Calf Intestine)	Roche, Mannheim
Prestained Protein Standard	Bio-Rad, Münich
Restriction Endonucleases	New England Biolabs, Bad Schwalbach
RNAse A	Boehringer, Mannheim
T4-DNA-Ligase	New England Biolabs, Bad Schwalbach
T4-Polynucleotide-Kinase	New England Biolabs, Bad Schwalbach
Taq-DNA-Polymerase	Pharmacia, Freiburg
Pfu-DNA-Polymerase	Stratagene, Heidelberg
TITANIUM™ *Taq*-DNA-Polymerase	Clonetech, Palo Alto, CA
Ultrapure dNTP Set	Pharmacia, Freiburg
Zymolyase®-20T	Seikagaku, Tokyo (Japan)

2.1.6 Radioactive substance

L-[^{35}S]-Methionin/Cystein, 10 mCi/mmol from Hartmann-Analytik, Braunschweig

2.1.7 Kits for DNA and Protein

ABI PRISM Dye Terminator Cycle Sequencing Ready Reaction Premix	Perkin Elmer Cetus, Norwalk (USA)
BioRad Protein Assay	Bio-Rad, Munich
QIAEX®II Agarose Gel Extraction Kit	Qiagen, Hilden
QIAprep Spin Miniprep Kit	Qiagen, Hilden
SuperSignal® West Pico Chemiluminescent Substrate	PIERCE, Rockford (USA)

2.1.8 Oligonucleotides

Name	Oligonucleotide	Purpose
*ENT3*HA f	TAACCATACATCATCCAAAGAAATCGATTTACTTTCCTTT CGG ATC CCC GGG TTA ATT AA	For genomic integration of HA tag to *ENT3*
*ENT3*HA r	TTATAAAACATTTACATATTGTGTAAACCAATAATATCAC GAA TTC GAG CTC GTT TAA AC	For genomic integration of HA tag to *ENT3*
*ENT3*UT5	CG GGA TCC ATT TTG CTA AGC CAA TTC	To amplify *ENT3* and also to delete *ENT3*
*ENT3*UT3	GC TCT AGA AGG GCA CTT CAA CTC TC	To amplify *ENT3* and also to delete *ENT3*
ENT3-Aux3	TTATAAAACATTTACATATTGTGTAAACCAATAATATCAC GGTATTTCACACCGCATA	To delete *ENT3*
ENT3-Aux5	CGTCGATAGGAGATCACATCGTTAATTAGTGTTAGGAAGA TTGTACTGAGAGTGCACCAT	To delete *ENT3*
6H*ENT3*f	GCAT AT GAG TTT AGA GGA TAC ATTAG	To tag ENTH domain of *ENT3* with 6xHIS

6H*ENT3*r	CGGATCC TCA AAA GGA AAG TAA ATC GAT TTC	To tag ENTH domain of *ENT3* with 6xHIS
ENT3 5	CGG GAT CCG AAT GAG TTT AGA GGA TAC ATT	To amplify and tag GFP to the C-term of *ENT3*
*ENT3*cfo	CGG GAT CCA AAG GCA AGA GAA ACG GCA AAG	To amplify C-term of *ENT3* (AA158-408)
*ENT3*cre	GCC CAA GCT TCA AAA GGA AAG TAA ATC GAT TTC	To amplify C-term of *ENT3* (AA158-408)
ENT3 GFP	TCC CCC GGG AAA GGA AAG TAA ATC GAT TTC□	To amplify and tag GFP to the C-term of *ENT3*
ENT5 5	CGGG ATC CAA ATG GAC TCA TTA TCA AAA AAG	To amplify and tag GFP to the C-term of ENT5
Ent5 GFP	CCCC AAG CTTG ACC AAC GACT TGG AGT AAG	To amplify and tag GFP to the C-term of ENT5
ENT5 delf	CAA TCTAGA TTT TAG TTTT CGG	To delete ENT5
ENT5 delr	TTT CTT CTG CAT GGA TAA TGAC	To delete ENT5
Ent5au5	ATTAAACGTTCCAATTGCATAAATACCAACACCATACAAA TTGTACTGAGAGTGCACCAT	To delete ENT5
Ent5au3	CTGTATTGAATGTATTGGGAGATGAAGGGGTATTTGGTGA GGTATTTCACACCGCATA	To delete ENT5
Pep12 5'	AATGCAGCGCAGAGGCTATC	To delete Pep12

Pep12 3'	CACTCTTCATTAGGGTATGATG	To delete Pep12
ubc7 f	AATAGTGTAATTTGGAAGGGC	To delete Ubc7
ubc7 r	ATCATTAACCTGCTACCTGC	To delete Ubc7
cue1 f	CATTACAATCTACGATCGCGC	To delete Cue1
cue1 r	TCCCGACAAGCACTTAAGCG	To delete Cue1

2.1.9 Yeast and bacterial strains

Yeast strains

Strain	Genotype	Reference
SEY6210	MATα *leu2-3,112 ura3-52 his3-Δ200 trp1-Δ901 lys2-801 suc2-Δ9 mel-*	(Robinson *et al.*, 1988)
SEY6211	MAT**a** *leu2-3,112 ura3-52 his3-Δ200 ade2-101 trp1-Δ901 suc2-Δ9 mel-*	(Robinson *et al.*, 1988)
FvMY7	MAT**a** *leu2-3,112 ura3-52 his3-Δ200 ade2-101trp1-Δ901suc2-Δ9 mel- vti1-1*	G. Fischer von Mollard
FvMY24	MAT**a** *leu2-3,112 ura3-52 his3-Δ200 ade2-101trp1-Δ901suc2-Δ9 mel- vti1-2*	G. Fischer von Mollard
FvMY29	MAT**a** *leu2-3,112 ura3-52 his3-Δ200 ade2-101trp1-Δ901suc2-Δ9 mel- vti1-1pho8Δ*	G. Fischer von Mollard
FvMY6pBK117	MAT**a** *leu2-3,112 ura3-52 his3-Δ200 ade2-101trp1-Δ901suc2-Δ9 melΔvti1::HIS3 vti1Q116-217*	G. Fischer von Mollard
FvMY6pBK119	MAT**a** *leu2-3,112 ura3-52 his3-Δ200 ade2-101trp1-Δ901suc2-Δ9 melΔvti1::HIS3 vti1M55-217*	G. Fischer von Mollard
FvMY6pBK120	MAT**a** *leu2-3,112 ura3-52 his3-Δ200 ade2-101trp1-Δ901suc2-Δ9 melΔvti1::HIS3 vti1Q29R W79R*	G. Fischer von Mollard
FvMY6pBK123	MAT**a** *leu2-3,112 ura3-52 his3-Δ200 ade2-101trp1-Δ901suc2-Δ9 melΔvti1::HIS3 vti1Q29R*	G. Fischer von Mollard
FvMY6pBK128	MAT**a** *leu2-3,112 ura3-52 his3-Δ200 ade2-101trp1-Δ901suc2-Δ9 melΔvti1::HIS3 vti1W79R*	G. Fischer von Mollard
BKY12	MATα *leu2-3,112 ura3-52 his3-Δ200 trp1-Δ901 lys2-801 suc2-Δ9 mel- pep4Δ::URA3*	Beate Veith
BKY13	MAT***a****his3Δ1leu2Δ0lys2Δ0ura3Δ0 ent5Δ::kanMX4 ent3Δ::LEU2*	Beate Veith

Strain	Genotype	Reference
BKY15	MAT***a*** *leu2-3,112 ura3-52 his3-Δ200 ade2-101 trp1-Δ901 suc2-Δ9 mel- vti1-1 ent5Δ::kanMX4*	Beate Veith
BKY16	MAT***a*** *leu2-3,112 ura3-52 his3-Δ200 ade2-101 trp1-Δ901 suc2-Δ9 mel- vti1-2 ent5Δ::kanMX4*	Beate Veith
BKY17	MAT***a*** *his3Δ1 leu2Δ0 lys2Δ0 ura3Δ0 ent4Δ::kanMX4 ent5Δ::URA3*	Beate Veith
BKY18	MAT***a*** *ura3-52 his3-Δ200 ent3Δ::LEU2 ent4Δ::kanMX4 ent5Δ::URA3*	Beate Veith
BKY19	MAT***a*** *ura3-52 his3-Δ200 ade2-101 trp1-Δ901ENT3Δ::LEU2 ent4Δ::kanMX4*	Beate Veith
BKY20	MAT***a*** *ura3-52 his3-Δ200 ade2-101 trp1-Δ901 ent3Δ::LEU2 ent5Δ::URA3*	Beate Veith
BKY21	MATα *ura3-52 his3-Δ200 ade2-101 trp1-Δ901ent4Δ::kanMX4 ent5Δ::URA3*	Beate Veith
BKY22	MATα *ura3-52 his3-Δ200 trp1-Δ901 ent3Δ::LEU2*	Beate Veith
BKY23	MAT***a*** *ura3-52 his3-Δ200 ade2-101 trp1-Δ901 ent4Δ::kanMX4*	Beate Veith
BKY24	MATα *ura3-52 his3-Δ200 trp1-Δ901 ent5Δ::URA3*	Beate Veith
BKY25	MAT***a*** *leu2-3,112 ura3-52 his3-Δ200 ade2-101 trp1-Δ901 suc2-Δ9 mel- ent3Δ::kanMX4 pho8Δ::ADE2*	Beate Veith
BKY26	MAT***a*** *leu2-3,112 ura3-52 his3-Δ200 ade2-101 trp1-Δ901 suc2-Δ9 mel- ent5Δ::kanMX4 pho8Δ::ADE2*	Beate Veith
SNY18	MAT***a*** *leu2-3,112 ura3-52 his3-Δ200 ade2-101 trp1-Δ901 suc2-Δ9 mel- pho8Δ::ADE2*	Steve Nothwehr
MDY7	MAT***a*** *leu2-3,112 ura3-52 his3-Δ200 ade2-101 trp1-Δ901 suc2-Δ9 mel- vti1-2 pep4Δ::URA3*	Meik Dilcher
BY4742	MAT***a*** *his3Δ1 leu2Δ0 lys2Δ0 ura3Δ0*	Euroscarf
ent3Δ	MAT***a*** *his3Δ1 leu2Δ0 lys2Δ0 ura3Δ0 YJR125CΔ::kanMX4*	Euroscarf
ent4Δ	MAT***a*** *his3Δ1 leu2Δ0 lys2Δ0 ura3Δ0 YLL038cΔ::kanMX4*	Euroscarf
ent5Δ	MAT***a*** *his3Δ1 leu2Δ0 lys2Δ0 ura3Δ0 YDR153cΔ::kanMX4*	Euroscarf
SCY1	MAT***a*** *leu2-3,112 ura3-52 his3-Δ200 ade2-101 trp1-Δ901suc2-Δ9 mel- ent3Δ::kanMX4 vti1-2*	This study

Strain	Genotype	Reference
SCY2	MAT*α leu2-3,112 ura3-52 his3-Δ200 trp1-Δ901lys2-801suc2-Δ9 mel-ent3Δ::kanMX4*	This study
SCY3	MAT***a*** *leu2-3,112 ura3-52 his3-Δ200 ade2-101 trp1-Δ901suc2-Δ9 mel-ent3Δ::kanMX4 vti1-1*	This study
SCY4	MAT*α leu2-3,112 ura3-52 his3-Δ200 trp1-Δ901lys2-801suc2-Δ9 mel- ent3Δ* c-term Myc tag	This study
SCY5	MAT***a*** *his3Δ1 leu2Δ0 lys2Δ0 ura3Δ0 ent3Δ::LEU2 ent4Δ::kanMX4*	This study
SCY6	MAT*α leu2-3,112 ura3-52 his3-Δ200 ade2-101 trp1-Δ901 suc2-Δ9 mel-Δvti1::HIS3 vti1 Q29R W79 ent3Δ::kanMX4*	This study
SCY7	MAT*α leu2-3,112 ura3-52 his3-Δ200 trp1-Δ901 lys2-801suc2-Δ9 mel-ENT3HA::TRP2*	This study
SCY8	MAT*α leu2-3,112 ura3-52 his3-Δ200 trp1-Δ901lys2-801suc2-Δ9 mel-Δvti1::HIS3 vti1 Q29R*	This study
SCY9	MAT*α leu2-3,112 ura3-52 his3-Δ200 ade2-101 trp1-Δ901 suc2-Δ9 mel-Δvti1::HIS3 vti1 W79R*	This study
SCY10	MAT***a*** *leu2-3,112 ura3-52 his3-Δ200 trp1-Δ901 lys2-801 ENT3HA::TRP2*	This study
SCY11	MAT***a*** *leu2-3,112 ura3-52 his3-Δ200 trp1-Δ901lys2-801 fab1Δ::LEU2 ENT3HA::TRP2*	This study
SCY12	MAT***a*** *leu2-3,112 ura3-52 his3-Δ200 ade2-101trp1-Δ901suc2-Δ9mel-ENT3HA::TRP2 vti1-2*	This study
SCY13	MAT***a*** *leu2-3,112 ura3-52 his3-Δ200 ade2-101 trp1-Δ901 suc2-Δ9Mel-ent3Δ::LEU2*	This study
SCY14	AT***a*** *leu2-3,112 ura3-52 his3-Δ200 ade2-01 trp1-Δ901 suc2-Δ9 Mel-:: vti1-Q29R 79R*	This study
SCY15	MAT***a*** *leu2-3,112 ura3-52 his3-Δ200 ade2-101 trp1-Δ901 suc2-Δ9 mel-ent3Δ::kanMX4 ent5Δ::URA3 vti1-2*	This study
SCY16	MAT***a*** *leu2-3,112 ura3-52 his3-Δ200 ade2-101 trp1-Δ901 suc2-Δ9 melΔvti1::HIS3 vti1Q116-217HA*	This study

Strain	Genotype	Reference
SCY17	MAT***a*** *leu2-3,112 ura3-52 his3-Δ200 ade2-101 trp1-Δ901 suc2-Δ9 melΔvti1::HIS3vti1M55-217HA*	This study
SCY18	MAT***a*** *leu2-3,112 ura3-52 his3-Δ200 ade2-101 trp1-Δ901 suc2-Δ9 Mel-:: vti1-Q29R W79R pep4Δ::URA3*	This study
SCY19	MAT***a*** *leu2-3,112 ura3-52 his3-Δ200 ade2-101 trp1-Δ901 suc2-Δ9 Mel-vti1-Q29R W79R pep4Δ::URA3*	This study
SCY20	MATα *his3Δ1 leu2Δ0 lys2Δ0 ura3Δ0 ent5Δ::kanMX4 pep4Δ::URA3*	This study
SCY21	MAT***a*** *leu2-3,112 ura3-52 his3-Δ200 ade2-101 trp1-Δ901 suc2-Δ9 Mel-:: vti1-Q29R W79R ubc7Δ::LEU*	This study
SCY22	MAT***a*** *leu2-3,112 ura3-52 his3-Δ200 ade2-101 trp1-Δ901 suc2-Δ9 Mel-:: vti1-Q29R W79R cue1Δ::LEU*	This study
SCY23	MAT***a*** *leu2-3,112 ura3-52 his3-Δ200 ade2-101 trp1-Δ901 suc2-Δ9 mel- vti1-2 ent5Δ::kanMX4 pep4Δ::URA3*	This study
SCY24	MATα *leu2-3,112 ura3-52 his3-Δ200 trp1-Δ901 lys2-801 suc2-Δ9 mel- pep4Δ::URA3 ent5Δ::kanMX4*	This study
SCY25	MATα *leu2-3,112 ura3-52 his3-Δ200 trp1-Δ901 lys2-801 ent5Δ::kanMX4*	This study
SCY26	MAT***a*** *leu2-3,112 ura3-52 his3-Δ200 ade2-101 trp1-Δ901 suc2-Δ9 mel- ent3Δ::LEU2 ent5Δ::kanMX4*	This study
SCY27	MATα *leu2-3,112 ura3-52 his3-Δ200 trp1-Δ901 lys2-801 pep12Δ::URA3*	This study
SCY28	MATα *leu2-3,112 ura3-52 his3-Δ200 trp1-Δ901 lys2-801ent3Δ::LEU2 pep4Δ::URA3*	This study
SSY1	MAT***a*** *leu2-3,112 ura3-52 his3-Δ200 ade2-101 trp1-Δ901 suc2-Δ9 mel – ent3Δ*::LEU2 *pep12Δ::URA3*	Sarah Schulz
SSY2	MATα *leu2-3,112 ura3-52 his3-Δ200 trp1-Δ901lys2-801ent5Δ::kanMX4 pep12Δ::URA3*	Sarah Schulz
SSY3	MAT***a*** *leu2-3,112 ura3-52 his3-Δ200 ade2-101 trp1-Δ901 suc2-Δ9 mel – ent3Δ::LEU2 ent5Δ::kanMX4 pep12Δ::URA3*	Sarah Schulz

Bacterial strains

Strain	Genotype	Reference
DH5α	supE44, thi-1, recA1, relA1, hsdR17(rK-mK+), thi-1, ΔlacU169 (Φ80 lacZΔM15), endA1, gyrA (Nal^r)	Gibco BRL, Eggenstein
XL1-Blue	recA1, endA1, gyrA96, thi-1, hsdR17, supE44, relA1, lac [F', proAB, $lacl^qZ\Delta M15$, Tn10(Tet^r)]^c	Stratagene, Heidelberg
BL21-(D3)-RIL	*E. coli* B F^- ompT hsdS(r_B^- m_B^-) dcm^+ Tet^r gal λ(DE3) endA Hte [argU ileY leuW Cam^r]	Stratagene, Heidelberg

2.1.10 Plasmids

Plasmid	Details	Reference
pSC2	C-terminus of *ENT3* (AA158-408 end, PCR) overexpressed under TPI promotor from pYX242 (2μ), cloned in BamH1-HindIII site.	This study
pSC4	1,7 kb PCR-amplified *ENT3* cloned in YEp351 by XbaI-BamH1	This study
pSC5	1.7 kb PCR-amplified *ENT3* cloned in pRS315 by PvuII	This study
pSC6	1.7 kb *ENT3*-3xHA -TRP1 (C-term) by, in vivo recombination with pFA6a-3HA-TRP1	This study
pSC8	PCR amplified mvti1b from AA105524 cloned in pCDNA3.1 by BamH1-Xho1	This study
pSC9	2kb vti1Q29RW79R from pBK120 in pRS306 by PvuII	This study
pSC10	PCR amplified *EpsinR* from pZ1 in pGEM-Teasy	This study
pSC11	*EpsinR* from pSC10 was subcloned in pcDNA3.1 by BamH1-Not1	This study
pSC14	2kb *vti1Q29RW79R* from pBK120 cloned in YEp351 (2μ) by PvuII	This study
pSC19	1.15 kb PCR-amplified *SYN8* with 3xHA after ATG in pRS315 by PvuII	This study
pSC20	PCR-amplified *ENT3* ENTH domain (AA1-160) into pGEM-Teasy	This study
pSC21	Nde1-EcoR1 fragment from pSC20 cloned into pET 28	This study
pSC22	PCR amplified *ENT3* in C-terminal pGFP vector in BamH1-Sma1 site	This study
pSC23	CHS7 subcloned from RSB2312 into pRS314	This study
pSC24	PCR amplified *ENT5* in C-terminal pGFP vector in BamH1-HindIII	This study
pKW5	ENTH-domain *ENT3* (aa1-172) with C-terminal Strep tag in pASK-IBA3	Katrin Wiederhold

Plasmid	Details	Reference
PTS15	*PEP4*Δ::URA3 in pBR322. Cut with EcoR1-Xho1 to distrupt *pep4*Δ locus.	Tom Stevens
pSN55	Eag1-EcoR1 fragment of A-ALP in pRS316	Steve Nothwehr
RSB2310	CHS3GFP in pRS313	Schekman

2.1.11 Antibiotics

Ampicillin Trihydrate	Serva, Heidelberg
Geneticin G418	Sigma-Aldrich, Munich
Kanamycin A Monosulfate	Sigma, Munich

2.1.12 Media for *S. cerevisiae* cells

YEPD Medium (1L)

20 g Peptone

10 g Yeast extract

were dissolved in 960 ml of ddH_2O and autoclaved. Then added,

40 ml 50% Glucose (final conc. 2%)

For preparing YEPD plates, 1.5% of agar was added to the YEPD medium, before autoclaving and poured in 20cm petridishes. For YEPD-G418 plates, Geneticin was added to the final concentration of 200 mg/L.

Synthetic minimal medium (SD) (1L)

6.7 g Yeast nitrogen base w/o aminoacids

was dissolved in 860 ml of ddH_2O, autoclaved and cooled down.

40 ml 50% Glucose (final conc. 2%)

100 ml 10X Aminoacid mix

The composition of 10X aminoacid mix is listed below. The mix was prepared without Methionine for the purpose of pulse chase labeling of yeast cells. The desired auxotrophic 10X mix was prepared by not adding the particular aminoacid in the mix. The mix was autoclaved and stored at 4°C.

Supplements	Concentration(g/L)
Adenine	0.20
L-Tyrosine	0.30
L-Phenylalanine	0.50
L-Arginine	0.20
L-Lysine-HCl	0.60
L-Threonine	2.00
Uracil	0.20
L-Leucine	1.20
L.Typtophan	0.20
L-Histidine	0.20

Nitrogen starvation medium

6.7 g Yeast nitrogen base w/o aminoacids and Ammonium Sulphate was dissolved in 1000 ml of ddH_2O and autoclaved.

Sporulation plate

10 g Potassium acetate (final conc. 1%)

1 g Yeast Extract (final conc. 0.1%)

15 g Agar (final conc.1.5%)

dissolved in 974ml of ddH_2O and autoclaved, then added

1 ml 50% Glucose (final conc.0.05%)

25 ml 10X Aminoacid mix (final conc.0.25X)

2.1.13 Media for *Escherichia coli*

Luria Bertani (LB) medium (1L)

1 g	Glucose
5 g	Bacto-yeast extract
5 g	NaCl
10 g	Bacto-Tryptone

The medium was autoclaved and stored at room temperature.

LB Agar Plates

1.5% of Agar was added to the LB medium, autoclaved and the medium was let to cool down to around 50 °C. 100 µg/ml Ampicillin or 50 µg/ml of Kanamycin was added to the medium and poured into Petri dishes.

For Blue/white screen, 100µl IPTG (25mg/ml in water, stored at -20°C) and 50 µl X-Gal (50mg/ml in DMF, stored at -20°C) was spreaded evenly on the LB-Amp plate.

2xYT medium (1L)

10 g	Bacto-yeast extract
5 g	NaCl
16 g	Bacto-Tryptone

SOC medium (1L)

5 g	Bacto-yeast extract
0.6 g	NaCl
0.19g	KCl
2g	$MgCl_2$ 6 H_2O
20 g	Bacto-Tryptone

2.1.14 Stock solutions and buffers

10x PBS (1L)		Final Concentration
87.70 g	NaCl	1.5 M
28.48 g	Na_2HPO_4	160 mM
5.52 g	NaH_2PO_4	40 mM

dissolve in ddH_2O, Adjust the pH to 7.4 with NaOH, make up the volume to 1000 ml.

50x TAE (1L)		Final Concentration
242 g	Tris	2 M
37 g	Na_2EDTA (Titriplex III)	0.1 M
57 ml	Acetic acid	

Make up the volume to 1000 ml.

TE (100 ml)		Final Concentration
1 ml	1 M Tris-HCl, pH 7.5	10 mM
20 µl	0.5 M EDTA	0.1 mM

TEβ (10 ml)		Final Concentration
1 ml	1 M Tris-HCl, pH 8.0	200 mM
200 µl	0.5 M EDTA	20 ml
50 µl	β-Mercaptoethanol	1 %

Sphereoblast-buffer (10 ml):		Final Concentration
6 ml	2 M Sorbitol	1.2 M
500 µl	1 M KPO_4, pH 7.3	50 mM
100 µl	0.1 M $MgCl_2$	1 mM

10 % SDS:

10 g Sodiumdodecylsulphate in 100 ml ddH_2O.

0.5 M EDTA:

Dissolve 14.61 g Ethylene-diamine-tetra-acetate (Titriplex II) in 100 ml of ddH_2O and adjust the pH with 10 N NaOH to pH 8.0.

1 M Tris-HCl:

Dissolve 12.11 g Tris in 80 ml of ddH_2O and adjust to the desired pH with conc.HCL and make up the volume to 100 ml.

1M DTT (20ml):

3.08 g DTT, dissolved in 20 ml of 0.01 M Sodium Acetate (pH 5.2). Filter sterilized and stored at -20°C.

2.2 Methods

2.2.1 Molecular Biology

2.2.1.1 Preparation of electrocompetent *E. coli*

A single *E. coli* colony was inoculated into 10 ml of LB media and allowed to grow overnight at 37 °C in a shaking incubator. This pre-culture was inoculated in 1 l LB media and allowed to grow at 37 °C to an OD_{600} of 0.4-0.6. Cells were pre-chilled on ice for 15 min and then pelleted in JA-10 rotor at 5000 rpm for 15 min at 4 °C. Pellet was washed twice with 1 l of ice cold water and centrifuged as mentioned above. Pellet was resuspended in 20 ml ice cold sterile 10% glycerol and centrifuged in JA-20 rotor at 6000 rpm for 15 min at 4 °C. Pellet was resuspended in 2 ml ice cold, 10% glycerol, and aliquots of 40 µl, 80 µl and 160 µl in sterile eppendorfs were stored at −80°C.

2.2.1.2 Electroporation

The electroporation cuvette was washed thoroughly with 70% alcohol, followed by sterile water and chilled on ice for 5 min. The 40 µl or 80 µl aliquot of the electro competent cells was used for each transformation. 1.2 µl or 2.5 µl of DNA was added to the cells and the contents were transferred into the pre-chilled, sterile electroporation cuvette. The cuvette was placed in the electroporater and a pulse of 1800 V was given. Immediately after the pulse, SOC medium was added to the cells and were allowed to recover in sterile tubes for 30 min at 37 °C in a water bath. Then, the cells were plated on LB plates containing appropriate antibiotic and incubated overnight at 37 °C.

2.2.1.3 Isolation of DNA from *E. coli*

A single *E. coli* colony was inoculated into 2 ml of LB medium or 2xYT medium containing appropriate antibiotic and grown overnight at 37 °C in a shaking incubator. Cells were pelleted in a table-top centrifuge at 13,000 rpm for 1 min. Cell pellet was resuspended in 100 µl Lysozyme solution and 200 µl of NaOH::SDS was added, mixed gently by inverting the tube 3-4 times and incubated at RT for 5 min. To this, 150 µl of 3M NaoAc, pH 4.8 was added gently, mixed and incubated for 5min at RT. It was centrifuged for 10 min at 13000 rpm in a table-top eppendorf centrifuge. The supernatant

was taken in a new eppendorf cup, 150 µl of Phenol-Chloroform-Isoamylalcohol (25:24:1) was added, mixed and centrifuged for 5 min at 13000 rpm. The upper (aqueous) phase was carefully taken into a new tube and 2.5 volumes of cold 100% ethanol was added and centrifuged for 15min at 13000 rpm at 4°C. The pellet was washed with 1ml of 70% ethanol and was air dried or dried with the help of vacuum. The pellet was resuspended in 20 µl of TE with 100 µg/ml RNase.

Lysozyme-solution

50 mM	Glucose	
10 mM	EDTA	
25 mM	Tris-HCl, pH 8,0.	It was stored at 4°C.

NaOH-SDS

0.2 M	NaOH	
1 % (w/v)	SDS	Stored at RT. Prepared freshly.

RNase A- Solution (10 mg/ml)

10 mg RNase A in 1 ml TE and stored at -20°C.

TE/RNase (100µg/ml)

5 µl of 10 mg/ml RNase A in 500 µl TE and stored at 4°C.

2.2.1.4 Determination of the concentration of DNA

DNA concentration was determined using a spectrophotometer at 260 nm. DNA was diluted in water and the absorbance was measured at 260 nm.

Absorbance or optical density (OD) of 1 at 260 nm corresponds to ~50 µg/ml of double stranded DNA or ~40 µg/ml of single stranded DNA and RNA or ~20 µg /ml of oligonucleotides. The ratio of the readings at 260 nm and 280 nm (OD_{260}/ OD_{280}) provides an estimate of the purity of the nucleic acid. Pure preparations of DNA and RNA have OD_{260}/OD_{280} values of 1.8 and 2.0, respectively. Any contamination with proteins or phenol would yield values less than mentioned above.

2.2.1.5 Cloning techniques

2.2.1.5.1 Polymerase Chain Reaction (PCR)

PCR is a rapid and versatile *in vitro* method for amplifying defined target DNA fragments by DNA polymerase which occurs naturally in living organisms, where it duplicates DNA when cells divide. It is used to amplify a short, well-defined part of a DNA strand. *Taq* polymerase is widely used but the disadvantage is that it lacks 3'→5' proof reading exonuclease activity, leading to mutations in the sequence. But polymerases such as *Pwo* and *Pfu* have proof reading mechanism, so, combinations of *Taq* and *Pfu* provide high fidelity and accurate amplification of DNA.

For example

95 °C	40 sec	(Denaturation)
50 °C	40 sec	(Anealing) (Temp. based on Tm of the primers)
72 °C	1 min	(Extension) (Time depends on the size of the fragment. *Taq* polymerase amplifies 1 kb in 1 min)

30 Cycles

PCR Mix

10X Taq buffer (100 mM Tris/HCl pH 9.0; 500 mM KCl)	10 µl
2.5 mM dNTPs (Amersham, Stock 100 mM)	10 µl
25 mM $MgCl_2$	5 µl
5'-primer (Stock 100 pmol/µl)	2 µl
3'-primer (Stock 100 pmol/µl)	2 µl
Template DNA	1 µl
Taq polymerase + 1/10 *Pfu*-Polymerase	1 µl

Final volume made upto 100 µl with HPLC water

2.2.1.5.2 *In vitro* mutagenesis by PCR

In vitro mutagenesis results in alteration of a specific amino acid or small component of the gene product in a predetermined way. Also, it is used to introduce restriction sites into

cloned DNA of interest. Both primers are phosphorylated by T4-PNK to facilitate ligation.

Phosphorylation of the Primer:

1 µl Primer 1
1 µl 10x T4-Polynucleotide Kinase buffer
1 µl 10 mM ATP
6 µl HPLC-H_2O
1 µl T4-Polynukleotide-Kinase (10 U/µl)

Incubate for 30 min, at 37°C.

PCR

1 µl diluted Plasmid (1:10 to 1:50)
5 µl 10x *Pfu*-buffer
5 µl dNTPs
1.5 µl phosphorylated Primer 1 (3 µl for *PfuTurbo*®-Polymerase)
1.5 µl phosphorylated Primer 2 (3 µl for *PfuTurbo*®-Polymerase)
35 µl HPLC-H_2O (32 µl for *PfuTurbo*®-Polymerase)

Denaturation for 4 min at 95°C

Add 1 µl *Pfu*-Polymerase

For example:

1 min at 95°C
1 min at 52°C (Temperature based on T_m of the Primers)
10 min at 72°C (*Pfu* amplifies 1 kb in 2 min)
10 cycles (maximum 12)

The PCR product was treated with *DpnI*. The *DpnI* endonuclease is specific for methylated and hemimethylated DNA and is used to digest the parental DNA template and to select the synthesized mutation containing DNA.

*Dpn*I-digestion

PCR product + 1 µl *Dpn*I (20 U/µl)

- Incubated for 1 h in 37°Cwater bath.
- Inactivated the enzyme by incubating for 30 min at 80°C.

2 µl was checked by an analytical agarose gel.

Ligation

12.5 µl *Dpn*I-digested PCR product

1.5 µl 10x T4-DNA-Ligase-buffer

1.0 µl T4-DNA-Ligase (400 U/µl)

-Incubate for overnight at 16°C in a waterbath.

The ligation mix was then transformed to *E. coli.*

2.2.1.5.3 Phenol Extraction and Ethanol precipitation

To 100 µl of PCR product, 10 µl of Sodium Acetate, pH 5.2 and 30 µl of Phenol-Chloroform-Isoamylalcohol (25:24:1) was added and vortexed. It was centrifuged for 2 min at 13000 rpm. The aqueous phase was taken carefully and 2.5 volumes of 100% ethanol were added. This was incubated for 20 min, at -70 °C or 10 min on dry ice or overnight at -20 °C. DNA was pelleted at 13000 rpm for 10 min. The pellet was washed with 70% ethanol. The DNA pellet was dried at 37°C and was resuspended in 50 µl TE/RNase.

2.2.1.5.4 Restriction endonuclease (RE) digestion of DNA

Restriction enzymes cut DNA at internal phosphodiester bonds. Different types of RE exist and the most useful one is Type II restriction enzymes which cleaves at specific sequences. The activity of restriction enzyme is measured in Units (U). One unit of restriction enzyme is the amount of enzyme required to completely digest 1 µg substrate DNA in 1 h.

For Analytical digestion

6,8 µl ddH_2O

1,0 µl 10x Enzyme buffer

1,0 µl 10x BSA (1 mg/ml) [on requirement]

0,1 µl Restriction enzyme A

0,1 µl Restriction enzyme B

- Incubated at 37°C for one hour and 6 µl of 1x DNA dye was added and 6 µl was checked on agarose gel.

For Preparative digestion:

41 µl ddH_2O

5 µl Plasmid-DNA (or 25 µl PCR product)

6 µl 10x Enzyme buffer

6 µl 10x BSA (1 mg/ml)

1 µl Restriction enzyme A

1 µl Restriction enzyme B

- Incubated for 2-3 h at 37°C or overnight for PCR product and the enzyme was inactivated by incubating at 80°C for 20 min and loaded on a preparative agarose gel. Using QiaexII-DNA-Extraction kit, DNA was purified and ligation was set up.

2.2.1.5.5 Agarose gel electrophoresis of DNA

Agarose gel electrophoresis is used to clean and separate specific DNA fragments. The agarose used for analysis is inversely proportional to the size of the DNA of interest, and can be used to differentiate the circular and linear DNA also. Thus the size and purity of DNA is analyzed.

Agarose concentration (%)	Resolved DNA size (kb)
0.7	12 - 0.8
1.0	10 - 0.5
1.2	6 – 0.4
1.5	3 – 0.2
2.0	2 – 0.05

6x DNA loading buffer

0.15% (w/v) Bromophenol blue (seen at 400 bp in the gel)

0.15% (w/v) Xylenecyanol FF (seen at 4 kb in the gel)

40% Sucrose in 1x TAE

Ethidiumbromide bath

Added around 20 µl Ethidiumbromide in 200ml of 1x TAE.

The required amount of Agarose was weighed, dissolved in 1x TAE by boiling and poured into the agarose gel cassette and allowed to solidify completely. The gel was immersed in 1x TAE, then the DNA marker and the sample DNA was mixed with gel loading buffer and loaded into the lanes. The gel electrophoresis was carried out at 70 V for preparative gel and at 95 V for analytical gel. When the dye reaches the front, the gel was removed from the tank and incubated in the Ethidium bromide bath for 5-10 min. Ethidium bromide is a fluorescent dye which contains a planar group that intercalates between the stacked bases of the DNA. Three kinds of transilluminators are used to detect DNA fragments, viz., 254 nm, 302 nm and 365 nm. The 302 nm transilluminator is recommended for easy detection of small amounts of DNA without inducing damage, thus allowing further cloning of the purified fragments. The gel was photographed using a gel documentation system.

2.2.1.5.6 Ligation

Joining linear DNA fragments together by a phosphodiester bond between the 3' hydroxyl of one nucleotide and the 5' phosphate of another is called ligation. T4 DNA ligase is used for this purpose which ligates the cohesive ends of the fragments. There are two types of ligation viz., cohesive end or sticky end ligation and blunt end ligation, depending on the restriction digestion of the DNA. For the blunt end ligation and also if digestion was with single sticky end enzyme, the vector should be dephosphorylated by alkaline phosphatase, and the ligation mix should be incubated for overnight.

For example

x µl linearised vector DNA

y µl Insert DNA [1(vector DNA):10 (insert DNA)]

1,5 µl 10x Ligase buffer

1,0 µl T4-DNA-Ligase (400 U/µl)

Made upto 15 µl with ddH_2O, incubated overnight at 16°C and transformed into E.coli competent cells.

2.2.1.6 Sequencing of the clone

DNA sequencing was done by Sanger's method using a DNA sequencer. The plasmid DNA to be sequenced was supplied with a mixture of all four nucleotides plus four ddNTPs, each labeled with a tag that fluoresces different color. For sequencing reaction, clean DNA should be used (prepared by QIAprep-Spin-Miniprep-Kit).

For example:

PCR mix

x µl Plasmid-DNA (0.2 – 0.5 µg)

3.2 µl Forward primer or reverse primer (1 pmol/µl)

2.0 µl ABI PRISM Dye Terminator Cycle Sequencing Ready Reaction Premix

x µl HPLC-H_2O (Make it upto 10 µl)

Programme

96°C --- 10 sec

50°C --- 5 sec

60°C --- 4 min

25 cycles

The PCR product for sequencing should be cleaned thoroughly to remove fluorecently labeled free ddNTPs to avoid background. To the PCR product 2 µl of 3 M Sodium aceteate (pH 5.2) and 50 µl 95 % EtOH (room temperature) was added, incubated at RT for 10 min and centrifuged for 20 min at 13000 rpm. The pellet was washed with 250 µl of 70% ethanol for 10 min at 13000 rpm, dried and resuspended in 25 µl of HPLC water and given for sequencing.

2.2.1.7 Glycerol stocks of *E. coli* and *S. cerevisiae*

The Bacteria was streaked on a LB plate and the yeast strain was streaked on a YEPD plate and incubated overnight at 37°C and 30°C respectively. A small scrape of cells were resuspended well in 7% sterile DMSO and was frozen immediately at -80°C.

2.2.2 Yeast Genetics

2.2.2.1 PLATE transformation

It is an easy method to transform plasmids into yeast cells. PLATE medium contains Lithium acetate which makes the cell wall permeable for DNA and PEG acts as a volume excluder and causes stronger proximation of DNA and yeast cells.

Yeast cells from fresh plates were scraped and resuspended in 500 µl of PLATE medium or overnight cultures were pelleted and resuspended in 500 µl of PLATE and 1-2 µl of plasmid DNA was added. The mix was incubated at 42°C for 30 min or 1-2 days at RT with slow shaking and centrifuged for 15 sec at 6500 rpm. The pellet was resuspended in 200 µl of SOS, incubated for 20-30 min at 30°C and plated on the respective SD-selection plate.

PLATE-Medium (100 ml):		Final conc.:
40 g	PEG 4000	40 %
10 ml	1 M Lithiumacetate	0.1 M
1 ml	1 M Tris/HCl, pH 7.5	10 mM
0.2 ml	0.5 M EDTA	1 mM

Autoclave the mix.

SOS-Medium (Prepared freshly):

500 µl	YEPD
500 µl	2 M Sorbitol
6.5 µl	1 M $CaCl_2$

2.2.2.2 Lithium Acetate transformation

This method is extremely efficient to transform PCR products, plasmids and libraries. The yeast cells are made competent freshly before the transformation. All materials used for this procedure should be sterilized well.

Preparation of competent yeast cells:

100 ml of overnight yeast culture was grown till OD_{600} 0.5-1.0. Cells were pelleted in a JA20 rotor for 5 min at 5000 rpm and were washed with 50 ml of sterilized water. The pellet was resuspended in 25 ml of Lisorb, incubated for 15-30 min at 30°C and pelleted

at 5000 rpm for 5 min. The competent cells were resuspended in 300 µl of Lisorb and kept on ice.

Transformation

DNA mix for library:

100 µl of Salmon Sperm (SS) DNA was boiled for 7-10 min, 400 µl of Lisorb was added and mixed by pipetting up and down. The mix was let to cool to RT and 10 µl of library DNA was added to it.

DNA mix for genomic integration:

10 µl of SS DNA was boiled and 100 µl of PCR product or 10 µl of digested plasmid was added and mixed well.

100 µl of competent yeast cells and 100 µl of DNA-mix were mixed well. 900 µl of 40% PEG3350 in LiAc/TE was added and mixed well by pipetting up and down. The transformation mix was incubated at 30°C for 30 min and shifted to 42°C for 15 min. The heat shock should not be given for more than 15 min, otherwise the cells would die. The transformation mix was pelleted down, resuspended in 300 µl of SOS medium and incubated at 30°C water bath for 30 min (except for Kanamycin selection which needs around 2-3 h of incubation). The mix was spreaded on an appropriate selection plate.

LiSorb (100 ml)		Final conc.:
18.2 g	Sorbitol	1 M
10 ml	1 M Lithiumacetate	100 mM
1 ml	1 M Tris/HCl, pH 8.0	10 mM
200 µl	0.5 M EDTA	1 mM

- Autoclave the mix

40% (w/v) PEG 3350 in LiAc/TE (50 ml)		Final conc.:
20 g	Polyethylene glycol MW 3350	40 % (w/v)
5 ml	1 M Lithiumacetate	100 mM
0.5 ml	1 M Tris/HCl, pH 8.0	10 mM
100 µl	0.5 M EDTA	1 mM

- Autoclave the mix

2.2.2.3 Plasmid isolation from *S. cerevisiae*

2 ml liquid culture of Yeast in SD medium was used for the isolation of plasmid DNA. Cells were taken in a micro centrifuge tube and centrifuged for 30 sec at 13000 rpm. Pellet was resuspended in 200 µl of Lysis buffer. Around 100 µl of glass beads and 200 µl of Phenol-Chloroform was added to remove the proteins. This was vortexed for 2 min and centrifuged for 5 min at 13000 rpm at 4 °C. The aqueous phase was carefully transferred into a new microfuge tube without taking any phenol. To this, 20 µl of 3 M Sodium acetate pH 5.2 and 550 µl of 100 % Ethanol (cold) was added and centrifuged for 10 min at 13000 rpm at 4 °C. The pellet was washed with 70 % Ehanol (cold) and centrifuged again for 1 min. Pellet was dried at 37 °C. DNA pellet was resuspended in 20 µl of TE.

Lysis Buffer

1 %	SDS
2 %	Triton X100
1 mM	EDTA pH 8.0
10 mM	Tris/HCL pH 8.0
100 mM	NaCl

2.2.2.4 Isolation of yeast genomic DNA

Yeast cells were grown in 10 ml YEPD till an OD_{600} 0.5-1.0. Cells were pelleted at 3000 rpm for 3 min in a 15 ml falcon tube and washed with 5 ml of 1M Sorbitol, 0.1 M EDTA pH7.5. Pellet was resuspended in 400µl of 1M Sorbitol, 0.1 M EDTA pH7.5 with 100 µl of freshly prepared Zymolyase from 2 mg/ml stock and incubated for 30-40 min at 37 °C. Spheroplasts were pelleted at 6500 rpm for 30 sec and resuspended in 500 µl TE. 90 µl of freshly prepared Lysis buffer was added and incubated at 65 °C for 30 min. 80 µl of 5 M Potassium acetate pH 5.0 was directly added to the lysis mix, incubated for 2 h on ice and centrifuged for 15 min at 13000 rpm at 4 °C. Supernatant was collected into a new eppendorf tube and 1 ml of 100 % ethanol (room temperature) was added. It was centrifuged for 1 min at high rpm and the pellet was washed with 70 % ethanol. The pellet was dried, resuspended in 300 µl of TE and phenol extraction was done three times with 200 µl of Phenol-Chloroform-Isoamylalcohol (25:24:1). To the clear aqueous phase,

30 µl 3 M Sodium acetate pH 5.2 and 750 µl of 100 % ethanol was added, centrifuged for 10 min at 13000 rpm. The pellet was dried and resuspended in 100 µl TE.

Lysis Buffer

2 %	SDS
0.1 M	Tris/HCL pH 8.0
10 mM	EDTA pH 8.0

2.2.2.5 Yeast deletion mutants

Genetic manipulations are very easy in yeast which makes it one of the best tools for research. The very high efficiency of homologous recombination in yeast is used to make the gene deletions and to introduce specific mutations. There are different methods to disrupt a yeast gene. The most commonly used methods are PCR based one-step gene disruption and two step gene replacement or allele replacement.

One step gene disruption:

This method is useful for gene deletions and to insert PCR products. PCR primers were designed such that they consist of around 40 nucleotides as a complementary sequence to the 5'- or 3' flanking region of the gene of interest, followed by approximately 20 nucleotides complementary to the selectable marker. Using these primers, a gene disruption cassette was amplified from a vector that consisted of a selectable marker (URA3, HIS3, LYS2, LEU2, TRP1 and MET15) flanked by sequences derived from the 5' and 3' ends of the target gene to be detected. The PCR mix was transformed into yeast cells and initial screening was done using the selection marker. Genomic DNA was isolated from the probable clones and again PCR was done to confirm the gene disruption.

Two step gene disruption:

By this method all kind of mutations can be inserted into the chromosome at any location. The desired mutations with flanking sequences are cloned into a conventional plasmid that also contains a marker that can be selected both for and against URA3. Then the plasmid was digested with a restriction enzyme that cuts once within the yeast sequences flanking the mutation and is introduced into yeast by transformation. The DNA break

stimulates recombination within the flanking sequences, leading to integration of all the vector sequences and the mutated yeast sequences into the chromosome of the yeast cell. The successfully transformed cells are selected by growth in medium lacking the uracil. Some of the cells are then subjected to medium containing Uracil and 5'-fluororatic acid (FOA). The 5-FOA is only toxic to cells expressing the *URA3* gene. The 5-FOA resistant colonies are the possible positive clones and further screening was done by looking for the desired mutant phenotype.

2.2.2.6 Mating and Sporulation

In heterothallic yeast strains, sex is determined by the alleles of mating-type present in a given cell. The mating-type ***a*** cells mate with the cells of mating-type ***α*** and vice versa. Cells containing both mating-types, ***aα*** diploids, do not mate but they are able to undergo meiosis and sporulation. Yeast can exist stably in either haploid or diploid states. A diploid cell grows indefinitely, but under starving conditions, it undergoes meiosis forming 4 haploid spores enclosed in a structure called ascus.

Mating of MAT**α** or MAT**a**

MAT**α** and MAT**a** were streaked heavily on a YEPD plate, like a cross. The plate was incubated at 30°C for 14-16 h. Then the possible diploid cells were checked on an appropriate selection plate. If there was no selection marker, the mating was allowed only up to 4-6 h on a YEPD plate, the zygotes were picked up using a micro manipulator and spotted on a YEPD plate to grow further. The mating types of the zygotes were checked and the diploids were selected.

Sporulation

When the diploid cells are exposed to nitrogen starvation conditions, they undergo meiosis. The four meiotic products from a diploid cell are contained together as four spores in an ascus sac, commonly called as a tetrad. Using a micro manipulator, the four spores were separated and grown as haploid cells separately. Then the mating-type of each spore was tested.

Procedure

The diploid strain was streaked freshly on a SD-minimal plate and was grown overnight at 30°C. Then, a heavy streak was made on a sporulation plate and incubated at 30°C for 3-5 days. The tetrads were analyzed and dissected using a micromanipulator.

2.2.2.7 Tetrad dissection

From the sporulation plate, cells were scraped and resuspended in 50 µl of 1M sorbitol with 2.5 µl of 10 mg/ml zymolyase. Cells were incubated for 7 min at 30°C in a water bath when the thick cell wall surrounding the ascus was digested. 25 µl was taken out for further incubation at 30°C for 7 min and 200 µl of 1 M sorbitol was added to the rest and kept on ice. After the incubation, 200 µl of 1M sorbitol was added to it and kept on ice. From each solution, 10 µl was taken on a YEPD plate as a line in the middle. Under an optical microscope, the four spores of an ascus were isolated using a fine needle of a micro manipulator and spotted individually in a line on the YEPD plate. The plate was incubated at 30°C or at 24°C for ts-mutants, until the spores grew up to a big colony. The spores were analyzed for deletions, on the selection plates for auxotrophic genes and the mating-type was tested. For the identification of ts-mutants, the growth was examined at different temperatures.

Halo test to identify the mating type

The strains to be tested and the control a (SEY6210) and α (SEY6211) strains were patched on a YEPD plate with at least 2 cm distance between each patch and grown overnight at 30°C. The tester strains [RC828(a) and/or sst(α)] were grown overnight in YEPD liquid medium till an OD_{600} 0.1-0.5 and were diluted to 0.01 OD/ml. 1.5% sterile agar was dissolved in water by microwave and let to cool till 55°C. 1.5 ml of agar and 1.5 ml of diluted tester strains were mixed well and poured on a YEPD plate. After 20 min, the strains to be tested were replica plated onto the agar poured plate and incubated at 30°C for 1-2 days to get a lawn like growth of the tester strains. The growth would be inhibited by the opposing mating type which resulted in a clear halo around the patch whereas the growth was not inhibited by the same mating type.

2.2.2.8 Growth test and growth curve

The growth patterns of wild type and mutants are compared by growth test. The yeast strains were inoculated in 8 ml of YEPD or SD-medium and grown overnight at 24°C till OD_{600} 0.2-1.0. The plates were pre-warmed at respective temperatures. For each strain, two dilutions were prepared in sterile water viz., 0.01 OD/ml and 0.05 OD/ml. 10 µl from each dilution is spotted onto the pre-warmed plates using a pattern. The spots were allowed to dry and the plates were incubated at the corresponding temperatures (usually 24°C, 30°C, 33°C and 37°C). The growth was scored after 24 h.

For growth curves, the log phase yeast cultures were diluted to 0.1 OD/ml in 5 ml medium and allowed to grow at desired temperatures. Every two hours, the OD_{600} was measured at least for 10 h and the growth curve was drawn.

2.2.2.9 APNE test for *PEP4* deficient mutants

This test is very fast and easy way to identify the *PEP4*, which codes for vacuolar Proteinase A, deletion strains. The strains to be tested, the *PEP4*-positive (wildtype) strain and the *PEP4*-deficient strains were streaked on a YEPD or SD plate and incubated overnight at 30°C. Next day, APNE mix was prepared as follows:

For 25 ml APNE-Mix

0.175 g	Agar
17.5 ml	ddH_2O
5.0 ml	1 M Tris-HCl, pH 7.4

Were taken in a 50 ml flask and boiled in the microwave and cooled down to 55°C. 20 mg of Fast Garnet GBC salt and 2.5 ml freshly prepared APNE solution (2 mg/ml in DMF) were added to the flask, mixed well and poured onto the overnight grown YEPD plate. After few minutes, strains would develop colors. The *PEP4*-deficient strain would be white in color whereas the *PEP4*-positive strain (wild type) would be red in color. Further confirmation of *PEP4*-deficient strain was done by checking the protein extract for the maturation of CPY by western blotting using anti-CPY antibodies. Since Proteinase A is needed for the processing of the p2CPY into mature CPY, only in the *PEP4*-deficient strains p2CPY would be present whereas in the *PEP4*- positive strain, only mCPY would be found.

2.2.2.10 Zymolyase sensitivity test

Zymolyase is an β-1, 3-Glucanse enzyme which hydrolyses the glucose residues from the cell wall of yeast cells by cleaving the β-1, 3-glucosidic linkages. If there are any changes in the composition of the cell wall, the sensitivity towards zymolyase would be altered. So, this test is used to screen cell wall defective mutants.

Yeast cells were grown in YEPD medium at 24°C and 2 OD of cells were pelleted in a 15 ml falcon tube at 3000rpm for 3 min and washed once with 4 ml of 10 mM Tris pH7.4. The pellet was resuspended in 5 ml of 10 mM Tris pH7.4. Zymolyase-20T (Seikagaku, Tokyo, Japan) was added to the cells to the final concentration of 5 µg/ml and incubated at 37°C with slow shaking. Every one hour the OD was measured for up to 3 h and graph was drawn by setting the initial OD to 100%.

2.2.3 Biochemical methods

2.2.3.1 Preparation of protein extract from yeast cells

10 ml of yeast culture was grown overnight till an OD_{600} of maximum 1.0 and 1-10 OD of cells were pelleted at 3000 rpm for 3 min. The pellet was washed with 1ml of water in an eppendorf at 6500 rpm for 30 sec. The supernatant was discarded and 50 µl of glass beads were added to the pellet. For 1 OD of cells, 40 µl of Thorner buffer was taken. The required volume of Thorner buffer + 5% β-Mercaptoethanol was heated at 70°C for 5 min. 1x Protease inhibitors was added to the Thorner buffer and the appropriate volume of buffer was added to the pellet. It was vortexed well, incubated at 70°C for 10 min and kept in the automatic vortexer for 2 min. Then the extract was collected at 13000 rpm for 5 min at 4°C. 10 µl of the protein extract + 10 µl of 2x stop buffer was boiled at 95°C for 5 min and 15 µl was loaded onto the SDS-gel.

Thorner-buffer

8 M	Urea
5 %	SDS
50 mM	Tris-HCl, pH 6.8

2.2.3.2 Determination of protein concentration

Protein estimation was done using Coomassie-G-250 coloring agent (Bradford reagent), which after binding to protein absorbs light at 595 nm. The absorption is directly proportional to the amount of protein bound to the coloring agent. A standard curve was made using BSA in the range of 5-20 µg. 2 µl or 5 µl of the sample was used for the protein estimation. The volume was made up to 200 µl with water. One part of Bradford reagent and three parts of water was mixed, 800 µl was added to the samples and were incubated for 20 min at room temperature. The optical density was measured at 595 nm in the Spectrophotometer.

Bovine Serum Albumin (BSA) stock solution 1 mg/ml

2.2.3.3 SDS gel electrophoresis

Proteins can be separated on the basis of mass by electrophoresis in a polyacrylamide gel under denaturing conditions. To the protein samples, sodium dodecyl sulphate was added to disrupt the noncovalent interactions and β-mercaptoethanol was added to reduce the disulfide bonds. Now, the SDS-protein complex has a net negative charge and moves under electric field. Thus, proteins are separated on the basis of mass from 200 kDa to 10 kDa by adjusting the pore size of the SDS gel.

Acrylamide concnetration	Molecular weight
8 %	200 – 40 kDa
11 %	100 – 20 kDa
12.5 %	40 – 10 kDa

SDS gel comprises of a stacking gel which is present on top of the resolving gel. Two clean glass plates (for small gel: 16 x 16 cm; big gel: 18 x 17.5) were fixed together with a spacer of 1 mm, using clips. 1 % agarose was used to seal the sides. The required percentage of resolving gel was prepared and poured in between the glass plates. On top of resolving gel, a small amount of water was added immediately. The gel was allowed to polymerize for about 30 min. The stacking gel was poured on top of the resolving gel and a comb with 16 wells was placed in the stacking gel and left undisturbed for about 15 min. After polymerization of the stacking gel, the combs were removed and the wells were cleaned with double distilled water to wash off any unpolymerized acrylamide. The

glass plates were fixed onto an electrophoretic apparatus with 1x Running buffer. The samples were denatured at 95°C for 5 min and loaded into the wells and 5 µl of molecular weight marker was also loaded. The small gel was run at 200 mA for 1 h and the big gel was run at 30 mA for 2 h.

Then the gels were stained with Coomasie-blue or with Ponseau-S stain or transferred to a nitrocellulose membrane by western blotting. For Pulse-chase immunoprecipitaion (radio-active) samples, the bigger gel was run at 15 mA for 5-6 h, dried and exposed to a phosphor imager screen for further analysis.

3x stop buffer (45 ml)

1 Spatula	Bromo phenol blue
15 g	Sucrose
4.5 g	SDS
18.8 ml	1 M Tris-HCl, pH 6.8
26.2 ml	ddH_2O

900 µl 3x stop buffer and 100 µl β-Mercaptoethanol was mixed before use.

10x Running buffer

10 g/L	SDS
30.2 g/L	Tris
144 g/L	Glycin

Acrylamide solution

30 % (w/v) Acrylamide

0.8 % (w/v) Bisacrylamide

Ammonium persulphate (APS)

10 % (w/v) Ammonium persulphate in ddH_2O

Resolving gel (15 ml)			
Acrylamide concentration	8 %	11 %	12.5 %
1.5 M Tris-HCl, pH 8.8	3.75 ml		
Acrylamide solution	4.0 ml	5.5 ml	6.25 ml
ddH_2O	6.9 ml	5.45 ml	4.65 ml
10 % (w/v) SDS	150 µl		
10 % (w/v) APS	150 µl		
TEMED	7.5 µl		

Stacking gel (7.5 ml)	
Acrylamide concentration	5.6 %
1 M Tris-HCl, pH 6.8	936 µl
Acrylamide solution	1.39 ml
ddH_2O	4.95 ml
10 % (w/v) SDS	75 µl
10 % (w/v) APS	150 µl
TEMED	7.5 µl

2.2.3.4 Coomassie blue staining

This is the most commonly used staining procedure for the detection of proteins for a range of 0.5 to 20 µg of protein and is both qualitative and quantitative. The SDS gel was incubated in Coomassie blue solution at RT for 1-2 hours with slow shaking to spread the dye evenly and the gel was destained for few hours with several changes of destaining solution until the background is clear. The gel was placed in double distilled water for few minutes and then dried in a gel drier.

Coomassie-blue stain

0.1 % (w/v) Serva blue R (Coomassie brilliant blue R-250)
25 % (v/v) Isopropanol
10 % (v/v) Acetic acid
65 % (v/v) ddH_2O

Destain

50 % (v/v) Methanol
10 % (v/v) Acetic acid
40 % (v/v) ddH_2O

2.2.3.5 Western blot analysis

For further immunological analysis, the proteins separated by SDS-PAGE were transferred onto a nitrocellulose membrane, by "semi dry" western blot procedure. The nitrocellulose membrane (0,2 µm) and 6 pieces of filter paper (Whatman, 3 mm) were cut

into shape according to the gel size and soaked in the Semi Dry blot buffer. The transfer was set as follows without any bubbles in a special blotting apparatus,

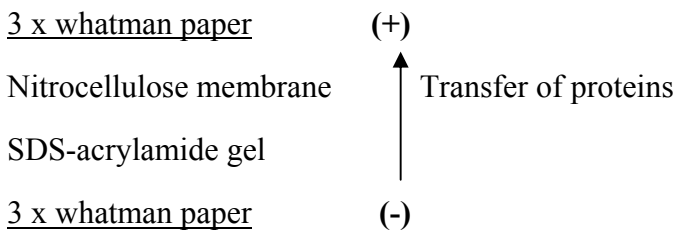

The transfer took place for 1 h with constant amperage from 1.0 mA/cm2. After the transfer, the membrane was stained with Ponceau-S (0,2 % in 3 % TCA, Serva) for 5 - 10 min to detect the proteins, the membrane was now cut into shape, washed with water for complete decolorization and stored up or continued with immunodetection.

On nitrocellulose membrane, the immobilized proteins (antigens) can be detected with very high sensitivity by specific primary anti-bodies and the corresponding secondary anti-bodies. By the enzyme Horse Radish Peroxidase (HRP), coupled to the secondary anti-body, the protein can be detected by "Enhanced Chemiluminescence" (ECL system, Amersham). Under alkaline conditions peroxidase catalyzes the oxidation of Luminol by H_2O_2, when Luminol emits the light. This reaction is strengthened by phenol derivatives such as p-coumaric acid. The chemiluminescent half-life of the reaction lasts to approximately 1h.

After the transfer, membrane was blocked with 2% Milk powder (Blotto) in PBS-T for 30 min at room temperature to block all non-specific interaction sites on the membrane. The primary antibody (polyclonal from rabbits and/or monoclonal from mouse) was diluted in Blotto at required concentration, was packed in a plastic foil with the membrane and incubated for 1-2 h at room temperature, on a rocker. If the signal is weak, the incubation was done in the cold room for overnight. The membrane was washed at least 3 x, each 5 min with PBS-T, the incubation with the secondary anti-body diluted in PBS-T (goat anti-rabbit HRP and/or goat anti- mouse HRP) was followed for 1 h. The membrane was washed for 5 x, each wash lasting for 5 min with PBS-T and washed finally with 1x PBS. Then, the membrane was treated with a 1:1 mix of the two ECL solutions for approx. 2 min. For detection and quantification, a CCD camera of the company Fuji with the soft wares AIDA image reader and AIDA image Analyzer was used.

Semi-Dry-Blot buffer

5.80 g/L	Tris
2.92 g/L	Glycin
3.7 ml/L	10 % (w/v) SDS
	Made upto 1 litre with ddH_2O
pH	9.2 (adjusted with NaOH)
200 ml/L	Methanol (added freshly)

PBS-T

0.1 % (w/v) Tween-20® in PBS

Blotto

2 % (w/v) Milk powder in PBS-T

ECL-solution:

SuperSignal® West Pico Chemiluminescent Substrate (PIERCE) package containing, Stable-Peroxide-solution and Luminol/Enhancer-solution was used.

2.2.3.6 Kar2p/BiP secretion test (TCA precipitation)

Kar2p/BiP is one of the molecular chaperones present in ER lumen to translocate proteins into ER and recycles between cis Golgi and ER. If there is any defect in the retrograde transport from the cis Golgi to ER, BiP would be secreted into the medium. This method was used in order to determine whether the *use1* mutants secrete Kar2p/BiP into the medium. The yeast strains were grown in 20 ml of YEPD medium or in the appropriate selection medium up to a density of OD_{600} of 0.3 to 0.5 OD/ml, 15 ml was pelleted down for 5 min at 3000 rpm and resuspended in 15 ml of medium. Afterwards the cultures were incubated for 2 h at the appropriate temperature. The density of the cultures was again determined and the cells were centrifuged at 3000 rpm for 5 min. The pellet was processed as described in 2.2.3.1 and the supernatant (medium) was transferred into Corex® tubes cooled on ice and 1/10 volume 100 % (w/v) of TCA (Final conc.: 10 %) was added, well mixed and incubated on ice for 10 min to precipitate the proteins secreted into the medium. The corex tubes were centrifuged for 15 min at 10000 rpm at 4°C in the JA20-Rotor. The pellet was loosened with 1 ml of -20°C cold acetone and transferred to an eppendorf tube. The tubes were sonicated for 20 seconds and centrifuged for 5 min at 13000 rpm at 4°C. The pellet was washed again with 1 ml of -20°C cold acetone and

dried. Subsequently, the pellet was resuspended in 8.3 µl 2x sample buffer per 1 OD of cells and was neutralized with 5 µl of 1 M Tris, pH 9.5 per 100 µl sample buffer. The pellet was resuspended completely by 20 seconds sonication.

A 1:2 dilution was made from the protein extracts of the cell pellets with 2x stop buffer. The protein extracts from pellet and the supernatant was boiled at 95°C for 5 min and 30 µl was loaded on 8% SDS PAGE and analyzed by Immunoblot with anti-Kar2p-antibody.

2.2.3.7 Cross linking of antisera to Protein A/G Sepharose beads

In an eppendorf tube, 100 µl bed volumes of protein A/G Sepharose beads were washed for 3 x with 1 ml KPi buffer (5 min on the turning wheel, thereafter 15 seconds of centrifugation at 4000 rpm). The protein A/G Sepharose pellets were resuspended into 100 µl KPi buffer.

50 µl washed protein A Sepharose beads + 25 µl Antibody + 200 µl KPi

50 µl washed protein A Sepharose beads + 25 µl preimmune serum + 200 µl KPi

The binding of the anti-body to the protein A Sepharose took place for 1 h at room temperature on the turning wheel. The Beads were washed 2 x each for 3 min incubation with 0.5 ml 0.1 M Sodium borate buffer pH 7.5. For cross linking, 300 µl of freshly prepared 0.1 M Sodium borate buffer with Dimethyl pimelinediimidate dihydrochloride (DMP) to a final concentration of 4.5 mg/ml was added to the tubes and incubated at room temperature for 30 min in the wheel. The beads were centrifuged for 20 seconds at 3000 rpm. After washing with 1 ml of 1M Tris HCl, pH 7.5 the Beads were incubated in the same for 2 h at 4°C on the turning wheel. The Beads were resuspended in 100 µl PBS, and sodium azide was added to a final concentration of 10 mM and stored at 4°C.

2.2.3.8 Native Immunoprecipitation

The yeast strain was grown in 40 ml YEPD medium, overnight at 24°C up to an OD_{600} of 0.5 to 1.0. Now 20 OD of cells were harvested by 5 min centrifugation at 3000 rpm, the pellet was resuspended in 2 ml TEβ and incubated for 10 min under slow shaking at 24°C. The cells were centrifuged thereafter for 3 min at 3000 rpm. The pellet was resuspended in 2 ml Sphereoplast buffer with 60 µl 10 mg/ml Zymolyase (Final conc. 300 µg/ml) and sphereoplasted for 1 h at 24°C under slow shaking. The sphereoplasts were washed with 1 ml YEPD/Sorbitol, for 2 times (centrifuged for 30 seconds at 6500 rpm).

If the mutants are temperature sensitive, then the cells were divided into 10 ml each into two falcon tubes. One tube was incubated at 24°C or permissive temperature and another at 37°C or restrictive temperature for 1 h under slow shaking. The cells were centrifuged for 2 min at 2000 rpm. The pellets were resuspended in 1 ml cold Lysis buffer + Proteaseinhibitors and were homogenized in each case 20 times in the ice-cold Potter ("loose"). The homogenized cells were incubated at 4°C for 15 min on the turning wheel. A centrifugation for 20 min at 50000 rpm at 4°C was done and the supernatant was collected. 40 µl of the supernantant was saved for the gel (Homogenate fraction), each 450 µl of the supernatant was transferred into two new eppendorf tubes:

A) 450 µl Homogenate + 48 µl antibody-Beads (see chapter 2.2.3.7)

B) 450 µl Homogenate + 48 µl Preimmune-Beads (see chapter 2.2.3.7)

Overnight incubation was done at 4°C on the turning wheel. On the next day they were centrifuged for 20 seconds at 6500 rpm. The Unbound fraction was saved for the gel. The Beads were washed, 3 x each for 5 min at 4°C with 1 ml Lysis buffer and resuspended afterwards in 50 µl 1x sample buffer without β-Mercaptoethanol.

For the Gel: 25 µl was taken from the Homogenate and the Unbound fractions, with 12.5 µl 3x sample buffers and the bead fractions were boiled at 95 °C for 5 min. On an 11 % gel, 30 µl from each sample was loaded followed by western analysis.

YEPD/Sorbitol

10 g/L	Yeast extract
20 g/L	Bacto-Peptone
182.2 g/L	Sorbitol (final conc.: 1 M)

after autoclaving, added

40 ml/L	50 % Glucose (final conc.:2 % (w/v))

Lysis-buffer (50 ml):		final conc.:
1 ml	1 M HEPES-KOH, pH 7.0	20 mM
5 ml	1 M KCl	100 mM
0.2 ml	0.5 M EDTA	2 mM
1 ml	25 % Triton X-100	0.5 % (w/v)

2.2.3.9 "Pulse-Chase" Immunoprecipitaion

Pulse-chase experiment is used to study the fate of a protein inside a cell. To analyze the transport and the specific processing, the yeast cells were grown in Methionine and Cysteine free medium, then marked with radioactive [^{35}S]-Methionine and [^{35}S]-Cysteine ("Pulse"). Non radioactive Methionine and Cysteine was added to the cells to stop the pulse and the samples were taken at different time points ("Chase"). Finally, immunoprecipitation was done to analyze the fate of the protein. In this study, the pulse chase immunoprecipitations were done for Carboxypeptidase Y (CPY), Alkaline Phosphatase (ALP), Vacuolar Sorting Protein 10 (Vps10p), A-ALP, Vti1p, Use1p and Pep12p.

CPY and ALP-IP:

The yeast cells were grown 2 days before the experiment and diluted evening before the experiment in a manner that the OD_{600} would be 0.1-1.1 in the next morning. 0.5 OD of cells were taken in 13 ml tubes and pelleted down at 3000 rpm for 3 min. The cells were resuspended in 500 µl SD-Met + 50 mM KPO4 pH 5.7 + 2 mg/ml BSA and incubated at 24°C for 15 min.

Pulse-Chase labeling:

For ts-experiment, cells were again preinucbated at 37°C or at desired temperature for 15 min. 10 µl (for CPY) or 15 µl (for ALP) of radioactive L-[^{35}S]-label ([^{35}S]-Methionine and [^{35}S]-Cystein, 14 µCi/µl) was added to the cells and pulsed for 10 min. 50 µl of cold Met + Cys (equal volumes of 10 mg/ml stocks were mixed) was added and chased for 30 min. 5 µl Na-Azide was added to stop the chase and the contents were transferred into screw cap eppendorf tubes. Cells were pelleted for 20 sec at 13,000 rpm and both the pellet and the supernatant fractions were processed for CPY-IP whereas only the pellet fraction was analyzed for ALP-IP.

Spheroplasting the yeast cells:

For spheroplasting the pellet fraction, the cells were pretreated with 1 ml of 50 mM Tris pH 9.5, 10 mM DTT and 10 mM NaAzide for 5 min at 30°C and centrifuged. To the pellet, 150 µl of Spheroplast-Mix with 250 µg/ml Zymolyase was added and incubated at 30 °C for 30 - 45 min. The spheroplasts were collected by centrifuging at 6500 rpm for 30 sec.

Lysis and Pre-absorption:

For CPY-IP:

To the cell pellet (I), 780 µl lysis mix was added which contained 100 µl 10x IP-buffer, 670 µl water and 10 µl 100x Protease inhibitors. To the Supernatant (E) with protease inhibitors, 250 µl of lysis mix (100 µl 10x IP-buffer and 150 µl water) was added. The samples were boiled at 95°C for 5 min and cooled for several min on ice. 270 µl of Pre-absorption mix (containing 50 µl washed Pansorbin and 220 µl water) was added to the cells and incubated on ice for 15 min.

For ALP-IP:

The cell pellet was resuspended in 50 µl lysis mix with 1 % SDS, 8 M Urea and 1x Protease inhibitors. The samples were boiled at 95°C for 5 min and cooled for several min at room temperature. 1ml of Pre-absorption mix (containing 100 µl 10x IP-buffer without SDS, 50 µl washed Pansorbin, 10 µl Protease inhibitors and 850 µl water) was added to the cells and incubated on ice for 15 min.

Immunoprecipitation:

The pre-absorbed cells were pelleted at 13000 rpm for 5 min. 5 µl of the supernatant was taken for counting at liquid scintillation counter and the rest was transferred to the new eppendorf tubes with 1 µl of anti-CPY or with 2 µl of anti-ALP antiserum. The cells were incubated on ice for 1h 30 min with frequent mixing. After the incubation, 50 µl Pansorbin was added to the cells and again incubated on ice for 1 h 30 min with frequent mixing. The eppendorf tubes were centrifuged at 12000 rpm for 30 sec and the pellet was washed three times with 1 ml ALP + CPY wash buffer. Finally the pellet was resuspended in 40 µl of 2x Stop buffer and frozen at -20°C.

A-ALP and Pep12p-IP

The pulse chase immunoprecipitaion of A-ALP and Pep12p was done as mentioned for CPY and ALP-IP, except that 1.6 OD of cells were taken in 3.1 ml of SD-met and labeled with 35 µl of radioactive L-[^{35}S]-label and pulsed for 25 min. 150 µl of cold Met + Cys was added and chased for 5 min, 60 min and 120 min for A-ALP and 10 min, 3 hr and 5 hr for Pep12p. For each chase point, 1 ml of cells was taken out and 10 µl of Na-Azide was added and kept on ice. The immunoprecipitation was continued as mentioned for ALP-IP and 2 µl of anti-ALP antibody was used for A-ALP-IP and 2 µl of anti-Pep12p antibody was used for Pep12p IP.

Vps10p-IP:

Vps10p IP was done as mentioned in CPY and ALP-IP with few modifications. 0.825 OD cells were taken in 3 ml of SD-met, labeled with 35 µl of radioactive L-[^{35}S]-label and pulsed for 25 min. 150 µl of cold Met + Cys was added and chased for 10 min, 3 hr and 5 hr. For cell lysis, the pellet was resuspended in 100 µl of Vps10p lysis mix (Containing 1% SDS, 50mM Tris-HCL pH7.4, 2 mM $MgCl_2$ and 3 µl/ml β-Mercaptoethanol), continued as in ALP-IP and 2.5 µl of anti-Pep1 (Vps10) antibody was used for IP.

Vti1p and Use1p-IP:

This IP was done exactly like Pep12p-IP**,** except that the cells were lysed with 50 µl of 0.5% SDS with 1X Protease inhibitors and heated at 65°C for 5 min. 2 µl of anti-Vti1p antiserum was used for Vti1p-IP and 4 µl anti-Use1p antiserum was used for Use1p-IP.

Spheroplast-Mix:

1.2 M	Sorbitol
50 mM	KPO_4, pH 7.3
10 mM	Sodiuim Azide

10x IP-buffer:

0.9 M	Tris-HCl, pH 8.0
1 %	SDS
1 %	Triton X-100
20 mM	EDTA

10x IP-buffer (without SDS):

0.9 M	Tris-HCl, pH 8.0
1 %	Triton X-100
20 mM	EDTA

CPY+ALP-Wash buffer:

10 mM	Tris, pH 8.0
0.1 %	SDS
0.1 %	Triton X-100
2 mM	EDTA

Washig of Pansorbin:

Pansorbin cells were washed 3 x with 20 mM Tris, pH 7.5 + 100 mM NaCl (centrifugation for 30 sec at 11000 rpm) and made up to the start volume with 20 mM Tris, pH 7.5 + 100 mM NaCl.

For the SDS-gel:

The samples were boiled at 95°C for 5 min, 20 µl was loaded onto 8 % SDS gel for CPY, ALP, A-ALP and Vps10p-IP and 11% SDS gel was used for Pep12p, Vti1p and Use1p. The gel was run at 15 mA for 5-6 hr, destained for 30 min, washed with water and dried for 2 hr. Then the gel was exposed to a phosphor-imager screen, scanned and analyzed by BAS1000 (Fuji).

2.2.3.10 Purification of Ent3p-Strep tag fusion protein

10 ml of pKW5 (Strep-tag Ent3p-ENTH) culture was grown overnight in 2xYT-Amp medium. The next day, the 10 ml culture was added to 250 ml of fresh 2xYT-Amp, grown at 30°C for 1 h 30 min till an OD_{600} of 0.5. The cells were induced with 12.5 µl of AHT (2 mg/ml anhydrotetracycline) for 4 h at 30°C. The cells were pelleted at 10000 rpm for 10 min at 4°C in JA20 rotor. The pellet was resuspended in 4 ml of buffer W and was frozen in -20°C. The next day, the pellet was thawed and 40 µl of protease inhibitors was added immediately before French Press lysis with 900 psi at medium for 3 times in the small cell. The cells were centrifuged for 10 min at 13000 rpm at 4°C. The supernatant was collected and filtered through 0.2 µm filter for the purification. 2 µl of the supernatant and the pellet (resuspended it in the same volume) was saved for SDS-gel.

IBA-Strep-Tactin Superflow column was equilibrated two times at 4°C with 4 ml buffer-W. The supernatant was loaded on the column, the unbound fraction was collected and saved for the gel. The column was washed five times with 1 ml buffer W and eluted five times with 0.5 ml buffer E. 0.5 ml fractions were collected and the fractions 3 and 4 were aliquoted and frozen immediately on dry ice. Protein concentrations of the fractions were analyzed. The column was regenerated by washing three time with 5 ml buffer R and stored in it.

Buffer W:

100 mM Tris, pH8.0

150 mM NaCl

1 mM EDTA

Buffer E:

Buffer W + 2.5 mM desthiobiotin

Buffer R:

Buffer W + 1mM 2-[4'-hydroxy-benzeneazo] benzoic acid (HABA)

2.2.3.11 Liposome binding assay

Preparation of liposomes:

Liposomes are lipid-bilayer bounded vesicles. They are prepared by hydrating lipids (from Sigma) in aqueous solutions. 1 mg of lipids consisting of 70 % phosphatidylcholine (PC), 20 % phosphatidylethanolamine (PE) and 10 % variable lipids were dried under nitrogen to form a thin lipid film. It should not be dried too fast. The thin lipid film was rehydrated by adding 150 µl of 0.3 M sucrose, incubated at room temperature for 1 hr and vortexed occasionally. 850 µl of water was added and centrifuged for 1 hr at 4°C at 20,000 rpm in a Beckmann table top ultracentrifuge with TLA-100.3 rotor. The pellet was resuspended in 500 µl of 20 mM Hepes pH7.4 and passed 15 times through a pre-wet extruder with 100 or 400 nm membrane. The liposomes were stored at 4°C and used within one week.

Liposome binding assay:

Bacterially expressed strep-tagged ENTH domain of Ent3p was diluted with buffer-L to required concentration. For each reaction, 6 µg of Ent3p in 100 µl of buffer-L and 100 µg of liposomes were used. The purified Ent3p protein concentration used in this experiment was 1.1 µg/µl. So, 5.5 µl of Ent3p in 94.5 µl of buffer-L was taken for each reaction. Totally, for 7 (6+1) reactions, (PC, PE, PI3P, PI4P, PI3,5P and a negative control (only protein)), 38.2 µl of protein in 661.5 µl of buffer-L was pre-incubated on ice for 10 min and pre-cleared at 50,000 rpm for 20 min in a Beckman table top centrifuge using TLA100.3 rotor. The final salt concentration of buffer-L with protein was 55 mM NaCl. 100 µl of the pre-cleared supernatant was incubated with 50 µl (100 µg) of liposomes on ice for 15 min and re-isolated at 25000 rpm for 20 min using TLA100.3 rotor. The pellet

was rinsed twice with 150 µl of buffer-L at 25000 rpm for 20 min. The pellet was resuspended in 20 µl of 2x stop buffer and analyzed by SDS-PAGE followed by Coomassie blue staining. 30 % (1.64 µl of Strep-Ent3p) of the starting material was loaded as a standard.

Buffer-L:

20 mM Hepes pH 8.0

50 mM NaCl

2.2.4 Cell Biology

2.2.4.1 Subcellular fractionation

The yeast cells were grown overnight to an OD_{600} of 0.5-1.0. And 20 OD of cells were pelleted at 3000 rpm for 3 min. The pellet was resuspended in 2 ml of TEβ and incubated at 30°C for 10 min under slow shaking. Cells were pelleted down at 3000 rpm for 3 min and spheroplasted with 60 µl of 10 mg/ml zymolyase in 2 ml spheroplast buffer for 1 h at 30°C. Spheroplasts were pelleted at 6500 rpm for 30 sec and washed 3 times with spheroplast buffer. Spheroplasts were resuspended in 1 ml of lysis buffer in the presence of protease inhibitors. Cells were homogenized 5 times in a tight glass potter. For some, experiments in which glass beads were used, the cells were washed once with 5 ml of ice cold lysis buffer containing 20 mM HEPES (pH6.8), 0.15 M potassium acetate, 10 mM $MgCl_2$ and 0.25 M Sorbitol with protease inhibitors, resuspended in 1 ml of the same buffer and transferred to prechilled 15 ml corex tube with 1.6 g glass beads. At 4°C, the cells were vortexed vigorously for 30 sec followed by chilling on ice for 30 sec which was repeated 10 times. The supernatant was transferred to an eppendorf cup. The homogenates from the gentle method (homogeneization) and the harsh method (with glass beads) were centrifuged at 2000 rpm for 5 min at 4°C, to remove the broken cells. The supernatant was transferred carefully to a new eppendorf cup, 400 µl was saved as **H** fraction and 500 µl was centrifuged at 13000 rpm for 10 min at 4°C to obtain the S13 and P13 fractions. S13 fraction was then centrifuged at 50000 rpm for 20 min at 4°C in a Beckman table top centrifuge using TLA100.3 rotor to obtain the **S200** (cytosolic proteins) and the P200 fraction (membrane proteins). **P13** and **P200** fractions were resuspended in 500 µl and 400 µl respectively with the lysis buffer containing protease

inhibitors. For some experiments, the pellet fractions were resuspended in 70 µl of lysis buffer.

Gel:

To 50 µl fractions of **H**, **P13**, **P200** and **S200**, 25 µl of 3x Stop buffer was added and boiled for 5 min at 95°C. From each sample 30 µl was loaded onto SDS-PAGE, for equal volume of load. For experiments in which equal amounts of protein were loaded: usually 10 µg per well. But it varied depending on the amounts of protein present in the fractions.

TEβ:

200 mM	Tris pH 8.0
20 mM	EDTA
1%	β-Mercaptoethanol

Lysis-buffer (10 ml):		Final conc.:
500 µl	1 M Tris, pH 7.5	50 mM
1 ml	2 M Sorbitol	0.2 M
20 µl	0.5 M EDTA	1 mM

2.2.4.2 CPY overlay assay

This assay was used to detect the mutants which secrete CPY. The strains to be checked were streaked on a YEPD plate with a positive (*vti1-1* or *vti1-2* cells) and a negative (wild type cells) control and a nitrocellulose membrane was placed on the top of the cells. The plate was incubated at the semi-permissive temperature for overnight. Then the membrane was removed from the plate, washed with water to clear up the adhering cells. The membrane was processed for immuno staining using antiserum against CPY.

2.2.4.3 Aminopeptidase I maturation test

Aminopeptidase I is a vacuolar hydrolase which is transported from the cytosol to the vacuole by the CVT pathway (during logarithmic and early stationary phases) and by the autophagy (during late stationary and starvation conditions). The pro form of the amino peptidase I would appear if the CVT pathway or the autophagy was blocked. The cultures from the log phase, stationary phase and nitrogen starvation were prepared as follows.

The strains were grown overnight at 30°C till OD_{600} 0.5 to 1.2, for the log phase cells. The stationary cultures were obtained by growing the cells for nearly 24 hours at 30°C to an OD_{600} above 4. The stationary cultures were pelleted down, resuspended in the nitrogen starvation medium and again grown for 4 h at 30°C to obtain the starved cells. Protein extracts from the log phase, stationary phase and starved cells were prepared as mentioned in 2.2.3.1 and analyzed by western immnuo blotting to check the maturation of aminopeptidase I using antibody against aminopeptidase I.

2.2.4.4 Indirect Immunofluorescence

5ml of SD or YEPD medium was inoculated with cells and grown overnight at 30 °C. Next day, cells equal to 2.5 OD_{600} were harvested and was inoculated in 10 ml of YEPD medium and incubated for 4 h at 30 °C. Cells were then fixed by adding 1-1.2 ml of 37% formaldehyde (final concentration 3.7%), incubated for 30 min in the shaker. Cells were harvested and resuspended in 2 ml fixative solution and incubated overnight at room temperature on the rocker. Fixed cells were harvested and suspended in 1 ml TEβ for 10 min. Spheroplasts were obtained by incubating with zymolyase at 30 °C with gentle shaking. While cells were spheroplasting, slides (8-well multitest slides) were prepared. 20 µl of 1 mg/ml poly-L-Lysine in water was added to each well and allowed to sit for 1 min. Each well was washed with 25 µl of water (6 times). Aspirated and allowed to air dry. Spheroplasted cells were pelleted at 6500 rpm, 30 sec and washed once with 1 ml of 1.2 M sorbitol containing 5 mM sodium azide and repelleted. Cells were resuspended in 1.2 M sorbitol containing 1-2 % SDS, incubated for 2 min and were pelleted at 6500 rpm, 30 sec and washed twice with 1 ml of 1.2 M sorbitol. The cells were resuspended in an appropriate volume of 1.2 M sorbitol depending on the size of the pellet. 40 µl of cells per well were added and allowed to settle for 10 min. Remaining cells were aspirated and each well was washed 3 times with 20-25 µl of PBS-BSA. The slides were allowed to sit in humid chamber for 15 min at room temperature. Wells were aspirated and primary antibody was added and incubated for 1h at room temperature. Cells were washed with 20-25 µl of PBS-BSA-azide 6 times. Secondary antibody was added and incubated for 1h. Cells were washed 6 times with PBS-BSA-azide. 10 µl of DAPI (1 mg/ml) was added, incubated for 10 min and washed with PBS-BSA-Azide 3 times. 8 µl of mounting media was added in each well, slides were covered with coverslip and allowed to settle.

After 5 min, ends of the cover slips were sealed with nail polish. Slides were viewed under a fluorescence microscope. DAPI staining was examined at 395 nm.

Fixative: 1 g of paraformaldehyde was dissolved in 25 ml of water by heating to 60 °C. 187.5 µl of 6 N NaOH was added and then 0.34 g of potassium hydrogen phosphate was added. The pH of the solution was 6.5.

TEβ buffer

Tris/HCl, pH 8.0	200 mM
EDTA	20 mM
β-mercaptoethanol	1%

Spheroplasting buffer

Sorbitol	1.2 M
Potassium phosphate pH 7.3	50 mM
Magnesium chloride	1 mM

Sorbitol-Azide

Sorbitol	1.2 M
Sodium azide	5 mM

Sorbitol-SDS

10% w/v SDS	2%
Sorbitol	1.2 M
Sodiumazide	5 mM

PBS-BSA-Azide

BSA	5 mg/ml
Sodiumazide	5 mM
10X PBS	1X

2.2.4.5 GFP fluorescence

Overnight grown yeast cells were washed once with PBS and directly viewed under the fluorescence microscope AxioCAM without fixation. If required, the nuclear staining was done with 1:1000 dilution of DAPI (1mg/ml) and incubated at room temperature for 10 min. Cells were washed twice with PBS. 1 or 3 µl of cells were examined under microscope.

2.2.4.6 FM4-64 staining

The cultures were grown overnight at 24°C in YEPD. When the cultures reached 0.4 OD to 1.0 OD, they were shifted to the restrictive temperatures for 15 minutes. 0.5 OD of the cells were pelleted down and resuspended in 120 µl of YEPD. The dye FM4-64 was added to the final concentration of 65 µM (from 16mM stock in DMSO) and inubated at the restrictive temperatures for 15 min. The samples were pelleted at 6500 rpm for 30 sec, washed once with YEPD and resuspended in 7 µl of YEPD. The cells were viewed immediately under a fluorescence microscope with texas red-filter.

2.2.4.7 Calcofluor and Phalloidin staining

Chitin in the yeast cell wall was stained using Calcofluor (Fluorescent brightener 28, Sigma-aldrich, Steinheim, Germany) and actin was localized after Phalloidin TRITC (Sigma, Steinheim, Germany) staining as described by Pringle et al. 20 ml Yeast cultures were grown overnight at 24°C and the log-phase cultures were shifted to 18°C or 30°C for 5 h or 2 h respectively. 2.2 ml of 37 % Formaldehyde was added to the cells, inucbated at the same temperature for 10 min and pelleted down at 3000 rpm for 5 min. The pellet was resuspended in 2 ml of PBS / 4 % formaldehyde for 1 h at RT. Cells were pelleted, washed thoroughly with PBS and resuspended in 500 µl of PBS. To 100 µl of cells, 10 µl of 1mg/ml calcofluor in water and 10µl of 6.6 µM phalloidin in methanol was added and incubated for 1h 30 min in the dark. Cells were washed five times with PBS, resuspended in 10 µl of mounting medium and 3µl was viewed under a fluorescence microscope.

3 Results

3.1 Characterization of Use1p mutants

During the doctoral studies of Dr. Meik Dilcher, he identified an uncharacterized open reading frame, YGL098w which shared the characteristic features of SNARE proteins. He showed that the 245 amino acids product from the ORF is really a SNARE protein and named it Use1p (Unconventional SNARE in the ER), since it was localized in the ER. *USE1* is an essential gene, so, Dr. Meik Dilcher created *ts* mutants by random mutagenesis to analyze its function. A 10 amino acid mutant allele (*use1-10AA*), which contained 5 amino acid replacements in the SNARE motif, including the mutation D183G in the 0 layer grew more slowly at 24°C than WT cells and did not grow at 30 and 37°C. To determine the importance of the 0 layer, the allele *use1-0* layer with the mutation D183G was created which didn't show any growth defect. He showed that *use1* mutants were defective in the retrograde traffic to the ER and co-immunoprecipitation of Use1p revealed that it formed a SNARE complex with Ufe1p, Sec20p and Sec22p. When the manuscript was submitted for publication, the reviewers asked for some more experiments. A small part of Use1p project was continued by me, by checking the vacuolar morphology of *use1* mutants with FM4-64 staining and repeating Kar2p/BiP secretion assays in *use1* mutants to support the finding that Use1p is involved in the retrograde trafficking.

3.1.1 Vacuolar morphology of *use1* mutants

The *use1-10AA* cells were larger, accumulated ER membranes and nuclei appeared fragmented in some cells. The morphology of vacuoles was studied by FM4-64 staining. Cells grown at 24°C were shifted to 30 or 37°C for 15 min and incubated with FM4-64 for an additional 15 min at the same temperature to stain vacuolar membranes. Vacuoles had wild-type morphology in most *use1* mutant cells, but were slightly more fragmented in some *use1-10AA* cells as showed in the Fig.10.

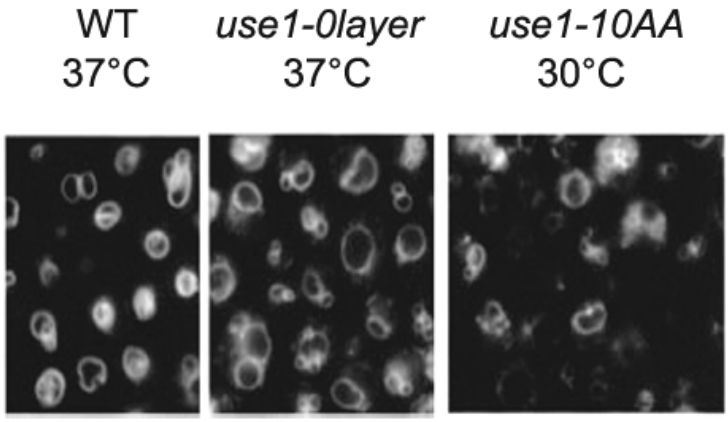

Fig.10. Vacuolar morphology in *use1* mutants: WT, *use1-0*layer and *use1-10AA* cells were incubated with FM4-64 at 37°C or 30°C to stain the vacuoles.

3.1.2 Kar2p/BiP secretion in the *use1*mutants

Kar2p/Bip is a soluble ER protein, which is retrieved from the Golgi (Semenza *et al.*, 1990). Kar2p is secreted into the medium if retrograde traffic to the ER is blocked. It is a specific assay to check the block in the retrograde traffic. The amount of Kar2p secreted by *use1* mutants was determined in a period of 2 h at permissive and restrictive temperatures. *use1-10AA* cells secreted some Kar2p at 24°C and slightly larger amounts at 30°C. A shift to 37°C increased Kar2p secretion from *use1-0*layer cells to levels clearly above that from wild-type cells. *use1-0*layer cells secreted less Kar2p at non-permissive temperature than *use1-10AA* cells. *sec20-1* cells were used for comparison since this defect primarily affects the retrograde traffic to the ER (Fig.11). Wild-type cells secreted 0.37% (SD 0.2), *sec20-1* cells 3.7% (SD 0.9) and *use1-10AA* cells 4.9% (SD 3.4) of the intracellular Kar2p within 2 h at 30°C in four independent experiments; *use1-0*layer cells secreted 0.8% in 2 h at 37°C.

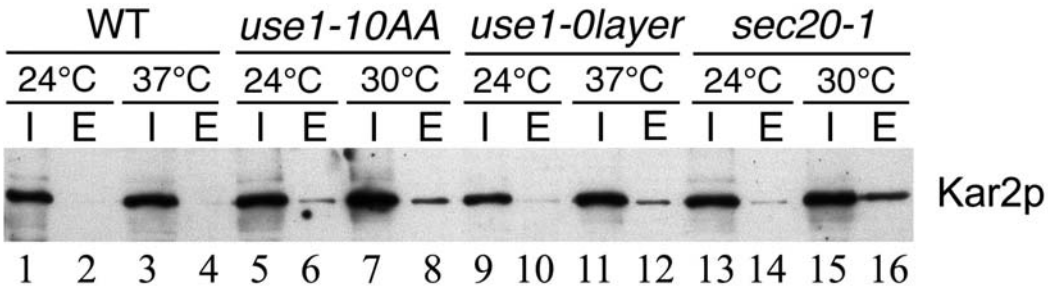

Fig.11. Kar2p/BiP secretion in *use1* mutants: Protein extracts from the cell pellet (I) and the TCA precipitated medium (E) were prepared from the WT, *use1-10AA*, *use1-0*layer and *sec20-1* cells at 24°C or 30°C or 37°C. Kar2p was detected by western immunoblotting using antibody against Kar2p/BiP. Load: Equivalents of 0.19 OD for the pellet fractions and 3.6 OD for the external fractions were subjected to SDS PAGE.

3.2 Function of the N-terminus of Vti1p

The function of the N-terminus of Vti1p is not known, so far. Using the N-terminal mutants of Vti1p, the function of N-terminus could be studied well. Random mutagenesis of *VTI1* gene generated a mutation with no big change in the SNARE motif and 7 amino acid exchanges. The N-terminus with 2 amino acid mutation till AA105 was cloned into wild type Vti1p. This 2 AA mutant allele, *vtiQ29RW79R* (2 AA mutant) caused phenotype. From the 2 AA allele, the 1 AA alleles (*vtiQ29R* and *vtiW79R*) were cloned separately, to study the effects of 1 AA replacement.

3.2.1 Localization of N-terminal mutants

The localization of the mutant Vti1p in FvmY6pBK120 cells (*vti1*Δ*vtiQ29RW79R* on *CEN* plasmid) was done by immunofluresecence with antibody against Vti1p. At 24°C, Vti1p is localized to Golgi and pre-vacuolar membrane as punctate structures both in WT and in the mutant, but in the mutant some staining around the ER could also be seen (Fig.12a). Protein synthesis was arrested by addition of 100 µg/ml Cycloheximide, to check whether the newly synthesized protein is accumulated in the ER or the localization of the mutant Vti1p itself is in the ER. Cycloheximide was added to the pre-incubated cells at 24°C, further incubated for 30 min and then fixed at the respective temperatures.

At 24°C with cycloheximide, vtiQ29RW79Rp was still localized to the punctate structures. When the cells were shifted to 37°C for 30 min, a clear relocalization of vtiQ29RW79Rp to ER was observed, even after the treatment of cycloheximide (Fig.12b). The effect was not altered by deleting *ENT3*, an interacting partner for the N-terminus of Vti1p, in the background of *vtiQ29RW79R*. But the 2 AA mutant was expressed from a *CEN* plasmid which led to mild over expression of the protein. When the mutation was integrated into the genomic locus, the ER staining had disappeared and normal punctate staining pattern was observed as shown in the Fig.12b (lower panel). Thus, vti1Q29RW49Rp was localized to ER under slightly over expressing conditions. This delocalization is due to the mutation because over expression of wild type *VTI1* using a 2 μ plasmid does not result in ER localization.

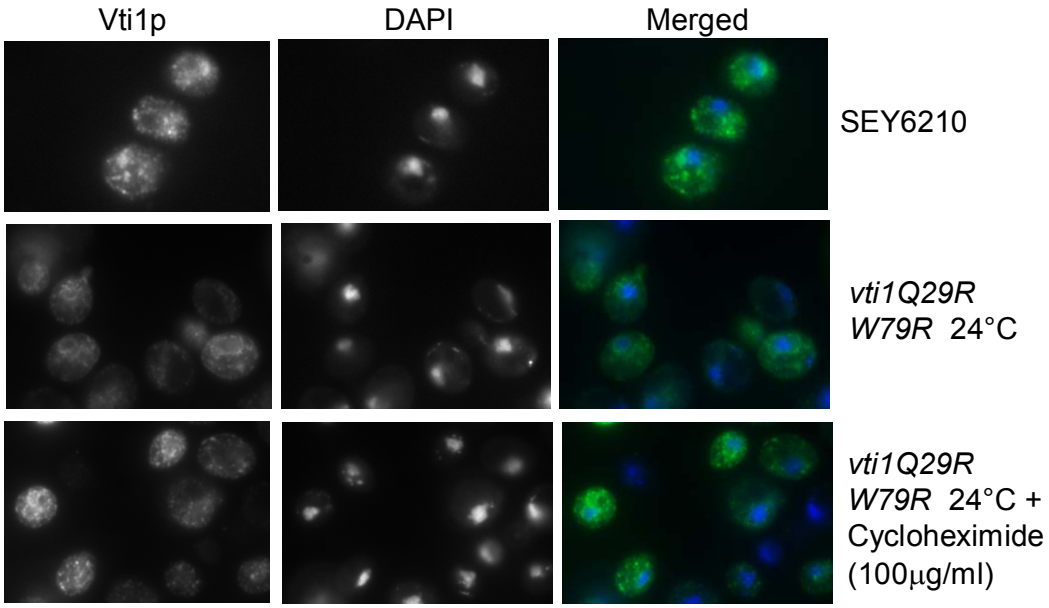

Fig.12a. Localization of vti1Q29RW79Rp at 24°C: The 2 AA mutant was pre-incubated at 24°C for 30 min, treated with cycloheximide (100 μg/ml) for 30 min and fixed at the same temperature. By Indirect immuno-fluorescence, the 2 AA mutant was detected using the antibody against Vti1p. DAPI staining was done to localize nucleus.

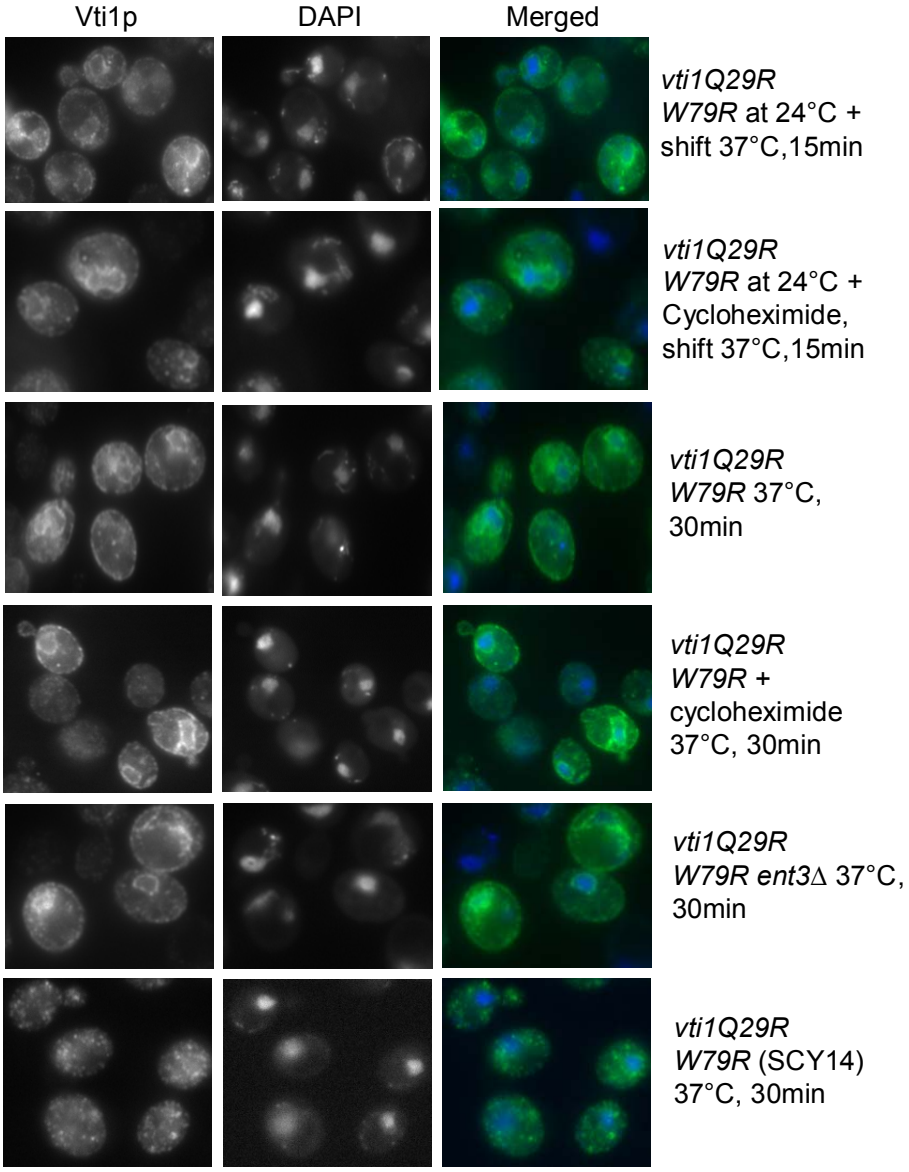

Fig.12b. Localization of vti1Q29RW79Rp at 37°C: The 2 AA mutant (*CEN* and SCY14) and the 2 AA mutant with the *ENT3* deletion was pre-incubated at 24°C for 30 min, treated with cycloheximide (100 µg/ml) for 30 min and shifted to 37°C for 15 min or 30 min and fixed at the same temperatures. By Indirect immuno-fluorescence, the 2 AA mutant was detected using the antibody against Vti1p. DAPI staining was done to localize nucleus. The 2 AA mutant was expressed from *CEN* plasmid except in the lower panel (SCY14).

The localization of 1 AA mutants were strikingly different from the 2 AA mutants which was also slightly over expressed from the *CEN* plasmids. Both the 1 AA mutants were found on vacuolar membranes and on internal small structures (Fig.12c).

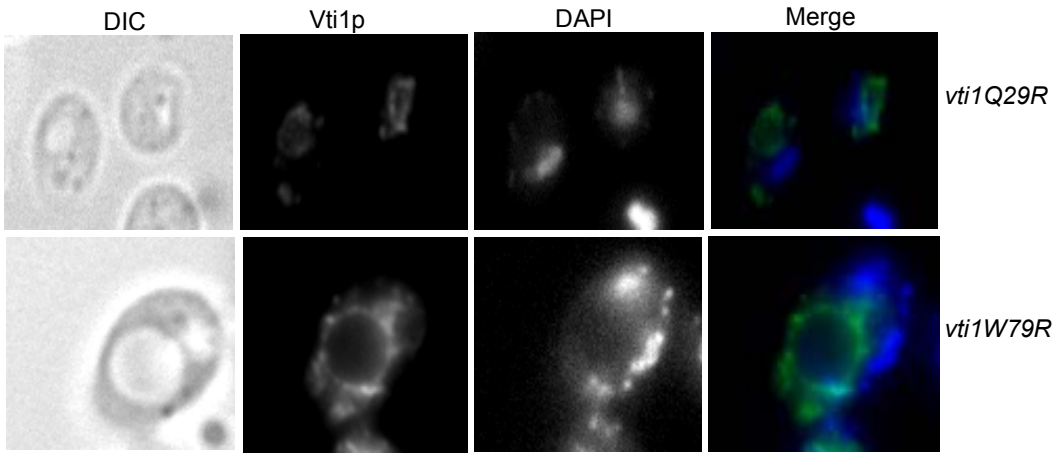

Fig.12c. Localization of 1 AA mutants at 37°C: The 1 AA mutants *vti1Q29R* and *vti1W79R* were fixed at 37°C and by Indirect immunoflurescence, the 1 AA mutatnt Vti1p was detected. The DIC pictures were made to clearly localize the vacuoles. DIC: Differential Interference Contrast.

3.2.2 CPY sorting by mutant Vti1p

Carboxypeptidase Y traffics from the ER to the vacuole via the pre-vacuolar compartment and exists in three different forms. When there is a block in the traffic step, the corresponding form of the CPY accumulates intracellular or the Golgi form is secreted into the medium which can be analyzed by SDS gel. The CPY pathway was analyzed in the 2 AA mutants by pulse chase immunoprecipitation at 24°C and 37°C and for 1 AA mutants at 37°C (Fig.13). IP was done both from the cell pellet (I) and the extracellular medium (E). In 2 AA mutants (*CEN*) at 37°C, only 33.5% of CPY was processed to the mature form (I) and p2CPY was secreted out into the medium (E) whereas this defect was not observed at 24°C. So, the 2 AA mutation is temperature sensitive. But in the case of 1 AA mutants, the CPY pathway was not affected. When the 2 AA mutation was integrated into the genome, the biosynthetic defect was even stronger and the percentage of mCPY was drastically reduced from 33.5 to 5 (Fig.14). Also, more p2CPY was present in the cell pellet (24%) with slightly increased levels of p1CPY. To check, whether the 2 AA mutation has a dominant negative effect, the mutation was over expressed from a 2μ plasmid in the wild type cells and the CPY pathway was analyzed by pulse chase immuno-precipitation. But the mutation did not show any dominant negative effect (Fig.14).

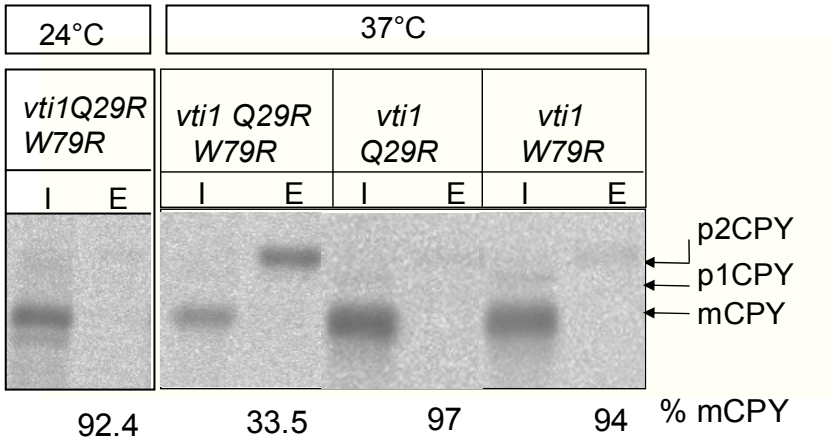

Fig.13. CPY pulse chase immuno-precipitation in 2AA and 1AA Vti1p mutants: Cells grown at 24°C were labeled with ^{35}S at 24°C or preincubated at 37°C for 15 min before labeling with ^{35}S for 10 min, chased for 30 min at 24°C or 37°C and immunoprecipitation was done from the cell pellet (I) and from the medium (E), using antibody against CPY. The three forms of CPY, p1CPY (from ER, 67 kDa), p2CPY (from Golgi, 69 kDa) and mCPY (from Vacuole, 61 kDa) were separated on a SDS gel. The percentage of mCPY was calculated.

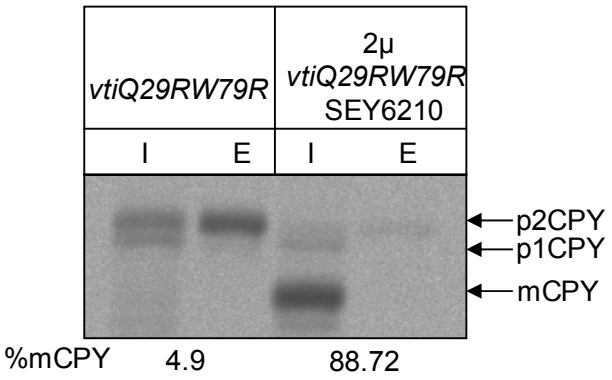

Fig.14. Pulse chase immunoprecipitation of CPY from overexpressed 2 AA mutant cells: The 2 AA mutant (SCY14) and the wildtype cells over expressing the 2 AA mutant from a 2µ plasmid were used for pulse chase labeling at 37°C and immunoprecipitaion of CPY. The percentage of mCPY was calculated.

Further, the onset of the defect in the CPY pathway was analyzed with and without pre-incubation at 37°C (Fig.15). The WT and the 2 AA mutant cells were labeled without pre-incubation (0'), with 5 min pre-incubation (5') and with 10 min pre-incubation (10') at

37°C. There was no time dependent change in the sensitivity of the defect. This indicates that the onset of the defect is extremely rapid.

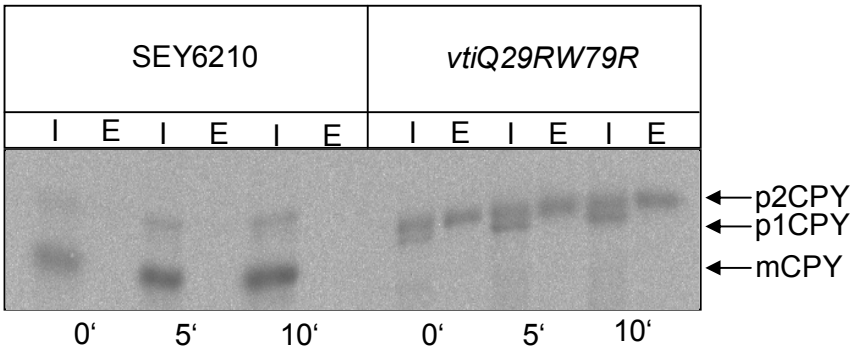

Fig.15. CPY-IP with and without pre-incubation in the 2 AA mutant.

3.2.3 Stability of N-terminal mutants

The stability of 1 AA and 2 AA Vti1p mutants (all from *CEN* plasmid) was analyzed by pulse chase immunoprecipitation of Vti1p at different chase points namely, 10 min, 2 h and 5 h at 37°C. The 2 AA mutant was very unstable, compared with 1 AA mutants (Fig.16). After 5 h of chase, only 33% of the Vti1p was present in the 2 AA mutant (on an average of 3 experiments) whereas in the wild type cells 85% of Vti1p was present which showed that wildtype Vti1p is very stable. The 1 AA mutants didn't show significant instability of Vti1p (average of 2 experiments). The genomically integrated 2 AA mutant Vti1p (SCY14) was highly unstable, only 17% was present after 5 h chase (on an average of three experiments).

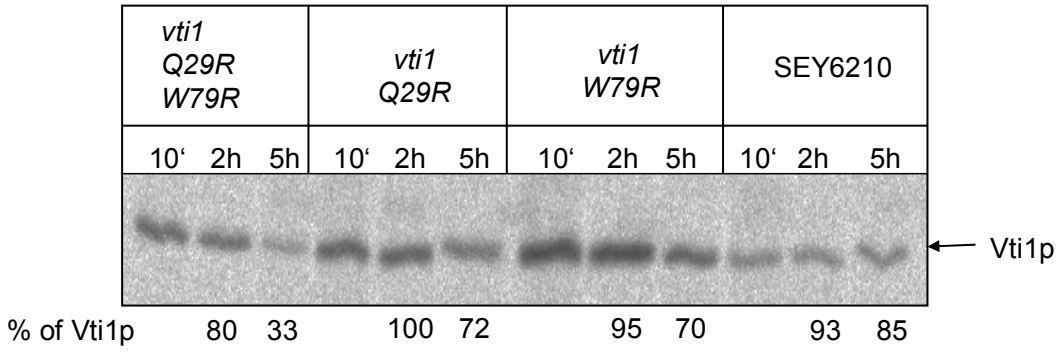

Fig.16. Stability of Vti1p in 1 AA and 2 AA mutants: The WT and the mutant cells were labeled with ^{35}S for 25 min, chased for 10', 2h and 5h at 37°C and Vti1p was immunoprecipitated. The percentage of Vti1p was calculated for each time point.

3.2.4 *vtiQ29RW79R*p is not degraded by Vacuolar proteases

Since the 2 AA mutant was highly unstable, it was very interesting to study how it would get degraded. Vacuolar proteinases are important for the vacuolar degradation of proteins, among which Proteinase A, coded by the *PEP4* gene plays an important role since it activates all vacuolar proteases. The stability of Vti1p was studied in the wild type, 2 AA mutant and in the *pep4* deletion strains by pulse chase immunoprecipitation of Vti1p at 10 min and at 5 h chase points, at 37°C (Fig.17). Vti1p was degraded by the vacuolar degradation pathway, because the *pep4* deletion in the wildtype cells stabilized Vti1p, increasing the percentage of Vti1p remaining after 5 h, from 49 to 113%. But in the 2 AA mutant, *pep4* deletion did not have any effect which demonstrated that the 2 AA mutant Vti1p was not degraded by the vacuolar degradation pathway.

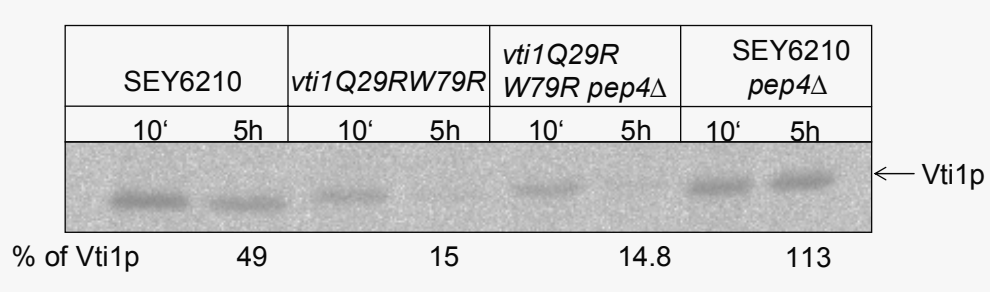

Fig.17. Stability of Vti1p in *pep4* deletion strains: Pulse chase immunoprecipitation of Vti1p was done from the wildtype, 2 AA mutant (SCY14), 2 AA mutant with *pep4* deletion (SCY18) and wildtype with *pep4* deletion (BKY12) cells at 10 min and 5 h chase points at 37°C. The percentage of Vti1p remaining after 5 h compared to the 10 min chase point was calculated.

3.2.5 Polyubiquitination is required for *vtiQ29RW79R*p degradation

Proteasome mediated proteolysis is the major pathway for protein degradation in the cells apart from the vacuolar/lysosomal degradation. Proteasomes are multi-protein complexes found in the cytosol and the nucleus (reviewed in: Coux *et al.*, 1996). The means of targeting proteins to proteasomes is by their modification with chains of ubiquitin. Ubiquitination is an essential cellular process effected by a multi-enzyme cascade involving classes of enzymes known as E1s (ubiquitin-activating enzymes), E2s (ubiquitin-conjugating enzymes or Ubcs), and E3s (ubiquitin-protein ligases) (reviewed in: Bonifacino and Weissman, 1998). Ubc7p is an ubiquitin conjugating enzyme, involved in the ER-associated protein degradation pathway which requires Cue1p for

recruitment to the ER membrane. Cue1p can bind ubiquitin to facilitate intramolecular monoubiquitination. The Cue1p-Ubc7p complex is not only required for degradation of luminal ER protein but also for membrane proteins which are anchored with their tails in the cytosolic face of the ER membranes (like SNAREs). Ubiquitin is attached to lysine on a target protein or to another ubiquitin chain at K48 of ubiquitin, resulting in the generation of chains of ubiquitin which is referred to as either polyubiquitination or multiubiquitination. The formation of the K48 linked polyubiquitin chains on proteins constitutes a potent targeting signal for degradation in 26S proteasomes.

To check whether the 2 AA mutant was degraded by the proteasomes, *CUE1* and *UBC7* genes were deleted in the 2 AA mutant background. Also, a plasmid expressing the mutant ubiquitin in which lysine 48 has been mutated to an arginine (*K48R*) was transformed into the 2 AA mutants. The *K48R* mutation renders ubiquitin unable to form poly-ubiquitin chains, thus preventing the proteasomal degradation. The stability of mutant Vti1p was studied in these strains by pulse chase immunoprecipitation (Fig.18). Vti1p was not stabilized in the *cue1* and *ubc7* deletions. But the *ubK48R* stabilized the mutant Vti1p from 16% to 63% at 3h and from 10% to 41% at 5 h. So, polyubiquitination was required for the degradation of the mutant Vti1p.

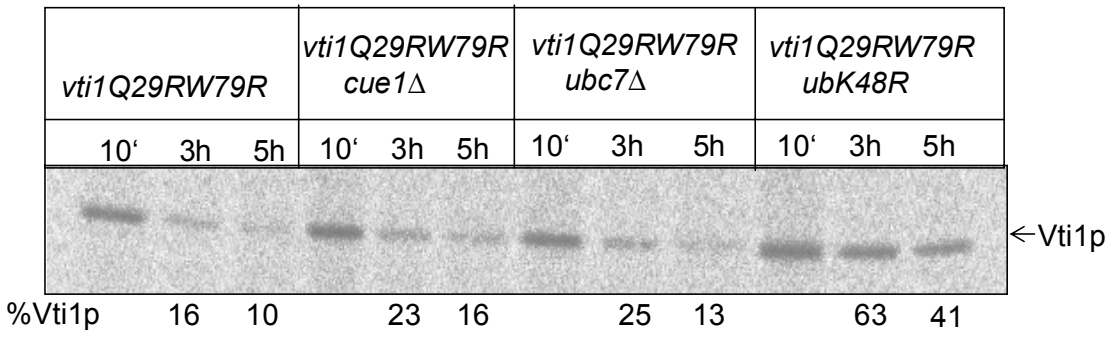

Fig.18. Vti1p stability in Proteasomal mutants: The 2 AA mutant (SCY14), 2 AA mutant with *cue1*Δ (SCY22), 2 AA mutant with *ubc7*Δ (SCY21) and 2 AA mutant with *ubK48R* (SCY14-pUB203) were used for the pulse chase immunoprecipitation of Vti1p at 10 min, 3 h and 5h, at 37°C.

3.3 Characterization of Ent proteins in *S.cerevisiae*

3.3.1 Role of Ent proteins in the trafficking of CPY and ALP

In several *ent* deletion mutants, CPY transport was analyzed by pulse chase labeling followed by immunoprecipitation at 37°C (Fig.19). No defects in CPY maturation were observed in ent*4*Δ and ent*5*Δ cells. Slightly elevated levels of p2CPY were secreted into the medium (E) by *ent3*Δ (6.2%) and *ent3*Δent*4*Δ (4.6%) cells even though most CPY reached the vacuole (mCPY in the intracellular fraction I). p2CPY is secreted from the cells if transport from the TGN to the vacuole is defective. *ent3*Δent*5*Δ and *ent3*Δent*4*Δ ent*5*Δ cells secreted even more p2CPY (9.3% and 8.1% respectively) and accumulated p2CPY within the cells. This slight transport defect indicates that Ent3p and Ent5p have a partially redundant function in CPY transport.

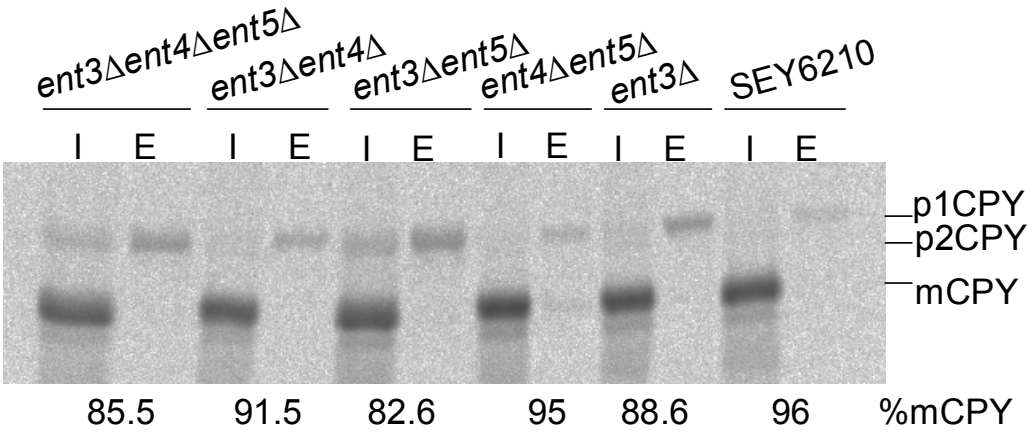

Fig.19. CPY transport in Ent mutants: CPY was immunoprecipitated from the cellular extracts (I) and the medium (E) after pulse-chase labeling at 37°C. p1CPY: ER proCPY (carboxypeptidase Y); p2CPY: Golgi proCPY; mCPY: vacuolar mature CPY.

The ALP pathway, which bypasses the pre-vacuolar compartment to reach the vacuole, was also analyzed in the *ent* mutants by pulse chase labeling and immunoprecipitaiton of alkaline phosphatase at 37°C (Fig.20). ALP pathway was not significantly affected in the *ent* mutants.

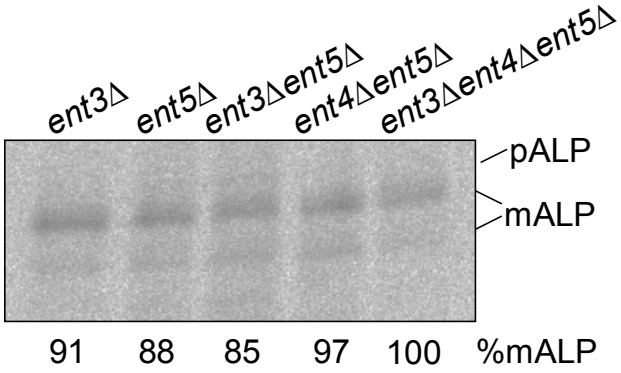

Fig.20. ALP transport in *ent* mutants: Pulse chase labeling and immunoprecipitation of ALP was done at 37°C. pALP: proALP; mALP: mature ALP (vacuolar form).

3.3.2 Ent3p binds phosphoinositides

Ent3p binds the clathrin adaptor Gga2p and has been implicated in clathrin coated vesicle formation at the Golgi or endosome (Duncan *et al.*, 2003). Different phosphoinositides are regulators of trafficking in these organelles in yeast (Simonsen *et al.*, 2001). PI(4)P is implicated in secretory traffic from the Golgi to the plasma membrane, PI(3)P in traffic to the endosome and autophagocytosis. PI(3,5)P_2 is required for sorting into the internal vesicles in prevacuolar endosomes to form multivesicular bodies. To detect whether Ent3p has any specificity towards phosphoinositides, the strep-tagged ENTH domain of Ent3p was bacterially expressed, purified and incubated with liposomes containing phosphatidylcholine (PC) and phosphoinositol (PI) as controls along with the above mentioned phosphoinositides. Ent3p bound specifically to liposomes with PI(3)P and PI(3,5)P_2 (Fig.21).

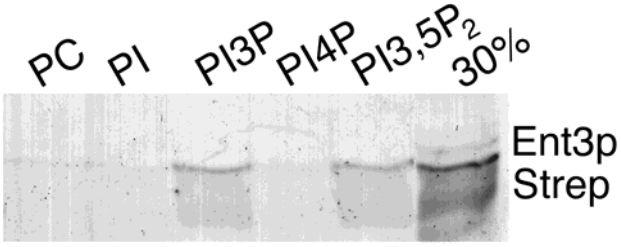

Fig.21. Ent3p binding to phosphoinositides: The ENTH domain of Ent3p with a C-terminal Strep tag was incubated with liposomes containing 70% PC, 20% PE and10% of the indicated lipids. Liposomes were pelleted and recruitment of Ent3p was followed by separation of the pellet fraction by SDS-PAGE and Coomassie blue staining. 30%: 30% of the protein used in the assay was loaded for comparison.

3.3.3 Localization of Ent3p and Ent5p in wildtype and in mutant cell

3.3.3.1 Localization of endogenous Ent3p using antibody against Ent3p

Initially, the localization of Ent3p was analyzed using Ent3p tagged with 3 copies of the HA epitope at the C-terminus which turned out to be non functional because it did not complement for the loss of Ent3p in Y24*ent3*Δ cells in the growth test at 37°C. Therefore we cannot rely on the Ent3p-HA data. Anti-Ent3p rabbit serum was raised against a Strep-ENTH domain of Ent3p which recognized specifically a protein with the expected molecular weight for Ent3p at around 50 kDa in a whole-yeast wild-type cell extract, but not in an *ent3*Δ cell extract both in SEY6210 and BY4742 background, as shown in the Fig.22a. Subcellular fractionation of wild type cells showed that Ent3p was more cytosolic (S200) and less associated with the membrane fraction (P13), when the lysis was done very gently after spheroplasting by homogenization with lysis buffer containing 20 mM HEPES (pH 6.8), 0.15 M potassium acetate, 10mM MgCl2 and 0.25 M Sorbitol with protease inhibitors (Fig.22b, SEY6210 cells). But when the lysis was done vigorously by glass beads with the same lysis buffer, Ent3p was more associated with membrane fractions (Fig.22b, SEY6210 cells). The P13 fraction contains vacuoles, mitochondrial and ER-membrane, the P200 fraction contains small vesicles and the Golgi and the S200 fraction derives all cyosolic proteins. Since, Ent3p and Vti1p are interacting partners, it was important to test whether Vti1p is required for the localization of Ent3p. Subcellular fractionation was done from several *vti1* mutants like SNARE motif mutants (*vti1-1* and *vti1-2*), N-terminal 2AA mutant (*vtiQ29RW79R*) and the N-terminal truncations (*vti1Q116-217* and *vti1M55-217*), to detect the localization of Ent3p, both by gentle (Fig.22b) and harsh (Fig.22c) methods of lysis. The N-terminal truncations express Vti1p amino acids from 55 to 217 [*vti1M55-217* (FvmY6-pBK117)], from 116 to 217 [*vti1Q116-217* (FvmY6-pBK117)] and an additional start ‘methionine’ under a constitutive promoter 789. These mutants exhibit slow growth, strong CPY sorting defects at all temperatures and lacks complete N-terminus involved in Ent3p interaction (amino acids 1-115).

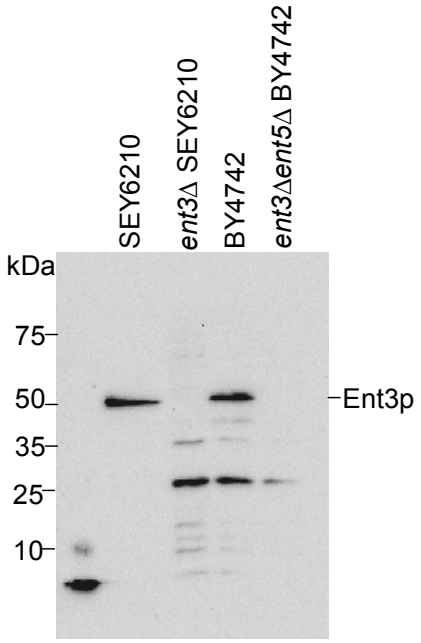

Fig.22a. Generation of anti-Ent3p rabbit serum: Serum from the terminal bleed of the strep-Ent3p injected rabbit (ywop (t)) was diluted to 1:500 and used for probing the blot with protein extracts from SEY6210, *ent3*Δ SEY6210 (SCY2), BY4742 and *ent3*Δ*ent5*Δ BY4742 (BKY13). In SEY6210 cells, a single band at 50 kDa, corresponding to Ent3p was detected. In other cells a mild cross reaction of anti-Ent3p was observed.

The cells were lysed in 1ml lysis buffer and fractionated. The pellet fractions were resuspended in 70 µl of lysis buffer, protein concentration was quantified and equal amounts of protein were loaded on the gel. In wild type cells, around 1.3% of Ent3p was present in the P13 fraction, 98% in S200 and rest in the P200 by gentle lysis (Fig.22b). But, by harsh method of lysis, 65% of Ent3p was present in the P13, 8% in P200 and 27% in S200 (Fig.22c). In *vti1* mutants, more or less, the same range of Ent3p was found by both the methods. Though, Ent3p was present more in the P13 fraction in the *vti1* mutants compared to wild type (Fig.22b), the consequent decrease in other fractions (S200) was not observed. On the other hand, fractionation done by the harsh lysis method (Fig.22b), showed that there was no apparent relocalization of Ent3p in the N-term truncations (since the N-term of Vti1p interacts with Ent3p, these mutants are the perfect tools to study the redistribution of Ent3p). The vacuolar ATPase, Vph1p was used as a control for the experiment (to check for rupture of vacuole during lysis). Vph1p is associated only with the P13 fraction but because of the glass beads, vacuoles might have got damaged,

so it was seen in the P200 fraction also. These data showed that there was no redistribution of Ent3p in the *vti1* mutants.

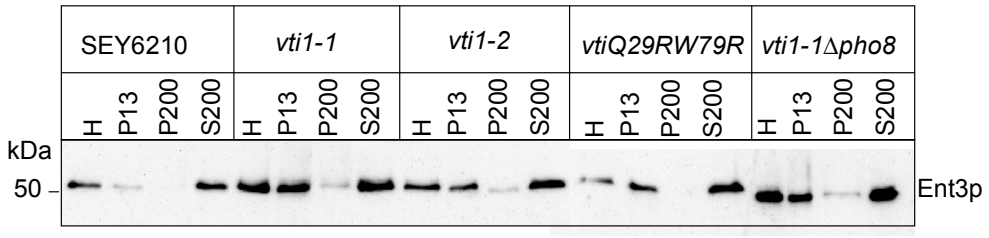

Fig.22b. Subcellular fractionation of Ent3p in *vti1* mutants by homogenization: Wild-type and the mutants *vti1-1* (FvmY7), *vti1-2* (FvmY24), *vtiQ29RW79R* (SCY14), *vti1-1Δpho8* (FvmY29) homogenates (H) (from 10 OD of cells) were fractionated (starting material 1ml) into a 13 000 g pellet (P13), a 200 000 g pellet (P200) and a 200 000 g supernatant (S200) by differential centrifugation. The pellet fractions P13 and P200 were resuspended in 70 µl of lysis buffer. Fractions were analyzed by immunoblotting using antiserum against Ent3p. Equal amount of protein was loaded. Load: 6 µg of the protein was loaded per well. In SEY6210 cells, total protein in H was 390 µg, in P13 (24.5 µg), in P200 (24.5 µg) and 200 µg in S200. The percentage of Ent3p present in P13 was 1.3, in P200 was 0.33 and 98.38 in S200. In other cells also the same range of total protein was protein.

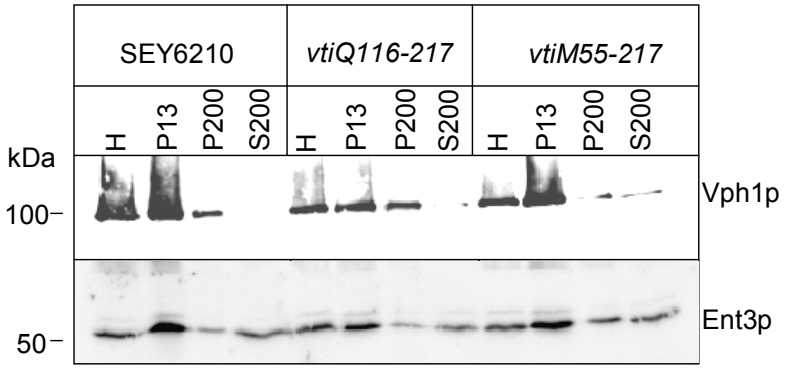

Fig.22c. Subcellular fractionation of Ent3p in *vti1* mutants by glass beads: Wild-type and the mutants *vti1Q116-217* (FvmY6-pBK117) and *vti1M55-217* (FvmY24-pBK119) homogenates (H) (from 25 OD of cells) were fractionated (starting material 1ml) and fractions were analyzed by immunoblotting using antisera against Vph1p (Vacuolar ATPase, 100kDa) and Ent3p. Equal amount of protein was loaded. Load: 70 µg of protein per well. In SEY6210 cells, total protein in H was 2800 µg, in P13 (710 µg), in P200 (720 µg) and 945 µg in S200. The percentage of Ent3p present in P13 was 65 %, in P200 was 8 % and 27 % in S200.

3.3.3.2 Fluorescence microscopy of Ent3p-GFP

Since the antiserum against Ent3p was not suitable for the immunofluorescence studies, Ent3p with a C-terminal GFP (pSC22) was constructed. This construct was transformed into the wildtype cells and *vti1* mutants and imaged using a fluorescence microscope (Fig.23). Ent3p was localized into few punctate structures possibly corresponding to endosomes and mostly diffused in the cytoplasm irrespective of the temperature. In the *vti1* mutants, there was no marked difference in the localization of the Ent3p. But, sometimes, in the N-term truncation, *vti1Q116-217* (Y6pBK117) (Fig.23b), a number of punctate structures were observed which was completely different from the wild type, although majority of the cells exhibited the same fluorescence pattern like the wild type (Fig.23a). Taking in account the subcellular fractionation and the fluorescence data, it was showed that Ent3p was not dependent on Vti1p for its localization.

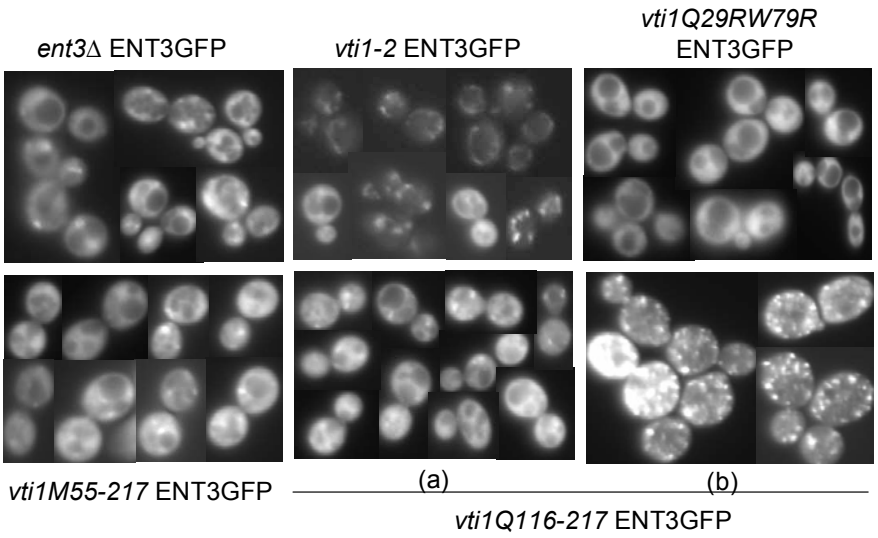

Fig.23. Fluorescence microscopy of Ent3p-GFP: The strains *ent3*ΔENT3GFP (SCY2 pSC22), *vti1-2* ENT3GFP (FvMY24 pSC22), *vti1Q29RW79R* ENT3GFP (SCY14 pSC22), *vti1M55-217* ENT3GFP (Y6pBK119 pSC22), *vti1Q116-217* ENT3GFP (Y6pBK117 pSC22) were grown overnight in the minimal medium at 30°C and were directly viewed (without fixation) under the microscope.

3.3.3.3 Subcellular fractionation of Ent5p- GFP

The C-terminal Ent5p-GFP construct was made to localize Ent5p in the wildtype and in the *vti1* mutants. The wildtype and the mutants harbouring the *ENT5GFP* plasmid (pSC24) were lysed gently by homogenization and fractionated (starting volume 1 ml). The P13 and P200 fractions were resuspended in 100 µl and 80 µl respectively and equal

volume was loaded on the gel. The blot was probed with antisera against GFP and Vph1p (Fig.24a). Ent5p-GFP was detected around 85 kDa and present nearly 20% in the P200, 74% in S200 fraction and rest in the P13 fraction in wild type cells. Interestingly, the membrane associated Ent5p-GFP was found predominantly in P200 while Ent3p-GFP was more prominent in P13 even though both proteins were largely cytosolic. No change in the localization of Ent5p was observed in *vti1* mutants (Fig.24b).

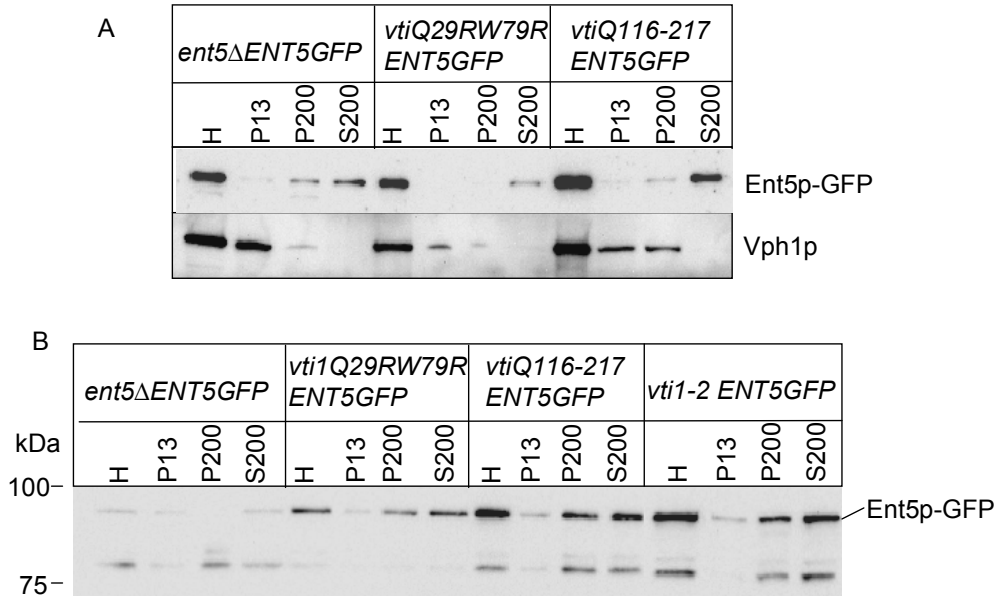

Fig.24. Subcellular fractionation of Ent5p-GFP: The strains (a) *ent5*ΔENT5GFP (SCY25 pSC24), *vti1Q29RW79R* ENT5GFP (SCY14 pSC24), *vti1Q116-217* ENT5GFP (Y6pBK117 pSC24) and (b) *vti1-2* ENT5GFP (FvMY24 pSC24), were gently lysed by homogenization and the homogenate (from 20 OD of cells) fractionated (starting material 1 ml). The fractions were detected with antisera against GFP and Vph1p (vacuolar ATPase, as a control) (a). Equal volumes of the samples were loaded. Some nonspecific band around 80 kDa with more or less same distribution pattern like Ent5p-GFP was observed in blot (b) which may be due to degradation.

3.3.3.4 Ent5p-GFP localization

Ent5p was localized to punctuate structures in wild-type cells as well as in *vti1-2* cells (Fig.25i). *vti1Q29RW79R* cells were stained like wild-type but sometimes it showed many punctuate structures which could not be seen after few hours even from the same culture. Like Ent3p-GFP, in some *vti1Q116-217* (N-terminal truncation) cells Ent5p was localized to many small punctuate structures and in some cells, it was localized to a few larger structure, sometimes close to vacuole possibly endosomes (Fig.25i (a)). Because of this

strange staining pattern in the *vti1Q116-217* cells, any change in the structure of the endosome and the vacuole was analyzed by uptake of FM4-64 dye (Fig.25ii). The uptake was delayed by 60 min when still some intermediate endosomal structures were also stained along with vacuoles. This indicates that transport from the endosomes to vacuoles was delayed in *vti1Q116-217* cells. The vacuolar morphology of the *vti1Q116-217* cells seems to be normal but the structure of the endosomes was not clear.

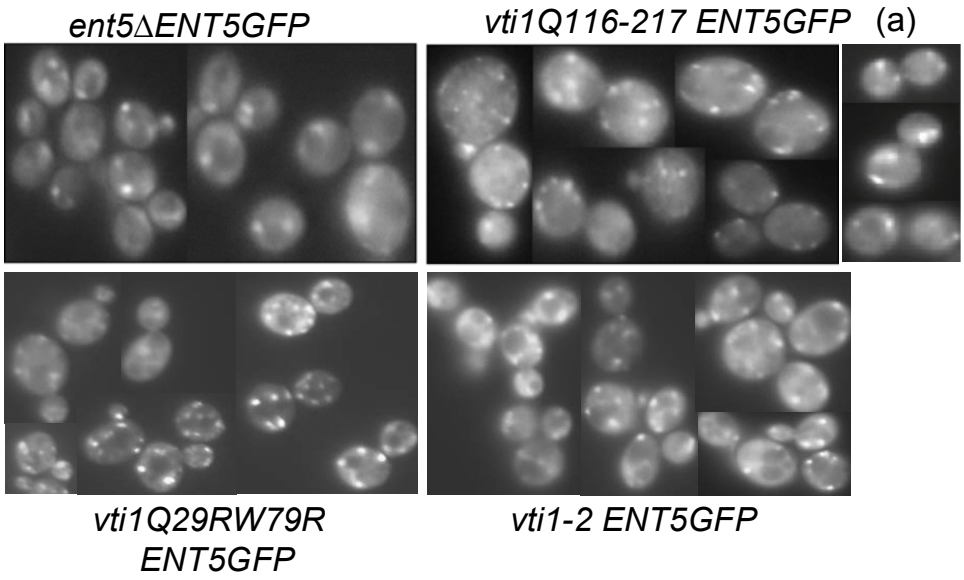

Fig.25(i). Fluorescence microscopy of Ent5p-GFP: The strains *ent5*ΔENT5GFP (SCY25 pSC24), *vti1Q29RW79R* ENT5GFP (SCY14 pSC24), *vti1Q116-217* ENT5GFP (FvMY6pBK117 pSC24) and *vti1-2* ENT5GFP (FvMY24 pSC24) were grown overnight at 30°C and the unfixed cells were imaged using a fluorescence microscope.

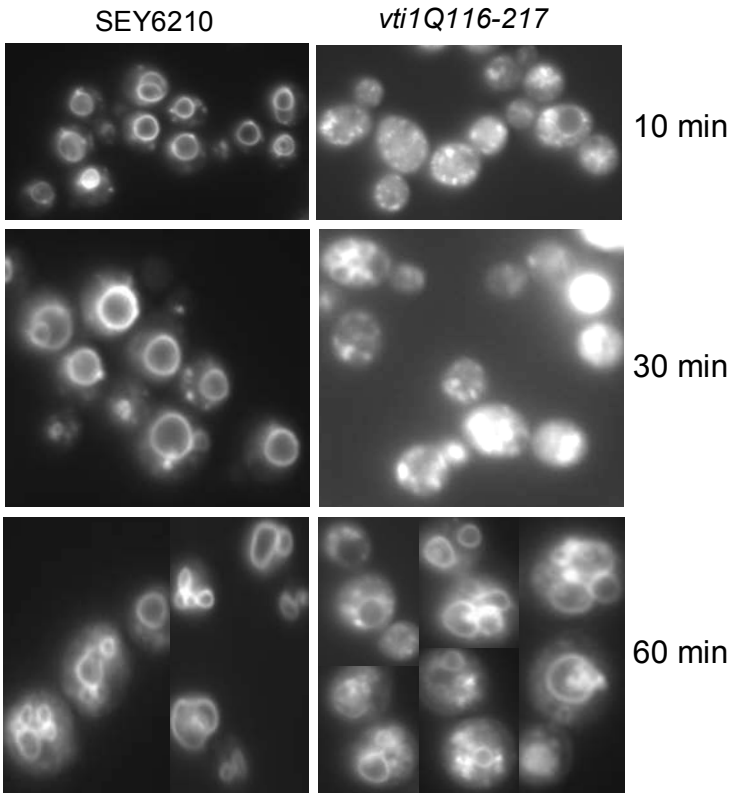

Fig.25(ii). Uptake of FM4-64 dye in N-terminal truncation: SEY6210 and *vti1Q116-217* cells were incubated with FM4-64 dye at 24°C for 10 min (pulse) and the cells were viewed after an additional incubation (chase) of 10 min or 30 min or 60 under the microscope.

3.3.4 Overexpression of Ent3p C-terminus and Ent3p in *vti1* mutants

The over expression of the C-terminus of the ENTH domain protein Epsin1 has a dominant negative effect in mammalian cells (Itoh *et al.*, 2001). A dominant negative effect can also be observed if a redundant protein is present. The C-terminus of Ent3p was over- expressed from a 2μ plasmid, to check whether it has a dominant negative effect on transport to the vacuole. Pulse chase immuno precipitation of CPY was done from SEY6210 and *vti1Q29RW79R* cells expressing the C-terminus of *ENT3* (pSC2) (Fig.26a). There was no dominant negative effect from the C-terminus of Ent3p. Then the full length Ent3p (pSC4) was overexpressed in the *vti1* mutants, to check whether the full length protein is able to suppress CPY sorting defects in *vti1* mutants (Fig.26b). It did not improve the sorting and showed neither dominant negative defect nor suppression in the 2 AA mutant.

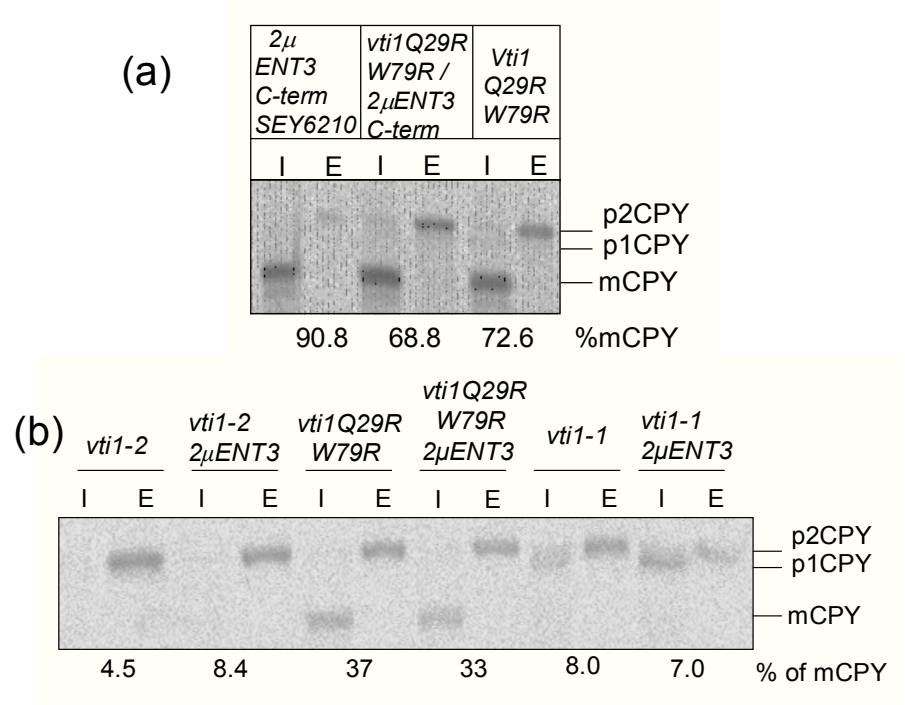

Fig.26. Overexpression of Ent3p in *vti1* mutants: Pulse chase immuno precipitation of CPY was done at 30°C (a) or at 37°C (b), from SEY6210 and *vti1Q29RW79R* (*CEN*) cells overexpressing the C-terminus of Ent3p (pSC2) (a) and from *vti1-2* (FvMY24), *vti1Q29RW79R* (*CEN*), *vti1-1* (FvMY7) cells overexpressing the full length Ent3p (pSC4) (b).

3.3.5 Vacuolar morphology of *ent* mutants by FM4-64 staining

The endocytosis and vacuolar morphology of *ent* mutants were studied by internalization of FM4-64 dye (Fig.27). The uptake was analyzed at different time points. There was no delay in the uptake of FM4-64 in the single *ent* mutants, *ent3*Δ*ent4*Δ and *ent4*Δ*ent5*Δ cells. In *ent3*Δ*ent4*Δ*ent5*Δ and *ent3*Δ*ent5*Δ, except very few cells which looked abnormal, in other cells the uptake was normal. There was no defect in the vacuolar morphology of the mutants.

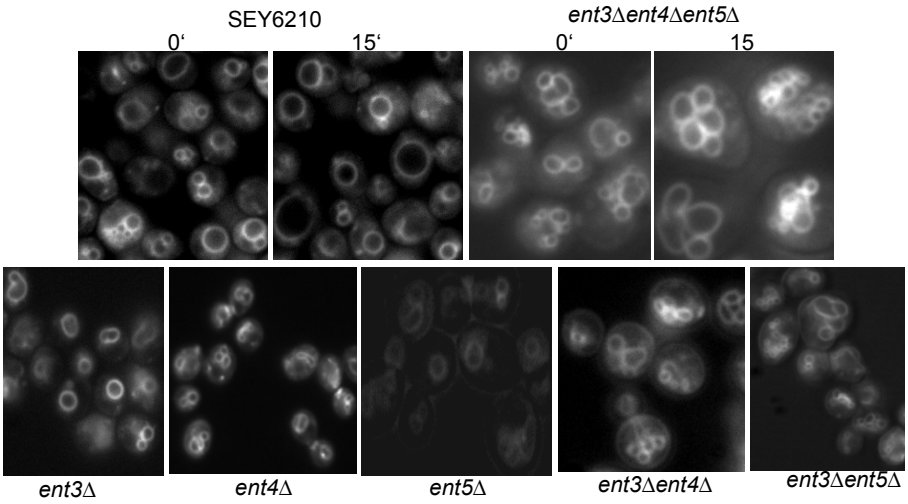

Fig.27. FM4-64 staining of *ent* mutants: SEY6210, *ent3*Δ (BKY22), *ent4*Δ (BKY23), *ent5*Δ (BKY24), *ent3*Δ*ent4*Δ (BKY19), *ent3*Δ*ent5*Δ (BKY20), *ent3*Δ *ent4*Δ*ent5*Δ (BKY18) cells were incubated with FM4-64 dye at 30°C for 15 min and viewed under microscope after an additional incubation of 0 min or 15 min for the top panel and 15 min for the lower panel.

3.3.6 Genetic interaction of Ent proteins with Vti1p

3.3.6.1 CPY pathway in *vti1* mutants with *ent* deletion

Different *vti1* mutant strains were used to investigate whether Ent3p or Ent5p have a functional connection with Vti1p and in which trafficking steps. *ent3* and *ent5* genes were deleted in the background of *vti1* mutants and pulse chase immuno precipitation was done (Fig.28). *vti1-1* cells are only defective in transport from the Golgi to the prevacuole. The absence of Ent3p reduced mCPY levels in *vti1-1* cells (SCY3) from 64.3% (SD 12.0) to 11.9% (SD 5.8, n=3) at a 33°C (Fig. 28a). Lack of Ent5p (BKY15) did not lead to a synthetic defect. *vti1-2* cells are defective in transport from the Golgi to the prevacuole as well as in transport to the vacuole. The deletion of Ent3p in the *vti1-2* cells (SCY1) reduced mCPY levels from 33% to 3.5%. The 2 AA N-terminal mutant, *vti1Q29RW79R* has a defect and only 33.5% of mCPY was present at 37°C (Fig.28b). The biosynthetic defect was pronounced in *vti1Q29RW79R* when *ent3* (SCY6) was deleted, in which only 13.5% of CPY was processed to the mature form at 37°C. There was no synthetic defect by the absence of Ent3p in the 1 AA mutants *vti1Q29R* (SCY8) and *vti1W79R* (SCY9).

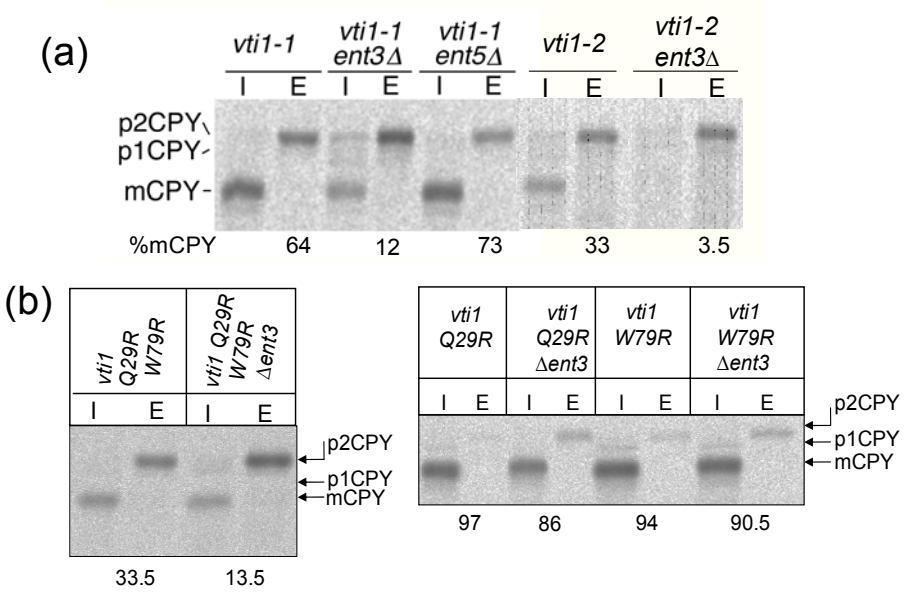

Fig.28. CPY pathway in *vti1* mutants with *ent* deletions: CPY was immuno precipitated from cellular extracts (I) and the medium (E) after pulse-chase labeling at 33°C for *vti1-1* (FvMY7), *vti1-1ent3*Δ (SCY3), *vti1-1ent5*Δ (BKY15) mutants, at 30°C for *vti1-2* (FvMY24), *vti1-2ent3*Δ (SCY1), mutants (a) and at 37°C for *vti1Q29RW79R* (FvMY6pBK120), *vti1Q29RW79R ent3*Δ (SCY6), *vti1Q29R* (FvMY6pBK123), *vti1Q29R ent3*Δ (SCY8), *vti1W79R* (FvMY6pBK128), *vti1W79R ent3*Δ (SCY9) mutants (b).

3.3.6.2 ALP pathway in *vti1* mutants with *ent* deletions

Vacuolar maturation of the pro form of alkaline phosphatase (ALP) was used as an assay for fusion with the vacuole because the pALP travels from the Golgi to the vacuole without passage through the prevacuole. Pulse chase immuno precipitation of ALP was done in the mutants (Fig.29). A deletion of *ent3* did not result in reduced appearance of vacuolar mALP in *vti1-1* and *vti1Q29RW79R* cells at semi permissive temperature (Fig. 29a). Slightly less mALP was found in the absence of Ent5p in *vti1-2* (BKY16) cells but not in the absence of Ent3p, after both a 5 min and a 30 min chase period (Fig.29b). After 30 min chase *vti1-2* and *vti1-2 ent3*Δ cells had 75.5% (SD 1.5) and 73.9% (SD 0.1) mALP respectively, but in the *vti1-2 ent5*Δ had 60% (SD1.0, n=2) of mALP.

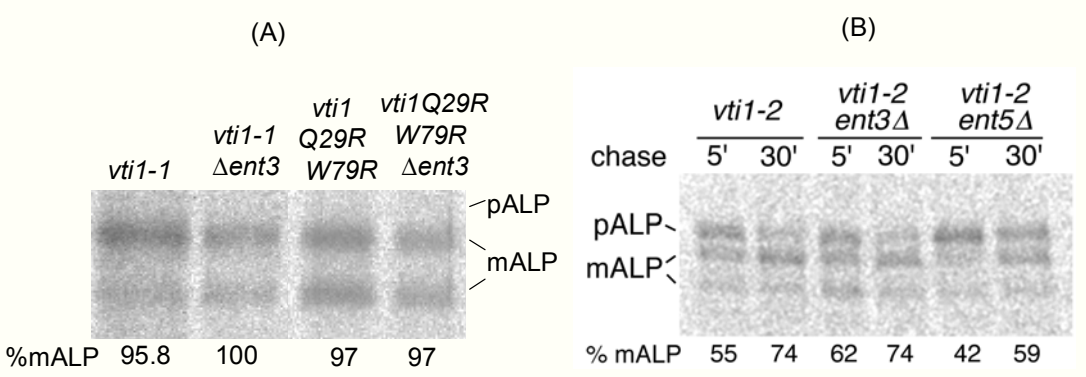

Fig.29. ALP pathway in *vti1* mutants with *ent* deletions: The cells were labeled at 30°C and chased for 30 min chase (a), for 5 min and 30 min (b) followed by immuno precipitation of ALP.

3.3.6.3 Synthetic growth defects of *ent* deletions in *vti1-2*

All the *ent* deletions in the background of *vti1* mutants were analyzed for their growth pattern to study the genetic interaction between the two proteins. There was no synthetic growth defect in the deletion mutants except in *vti1-2* mutants. *vti1-2* cells grow very slowly at 37°C. Both *vti1-2ent3*Δ and *vti1-2ent5*Δ cells were unable to grow at 37°C (Fig.30). The synthetic growth defect in *vti1-2ent3*Δ cells is probably due to reduced trafficking through the prevacuole which was detected as synthetic defect in CPY maturation (Fig.28a). The small synthetic defects in ALP maturation may be the reason for the synthetic growth defect in *vti1-2ent5*Δ cells (Fig.29b).

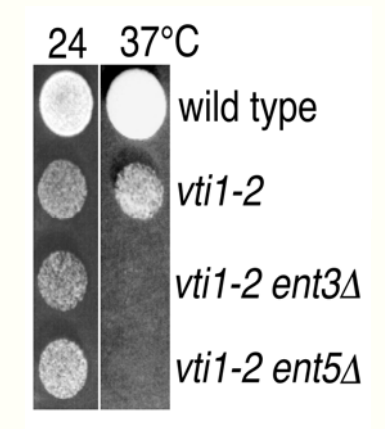

Fig.30. Synthetic growth defect in *vti1-2* mutants: The strains were grown overnight at 24°C and diluted cells were spotted on a YEPD plated, incubated at 24°C and 37°C and the growth was observed.

3.3.7 Cell wall defects in *ent3*Δ *ent5*Δ mutants

3.3.7.1 Abnormal cell shapes in *ent3*Δ *ent5*Δ

In the transmission light *ent3*Δ*ent5*Δ cells looked abnormal. To study the cell morphology clearly, chitin present in the cell wall and in the bud scar was stained with calcofluor (Fig.31). Some *ent3*Δ*ent5*Δ (BKY20) cells looked very abnormal in shape and displayed branched chain like budding pattern. They were larger than wild-type cells. The chitin ring was present in the bud neck of completely grown branched cells but the freshly budding cells lacked chitin in the bud neck (Fig.31, lower panel, 30°C). The mutant cells might have delayed formation of the septum or may be defective in cell separation process. But this abnormality was not a homogenous defect. In *ent3*Δ*ent5*Δ, the percentage of abnormal cells at 18°C was 20% and at 30°C, it was 12.8%. *ent3*Δ*ent4*Δ*ent5*Δ (BKY18) cells displayed similar phenotypes as *ent3*Δ*ent5*Δ cells. The rest of the cells were normal and the size was comparable to wild-type.

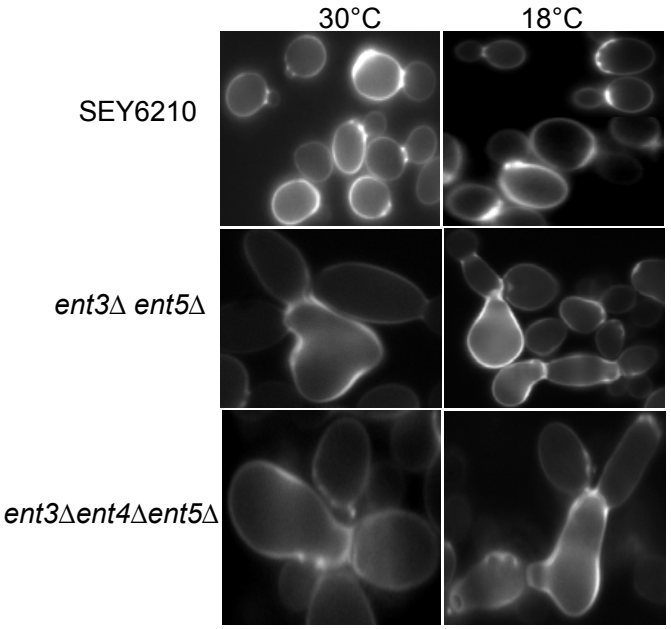

Fig.31. Calcofluor staining of *ent* mutants: SEY6210, *ent3*Δ*ent5*Δ (BKY20) and *ent3*Δ*ent4*Δ*ent5*Δ (BKY18) were grown at 24°C and shifted to 18°C or 30°C for 5 hrs or 2 hrs respectively. 10 µl of 1mg/ml calcofluor was added to the cells, incubated for 1h 30 min and imaged using a microscope.

3.3.7.2 Irregular distribution of Chitin and Actin assembly in *ent3*Δ*ent5*Δ

Since the cells were abnormal in shape, it was important to study the localization of actin assembly using phalloidin-fluorophor which binds polymerized actin, along with calcofluor (Fig.31). The yeast actin cytoskeleton is organized into atleast four biochemically and morphologically distinct structures, namely, cortical patches (discrete cytoskeletal bodies), actin cables (long bundles of actin filaments), the cap (polarized accumulation of cytoskeletal and regulatory proteins) and a cytokinetic ring (reviewed in: Pruyne and Bretscher, 2000). Cell polarity in budding yeast is established by a polarized actin cytoskeleton throughout the cell cycle. A cap (the bud site) of regulatory and cytoskeletal proteins establishes the polarity of actin cables and cortical patches (G1 phase). Actin cables then guide secretory vesicles to the cap, where they accumulate and fuse, thus polarizing growth. During isotropic growth (G2 and M phase), the proteins of the cap are more diffusely distributed, cortical patches are isotropically distributed and actin cables form a meshwork. A fourth cytoskeletal structure, a cytokinetic ring, mediates cell division when all the actin components reorient to the mother-bud junction.

The chitin and actin localization in some abnormal cells were shown in Fig.31a (Actin and chitin localization in the same cells). The actin filaments were absent in the abnormal cells from *ent3*Δ*ent5*Δ (BKY20). Also the number of actin patches was more in the abnormal cells. Chitin was deposited irregularly in the abnormal cells independent of the temperature. As shown in the middle panel of Fig.31a, all the cells were attached with each other but the cell having irregular chitin deposition lacks actin staining. The initial cells in the branch lost their actin staining as the branch grew. In the abnormal cells actin cap was formed properly even if the cells were not separated and elongated (Fig.31a, lower panel). Though the actin assembly was disorganized, the abnormal cells could form new buds, but could not get separated, resulting into branched cell morphology. These observations were restricted only to the 20% of the abnormal cells in the mutants whereas the rest of the cells exhibited wild-type phenotype. The cell cycle dependent actin localization in the normal cells of *ent3*Δ*ent5*Δ was shown in Fig.31b.

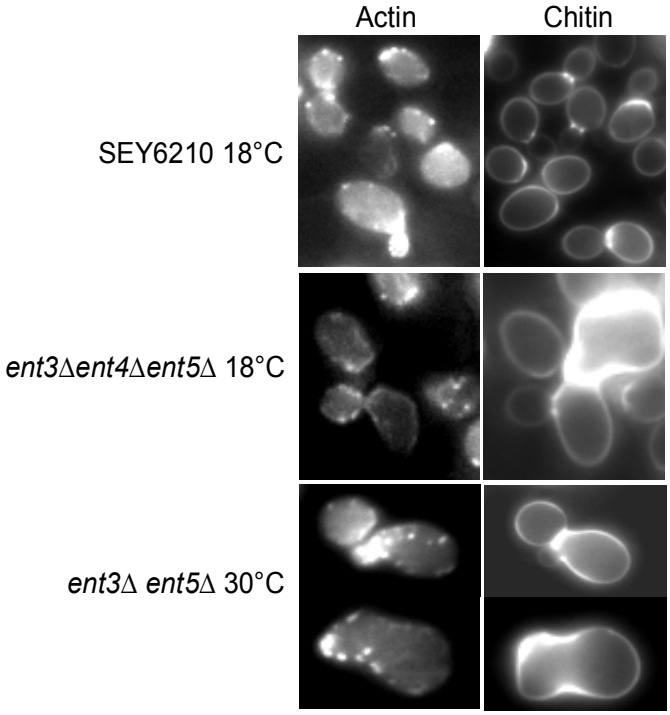

Fig.32a. Phalloidin and calcofluor staining of abnormal cells in *ent* mutants: SEY6210, *ent3*Δ*ent4*Δ*ent5*Δ (BKY18) and *ent3*Δ*ent5*Δ (BKY20) cells were grown at 24°C, shifted to 18°C or 30°C for 5 h or 2h respectively, incubated with phalloidin and calcofluor at the corresponding temperature for 1h 30 min and imaged using a fluorescence microscope.

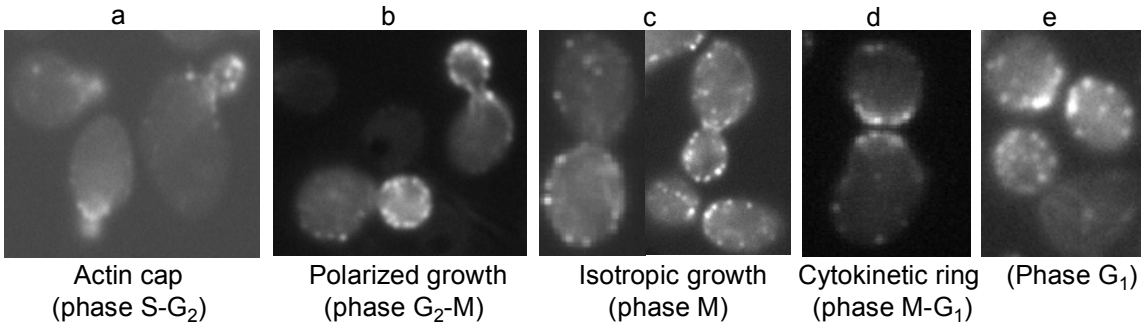

Fig.32b. Actin staining of normal cells in *ent3*Δ*ent5*Δ cells: Nearly 80 % of the cells displayed normal actin assembly. *ent3*Δ*ent5*Δ cells were stained with phalloidin as mentioned before. (a) Formation of actin cap structure in the bud site during the cell cycle phase S-G_2. (b) Actin patches and actin cables start distributing from the polarized growth at the beginning of M phase. (c) Isotropic distribution of actin patches and cables during M phase. (d) Actin structures are concentrated to form a cytokinetic ring in the beginning of G_1 phase. (e) After cytokinesis, actin patches are redistributed again isotropically.

3.3.7.3 Localization of Chs3p-GFP in *ent* mutants

The three chitin synthases of Saccharomyces cerevisiae, Chs1p, Chs2p, and Chs3p, participate in septum and cell wall formation of vegetative cells and in cell wall morphogenesis of conjugating cells and spores. Since in the *ent3*Δ*ent5*Δ cells, chitin deposition was irregular and also bud scar was not clearly present in some cells which indicated that the septum might not have formed well. Chs3p is responsible for the chitin synthesis in the septum wall formation (Shaw *et al.*, 1991) which is transported out of ER with the help of Chs7p and targeted to the plasma membrane via the Golgi with the help of Chs5p. Before being delivered to the bud neck, chs3p is recovered from the cell surface, stored in an endocytic structure and delivered to the bud neck by the vesicles that contain Tlg1p (Chuang and Schekman, 1996; Holthuis *et al.*, 1998). The plasmids, *CHS3GFP* (RSB2310) and *CHS7* (pSC23) were transformed into all the *ent* mutants and the localization of Chs3p was studied by GFP fluorescence (Fig.33). Chs3p-GFP was localized into the bud neck in small budded cells and in some internal compartments in wild-type. In some wild-type cells, ER localization was also observed. It could be because of the uneven expression of Chs7p which is needed for the exit of Chs3p from the ER. In all the mutant cells, Chs3p was present in the bud neck, in some internal compartments and also in the ER. In *ent3*Δ*ent4*Δ*ent5*Δ cells, the localization of Chs3p-GFP was analyzed at 18°C, 30°C and 37°C. This experiment showed that Chs3p reached its destination in the mutants, for example, in the budding cells, Chs3p was present in the bud site and in the bud neck. The localization of Chs3p-GFP was very heterogeneous in different cells from wild type as well as in mutants. No differences in overall staining pattern were detected.

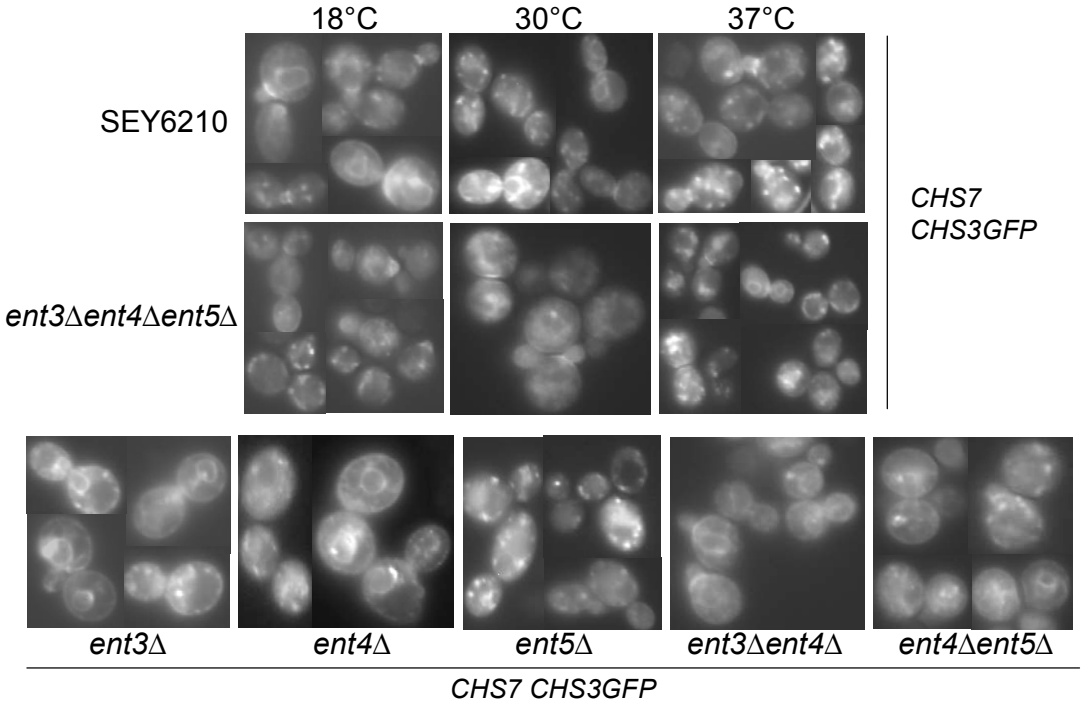

Fig.33. Chs3p localization in *ent* mutants (mixed background): SEY6210, *ent3*Δ (BKY22), *ent4*Δ (BKY23), *ent5*Δ (BKY24), *ent3*Δ*ent4*Δ (BKY19), *ent4*Δ*ent5*Δ (BKY21), *ent3*Δ*ent4*Δ*ent5*Δ (BKY18) cells expressing Chs7p and Chs3p-GFP were grown overnight at 18°C or 30°C or 37°C and viewed under microscope. In the lower panel, cells from 30°C were shown.

3.3.7.4 Aniline blue staining of *ent* mutants

The yeast cell wall represents a complex structure of cross linked chitin, 1, 3-β-Glucan, 1, 6-β-Glucan and mannoproteins. Since chitin deposition was not regular in *ent* mutants, it was interesting to check whether 1, 3-β-glucan deposition was normal. Aniline blue (also called as Methyl blue) specifically stains the 1, 3-β-glucan layer in the cell wall. All the *ent* mutants were stained with aniline blue (Fig.34). No defect in the 1,3-β-glucan layer of *ent* mutants was observed.

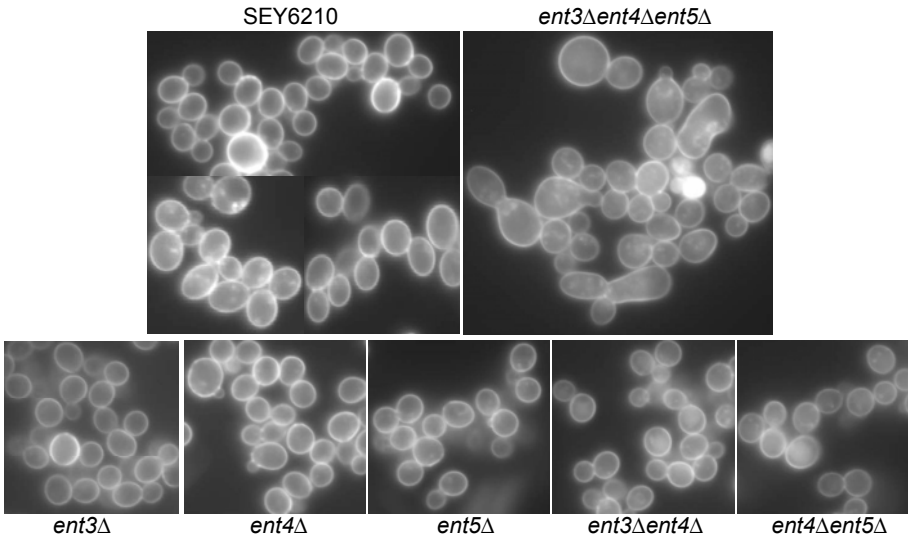

Fig.34. Aniline blue staining of *ent* mutants (mixed background): SEY6210, *ent3*Δ (BKY22), *ent4*Δ (BKY23), *ent5*Δ (BKY24), *ent3*Δ*ent4*Δ (BKY19), *ent4*Δ*ent5*Δ (BKY21), *ent3*Δ*ent4*Δ*ent5*Δ (BKY18) cells were grown overnight at 30°C and viewed under microscope.

3.3.7.5 Growth defects caused by cell wall perturbing agents

The growth pattern of *ent* mutants were analyzed on 1M NaCl, 1.4 M NaCl, 50 µg/ml calcofluor and on 0.05% SDS (Fig.35). These agents are generally used to screen cell wall mutants. Yeast cell have a rigid cell wall and higher internal turgor pressure. If the cell wall is defective, the cells can not grow on high osmotic or salt stress (NaCl) because of the loss of the turgor pressure. SDS, as a detergent, will solubilize protein and disrupt the architecture of the cell wall. Calcofluor white is a negatively charged fluorescent dye that binds to nascent chains of chitin and, to a lesser extent, glucan through hydrogen bonding and dipole interactions and, by preventing microfibril assembly, interferes directly with the supramolecular organization of the cell wall (Elorza *et al.*, 1983; Murgui *et al.*, 1985; Ram *et al.*, 1994). A disturbed or weakened cell wall is not able to withstand drug concentrations that do not affect normal wild-type cells. *ent3*Δ*ent4*Δ*ent5*Δ and *ent3*Δ*ent5*Δ cells were sensitive to all the tested cell wall perturbing agents except that *ent3*Δ*ent5*Δ was not sensitive to 1 M NaCl. *ent3*Δ was sensitive to SDS and calcofluor. This shows that *ent* deletions have a defective cell wall.

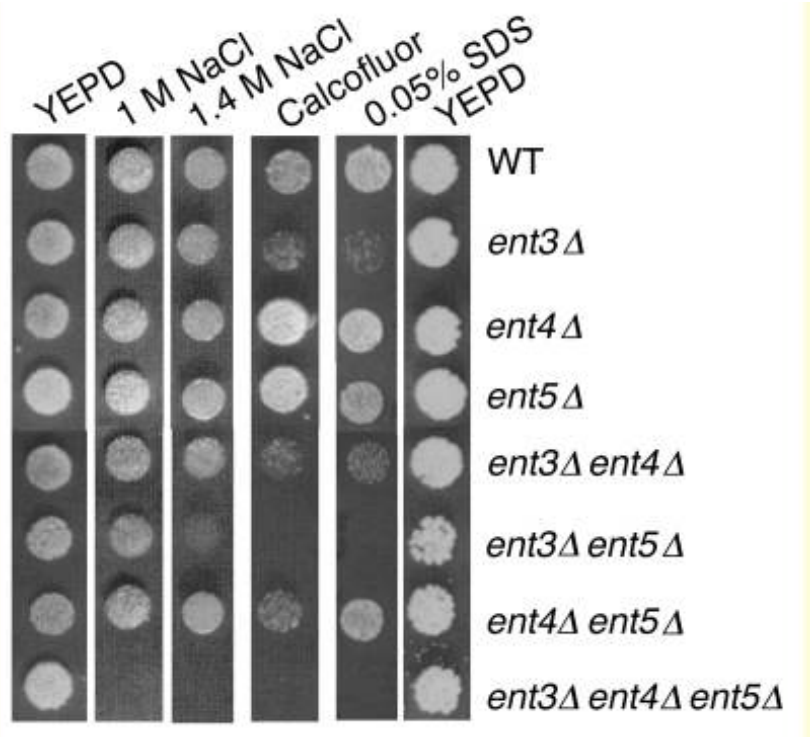

Fig.35. Growth defects of *ent* mutants by cell wall perturbing agent: BY4742, *ent3*Δ, *ent4*Δ, *ent5*Δ, *ent3*Δ*ent4*Δ (SCY5), *ent3*Δ*ent4*Δ (BKY13), *ent4*Δ*ent5*Δ (BKY17), *ent3*Δ*ent4*Δ*ent5*Δ (BKY18). Cells were grown at 24°C and different dilutions were spotted on YEPD plate and YEPD containing 1M NaCl, 1.4 M NaCl, 50 µg/ml calcofluor, 0.05% SDS and incubated at 30°C. All mutants are in BY4742 background except *ent3*Δ*ent4*Δ*ent5*Δ cells which is in the mixed BY4742 x SEY6210 background.

3.3.7.6 Zymolyase sensitivity curve

Zymolyase is a β-1, 3- Glucanase enzyme which cleaves the β-1, 3- glucosidic linkages. Cells would show altered sensitivity to zymolyase, if the cell wall composition was altered. Sensitivity to zymolyase may reflect changes in the β-1, 3-glucan layer (Ovalle *et al.*, 1998) or changes in the external mannoprotein layer that result in altered permeability to cell wall degrading enzymes (De Nobel *et al.*, 1991). *ent* mutants were incubated with zymolyase and every one hour the optical densitiy was measured (Fig.36). Δ*ent3* cells behaved like the wild type cells whereas Δ*ent5* and Δ*ent3*Δ*ent5* were more resistant to zymolyase which showed that the cell wall composition was altered in Δ*ent3*Δ*ent5* and Δ*ent5* mutants.

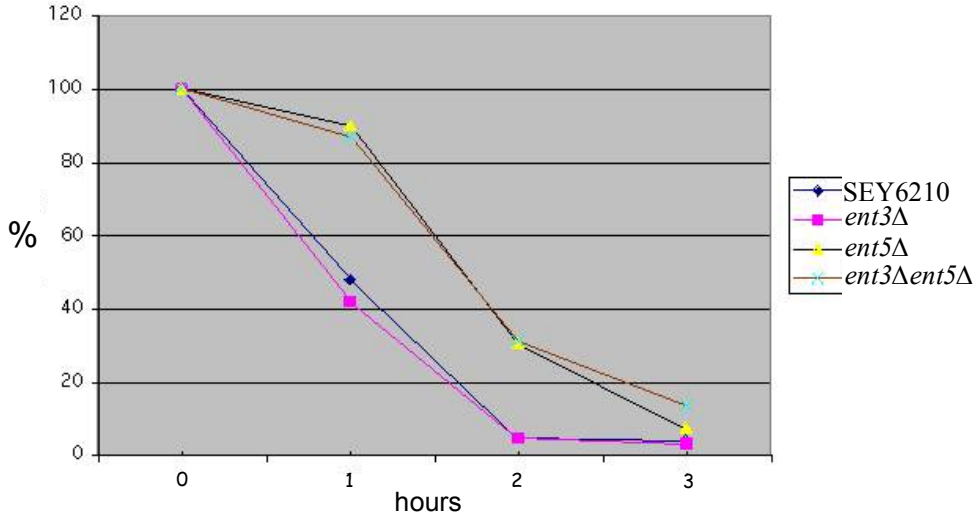

Fig.36. Zymolyase sensitivity curve: SEY6210, Δ*ent3* (SCY2), Δ*ent5* (SCY25) and Δ*ent3* Δ*ent5* (SCY26) cells were grown overnight at 24°C and incubated with zymolyase (5µg/ml) at 37°C. Every one hour the OD_{600} was measured for 3 h and the percentage of the final OD was calculated. OD: optical density.

3.3.8 Interaction of Ent3p with Pep12p and Syn8p

3.3.8.1 Two hybrid interactions of Ent3p

A two hybrid assay was done in the group to find out whether Ent3p interacts with other SNARE proteins apart from Vti1p (Fig.37a). Interestingly, Ent3p interacted with the N-terminal domains of Syn8p and Pep12p which are present in the endosomal SNARE complex with Vti1p and didn't interact with Tlg1p. EpsinR was used as a control. This two hybrid interaction was confirmed further by an *in vitro* pull down assay using His tagged Vti1p, Pep12p, Tlg1p and Syn8p with Strep tagged Ent3p (Fig.37b).

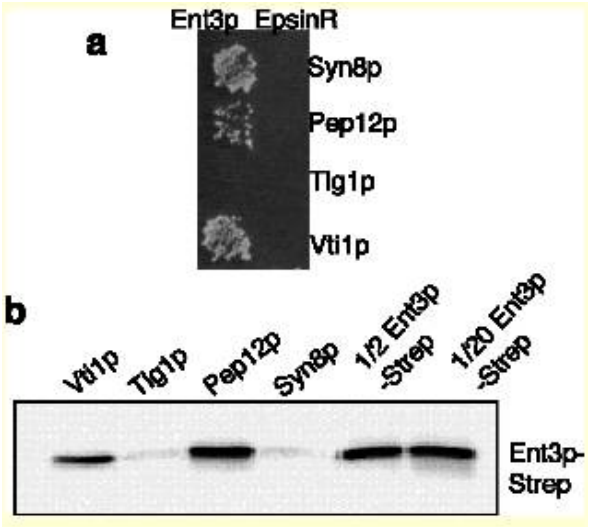

Fig.37. **(a) Two hybrid interactions** were detected between Ent3p and Syn8p and Pep12p. No interaction was found with Tlg1p. The interactions with EpsinR were used as a negative control. **(b) In vitro binding assay** was done as mentioned before with slight changes in the binding buffer. 1/20 Ent3p-Strep: 1/20 of the protein used in the assay.

3.3.8.2 Pep12p and vti1-2p are stabilized in *ent3*Δ cells

The stability of Pep12p and vti1-2p were studied in the *ent* mutants by pulse chase immuno precipitation of Pep12p and Vti1p (Fig.38). vti1-2p was more stable when *ent3* was deleted (Fig.38a) and the same was true for Pep12p (SCY2) (Fig.38b). The amount of vti1-2p after 2 h chase in *vti1-2* was 81.37 % (SD 41, n=3), in *vti1-2ent3*Δ 116.4 % (SD 26) and in SEY6210 97 % (SD 5.7). Absence of Ent5p (SCY25) did not lead to stabilization of Pep12p. In Δ*ent3*Δ*ent5* (SCY26), a slight stabilization of Pep12p could be observed. After 3 h of chase, 26.9 % [SD 0.2, n=3] Pep12p was present in the wild type, 28.25 % (SD 8.13) in *ent5*Δ cells whereas in *ent3*Δ, 56.5% [SD 10.6, n=3] was present. In Δ*ent3*Δ*ent5* cells, 34.7 % (SD 5.6) Pep12p was found. After 5 h of chase, the amount of Pep12p in wild type was 13 % (n=1), in *ent3*Δ 33.6 %, in *ent5*Δ 10.5 % and in Δ*ent3*Δ*ent5* 25.6 %. The epistatic effect of *ENT5* might have masked the effect of *ENT3*, resulting in less stabilization of Pep12p in Δ*ent3*Δ*ent5*. Three experiments were done which were reproducible both for vti1-2p and Pep12p. Ent3p might be required for the anterograde transport of Pep12p and vti1-2p.

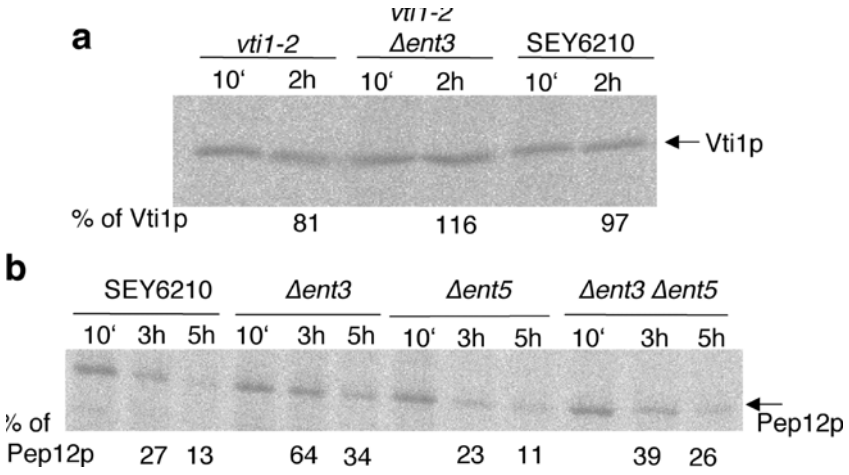

Fig.38. Stability of Pep12p and vti1-2p in *ent* mutants: Cells grown at 24°C were labeled with radioactive methionine for 30min and chased for 10 min or 2h or 3h or for 5h at 37°C. Vti1p (a) and Pep12p (b) were immunoprecipitated from cellular extracts, separated by SDS-PAGE and quantified by phospho imager.

3.3.8.3 Localization of Pep12p in *ent* deletion cells

Indirect immuno fluorescence of Pep12p was done in the *ent* mutants to study the localization of Pep12p (Fig.39). Both in wildtype and mutant cells, Pep12p was localized to punctuate structures corresponding to prevacuolar endosomes. Pep12p localization was not affected in the *ent* mutants. This should be further confirmed by sucellular fractionation of the *ent* mutants.

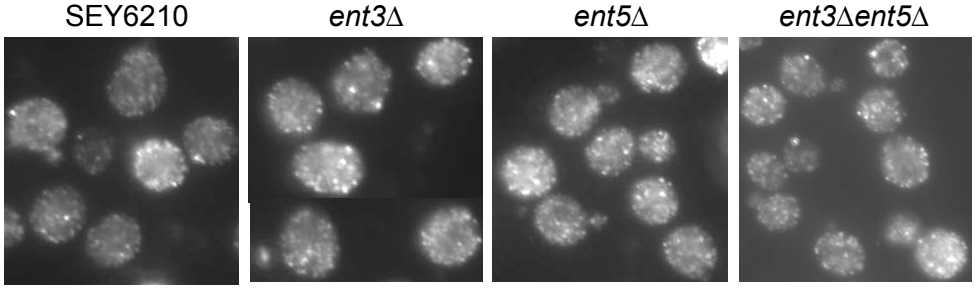

Fig.39. Immunofluorescence of Pep12p in *ent* deletion cells: SEY6210, Δ*ent3* (SCY2), Δ*ent5* (SCY25), Δ*ent3*Δ*ent5* (SCY26) cells were fixed, treated with monoclonal antibody against Pep12p and using a fluorescing secondary antibody, Pep12p was localized.

3.3.8.4 Synthetic growth defect of *pep12* deletion in *ent* mutants

To study the genetic interaction between *PEP12* and *ENT*, the mutants were scored for growth at 37°C (Fig.40). *ent3*Δ*pep12*Δ and *ent3*Δ*ent5*Δ*pep12*Δ cells could not grow at 37°C. When cells were grown on plates containing 1 M NaCl and 1.4 M NaCl at 30°C, *ent3*Δ*pep12*Δ and *ent3*Δ*ent5*Δ*pep12*Δ showed a synthetic growth defect. The cells did not grow on plates containing calcofluor and SDS (even the SEY6210 wild type). Only cells from the BY4742 background could grow on calcofluor and SDS.

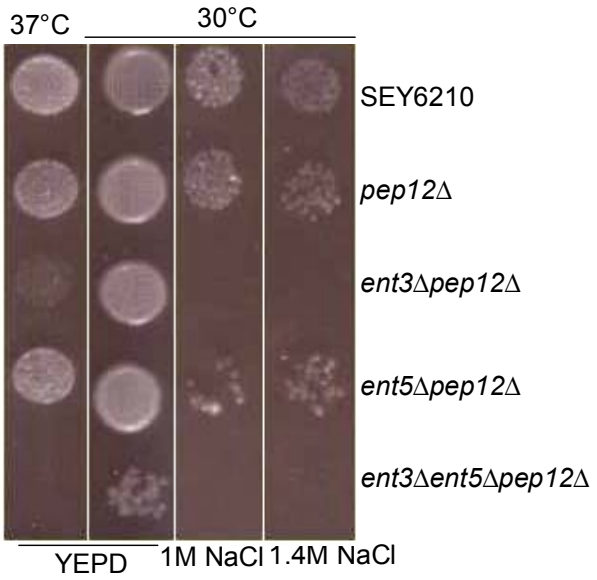

Fig.40. Growth test for *pep12* deletion in *ent* mutants: SEY6210, *pep12*Δ (SCY27), *ent3*Δ*pep12*Δ (SSY1), *ent5*Δ*pep12*Δ (SSY2), *ent3*Δ*ent5*Δ*pep12*Δ (SSY3) cells were spotted on YEPD and plates containing 1 and 1.4 M NaCl and incubated at 37°C or 30°C. All the mutants are in SEY6210/6211 background.

3.3.8.5 vti1-2p was destabilized in *ent5*Δ

The vti1-2p was stabilized in the absence of Ent3p but destabilized by the absence of Ent5p (SCY25), shown by pulse chase immuno precipitation of Vti1p at 37°C (Fig.41a). After 5 h of chase the amount of vti1-2p in *vti1-2* cells was, 71 % [SD 4.2 (n=3)], which was reduced to 47 % [SD 1.3, (n=3)] in *vti1-2ent5*Δ cells. In *vti1-2ent5*Δ*pep4*Δ (SCY23) cells, similar amounts of vti1-2p remained after 3 h and 5 h compared to *vti1-2pep4*Δ (MDY7). This indicated that the vti1-2p was degraded by the vacuolar degradation pathway. But this effect was temperature dependent. At 30°C, vti1-2p was neither destabilized in the absence of Ent5p nor stabilized in the absence of Ent3p (Fig.41b).

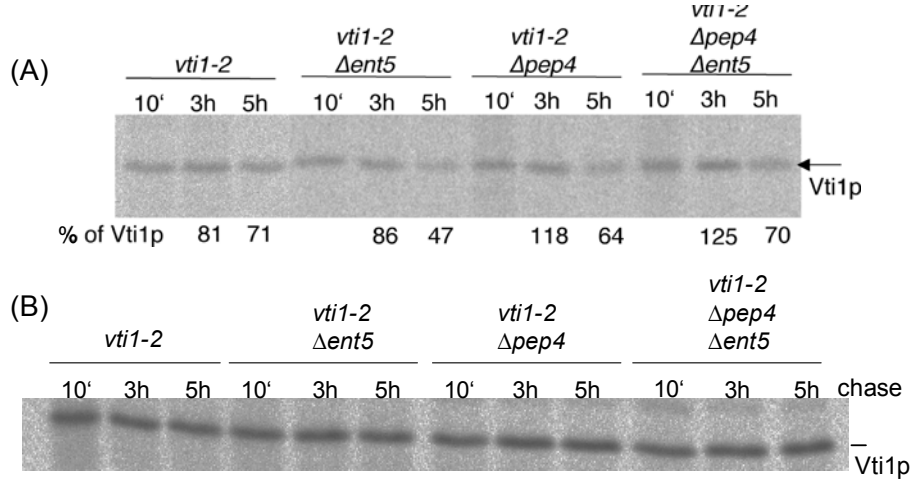

Fig.41.Stability of vti1-2p in *ent* mutants: cells were labeled at 37°C (A) or 30°C (B), chased for 10 min or 3 h or 5 h and Vti1p was immuno precipitated.

3.3.8.6 Stability of Vti1p in *ent* mutants

The vti1-2p showed temperature dependent stability which did not give a clear idea of whether absence of Ent5p leads to destabilization of Vti1p. Pulse chase immuno precipitation of Vti1p was done at 37°C from the *ent* mutants (Fig.42). There was no difference in the stability of Vti1p between the wild type and *ent3*Δ (SCY2), *ent5*Δ (SCY25) and *ent3*Δ*ent5*Δ (SCY26). Vti1p was stabilized in *pep4*Δ (BKY12), *ent3*Δ*pep4*Δ (SCY28) and *ent5*Δ*pep4*Δ (SCY24). Vti1p was neither destabilized in *ent5*Δ nor stabilized in *ent3*Δ.

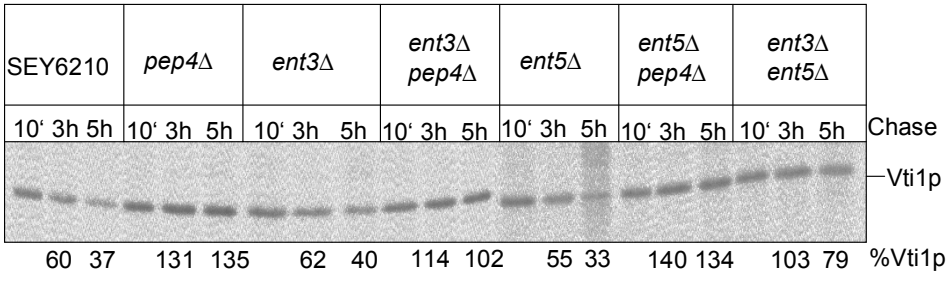

Fig.42. Stability of Vti1p in *ent* mutants: Cells were labeled at 37°C and chased for 10 min or 3 h or 5 h and Vti1p was immunoprecipitated.

3.3.8.7 Subcellular distribution of Vti1p in *ent* mutants

Subcellular fractionation of wild type and *ent* mutants were done to study the redistribution of Vti1p in *ent* mutants (Fig.43). Both in the wild type and in the mutants, Vti1p was present in the P13 and P200 (in pre vacuolar membrane and in Golgi). Vph1p, vacuolar ATPase and PGK, a soluble protein were used as controls. There was no redistribution of Vti1p in the *ent* mutants. But it is difficult to differentiate subtle changes by subcellular fractionation.

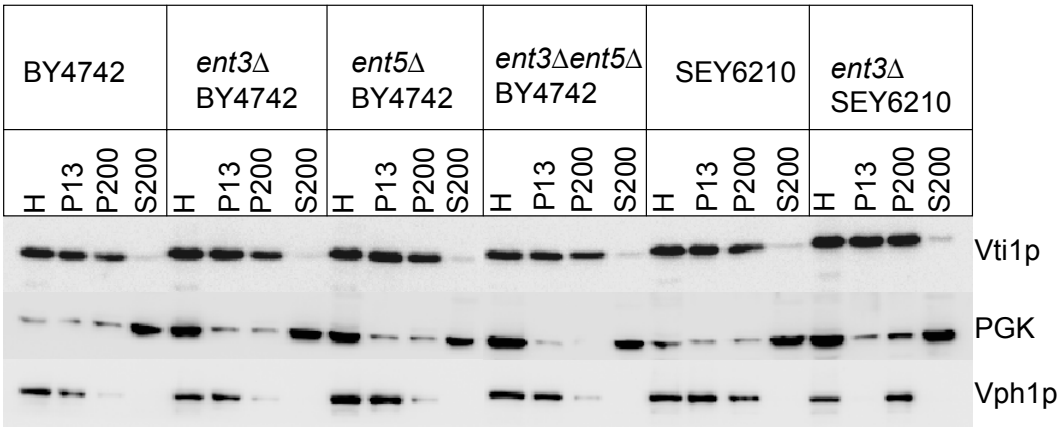

Fig.43. Subcellular fractionation of *ent* mutants: BY4742, *ent3*ΔBY4742, *ent5*Δ BY4742, *ent3*Δ*ent5*ΔBY4742 (BKY13), SEY6210 and *ent3*ΔSEY6210 (SCY2) homogenates were prepared by gentle lysis method, fractionated and the blot was probed with antisera against Vti1p, PGK and Vph1p. Starting volume was 1ml and equal volume was loaded.

3.3.8.8 Vti1p Immunofluorescence in *ent* mutants

Vti1p was localized to the punctuate structures of Golgi and PVC, both in the wild type and *ent* mutants studied by indirect immuno fluorescence of Vti1p (Fig.44). No change in the localization of Vti1p in *ent* mutants was observed.

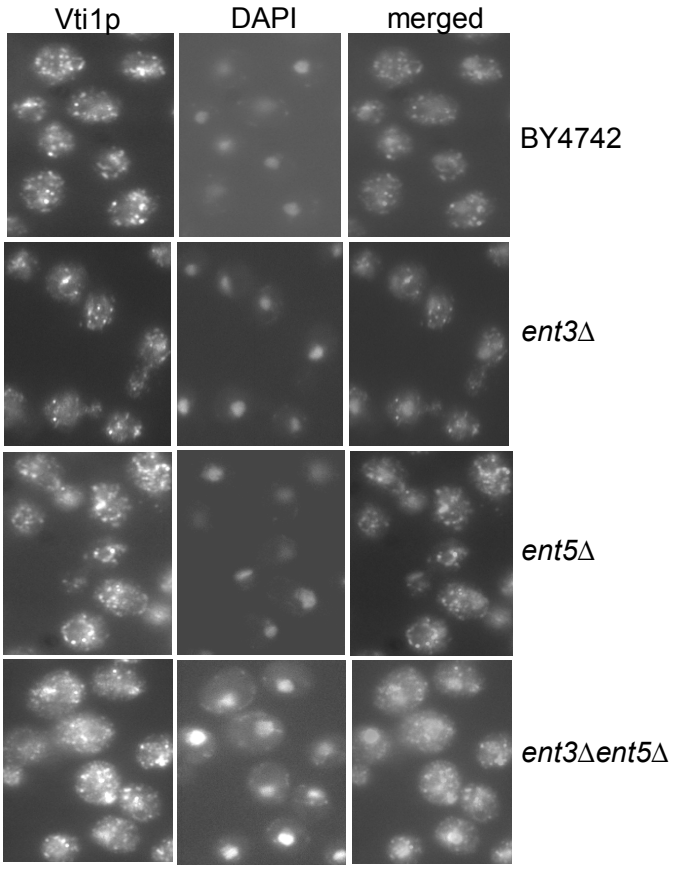

Fig.44. Immunofluorescence of Vti1p in *ent* mutants: Vti1p was localized in BY4742, *ent3*Δ, *ent5*Δ and *ent3*Δ*ent5*Δ (BKY13). DAPI staining was done to localize nucleus.

3.3.9 The composition of endosomal SNARE complex in *ent3*Δ*ent5*Δ

Since Ent3p interacted with Vti1p, Pep12p and Syn8p from the endosomal SNARE complex, it might be possible that Ent3p interacts with the whole SNARE complex and regulate the formation and dissociation of the complex. To check whether deletion of *ent3* or *ent5* affected the amounts of SNAREs present in the complex, immunoprecipitaion was done using Pep12p antibody from *ent3*Δ*ent5*Δ (SCY26) (Fig.45). A co-immuno-precipitation of Vti1p was observed. There was no change in the amounts of Vti1p which co-immnuoprecipitated with Pep12p in the *ent* mutant.

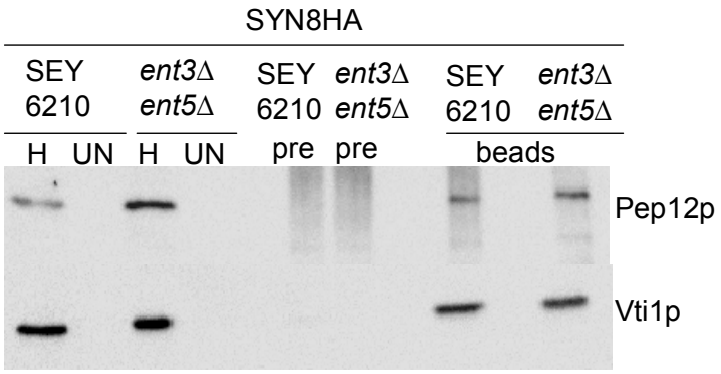

Fig.45. Immunoprecipitation of SNARE complex in *ent3*Δ*ent5*Δ: SEY6210 and *ent3*Δ*ent5*Δ (SCY26) cells expressing Syn8pHA (pSC19) were used to precipitate SNARE complex using beads crosslinked with antisera against Pep12p. H: homogenate; UN: unbound; pre: preimmune.

3.3.10 Retrograde transport of A-ALP and Vps10p

To study if Ent5p or Ent3p were involved in the retrograde transport, the stability of A-ALP and Vps10p which recycle between TGN and endosome, was analyzed (Fig.46). Vps10p is a receptor that sorts several different vacuolar proteins by cycling between a late Golgi compartment and the endosome. Vps10p is the receptor for CPY. A-ALP consists of the cytosolic domain of dipeptidyl aminopeptidase A [DPAP A] fused to the transmembrane and lumenal domains of the alkaline phosphatase [ALP]), which localizes to the yeast TGN. The cytosolic tail of DPAP A confers recycling between the TGN and the endosome. The delivery of this protein to the vacuole can be monitored by proteolytic maturation of proALP. Pulse chase immuno precipitation of A-ALP was done from *ent* deletions in *pho8* (which codes for ALP) deleted cells, transformed with the A-ALP plasmid (Fig.46a). After 120 min of chase, 59.4 % (n=1) mALP was present in *pho8*Δ cells, 52.8 % in *pho8*Δ*ent3*Δ (BKY25), 54.4 % in *pho8*Δ*ent5*Δ (BKY26). There was no destabilization of A-ALP in the mutants. The amount of Vps10p in wild type cells was 110 % (n=1), in *ent3*Δ (SCY2) 119 %, in *ent5*Δ (SCY25) 272 % and in *ent3*Δ*ent5*Δ (SCY26) 115 % (Fig.46b). The high value in *ent5*Δ cells might be due to technical problems since the 3 h band was optically comparable with other strains. Vps10p was also not affected in the *ent* mutants.

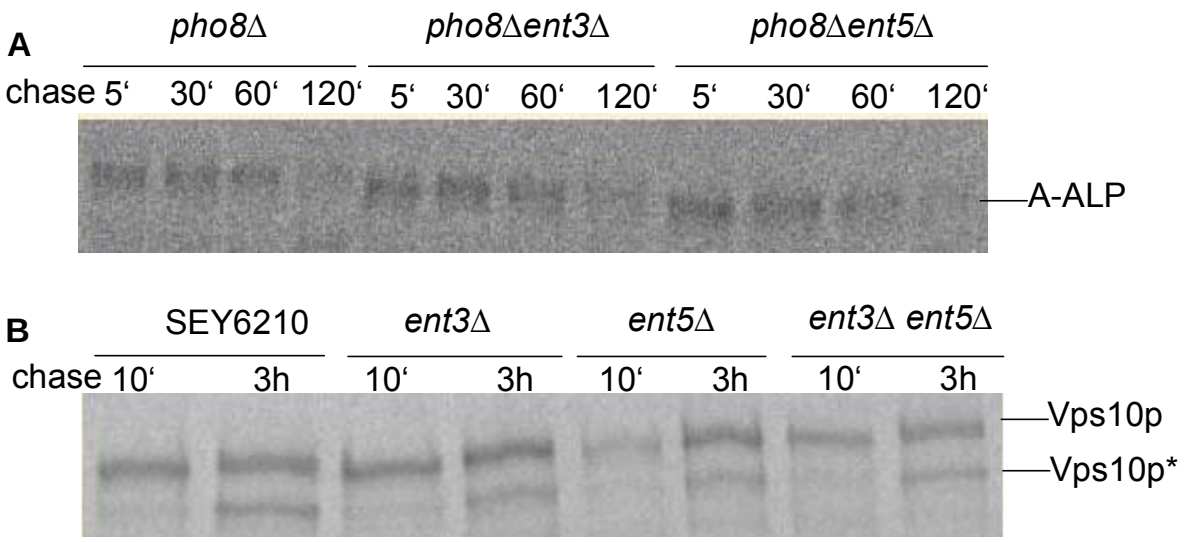

Fig.46. Pulse chase immunoprecipitation of A-ALP (a) and Vps10p (b): Cells were labeled at 37°C and chased for 5 min or 30 min or 60 min or 120 min for A-ALP and 10min and 3 h for Vps10p. Vps10p*: degraded Vps10p.

3.3.11 Role of Ent proteins in pApe1p processing

Amino peptidase I reach the vacuole through the CVT pathway in logarithmically growing cells and in early stationary cells and through autophagy in stationary and starved cells. These pathways were analyzed in the *ent* mutants to investigate the involvement of Ent proteins in this transport route (Fig.47). pApe1p would appear if the CVT pathway or the autophagy was blocked. In *ent3*Δ, pApe1p was present more in the log phase cells. But, the *ent3*Δ*ent5*Δ cells did not have pApe1p in both the phases. There may be some factors in *ent3*Δ*ent5*Δ cells which rescued the effect of *ent3*Δ or the comparatively slow growth of *ent3*Δ*ent5*Δ cells might have induced autophagy and pApe1p was processed. In the nitrogen starved cells, Ape1p was processed properly showing that autophagy was not affected by Ent proteins.

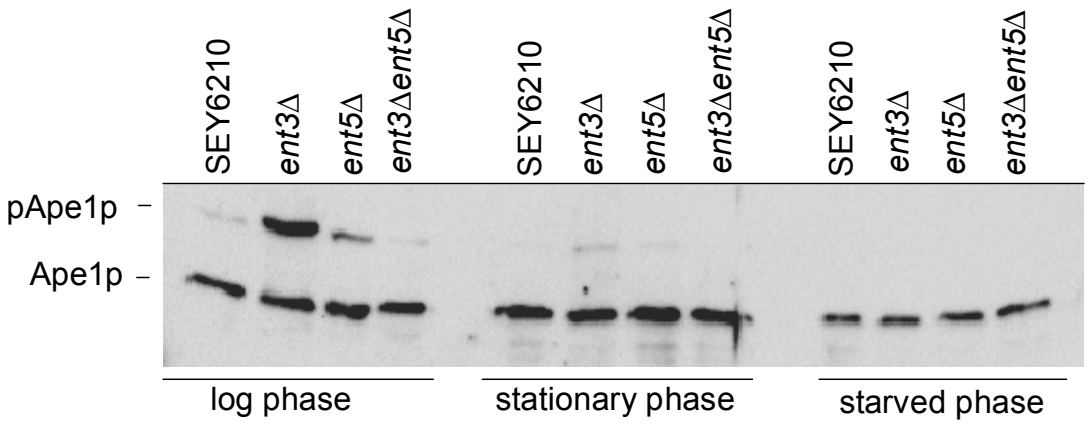

Fig.47. Ape1p processing in *ent* mutants: protein extracts were prepared from SEY6210, *ent3*Δ SEY6210 (SCY2), *ent5*ΔSEY6210 (SCY25) and *ent3*Δ*ent5*Δ (SCY26) cells from log phase, stationary phase and nitrogen starved condition. pApe1p:proApe1p. log phase: till OD_{600} 1.2; stationary phase: around 24 h growth, OD_{600} 3 to 8.

4 Discussion

The main aim of this study was to identify and characterize the interaction partners of Vti1p and to unravel the function of the N-terminus of Vti1p. In the first part, the importance of the N-terminus of Vti1p is discussed and in the second part the interaction between Vti1p and Ent3p is elaborated with comments on the characterization of the *ent* mutants.

4.1 Function of the N-terminus of Vti1p

The N-terminal domains of all syntaxins have overall similar structures. The N-terminal domain of neuronal syntaxin 1 and its yeast plasma membrane homologue Sso1p consists of a three-helix bundle which interacts with its own SNARE motif resulting into closed conformation and can down regulate the capability to form SNARE complexes (Dulubova *et al.*, 1999; Munson *et al.*, 2000). But when the N-terminal domain of Sso1p was removed, formation of the SNARE complex assembly was accelerated (Nicholson *et al.*, 1998). The SNAREs classified in the group of Qb and Qc are more divergent, and only few structures are known. Vti1p is a Qb SNARE and the function of the N-terminal domain is completely unknown. The identification of structurally related regions in Tlg1p and Vti1p argue that the N-terminal regions of these nonsyntaxin SNAREs are likely to mediate equal inhibitory intramolecular interactions that regulate fusion. The N-terminus of vti1b forms 3-helix bundles resembling syntaxin1, Sso1p and Vam3p but do not bind with the SNARE motif and has no influence on the assembly kinetics (Antonin *et al.*, 2002a). *In vitro* liposome fusion assays of N-terminal truncated Pep12p/Tlg1p and Vti1p (111-216) with all of the potential v-SNAREs in yeast showed that the specificity of fusion is fully conserved in the absence of any of the N-terminal domains (Paumet *et al.*, 2004). The removal of the N-terminal domains of Vti1p (1-118) and Tlg1p increases the fusion kinetics of the early endocytic/TGN complex and late endocytic complex in, *in vitro* liposome fusion assays (Paumet *et al.*, 2005). In this study, *vti1Q29RW79R,* a mutant having two amino acid replacements in the amino terminal region (2 AA mutant) has been employed to study the function of the N-terminus of Vti1p. Vti1p has high content of α-helices, 82.95% determined by PROF predictions of secondary structure of

proteins. In vtiQ29RW79Rp, the predicted α-helix content is 83.4%, the increase in the α-helix content is provided by the replacement of tryptophan at 79 with arginine which also created a phosphorylation site for cAMP- and cGMP-dependent protein kinase in the mutant Vti1p. *vti1Q29RW79R* is not a dominant negative mutation indicating that it does not sequester binding partners which are rate limiting.

A portion of the slightly overexpressed vti1Q29RW79Rp is localized to the ER. The fraction of ER localized vti1Q29RW79Rp increased upon shift to 37°C. The 1AA mutants, vti1Q29Rp and vti1W79Rp are partially localized to the vacuole whereas the genomically integrated 2 AA mutant did not show a strong ER localization. But, when Vti1p-HA was slightly overexpressed, it did not localize to the ER. This gives a hint that the N-terminal domain might contain some signal for the localization of Vti1p. The N-terminal extension of VAMP-4 contains a target signal for the TGN (Zeng *et al.*, 2003). The N-terminal (longin) domain of rat Ykt6 is required for its sub-cellular particle localization (Hasegawa *et al.*, 2003). The longin domain of the Vamp7p from *Arabidopsis thaliana* is necessary for its vacuolar and sub-cellular targeting (Uemura *et al.*, 2005). However, further studies on the localization of the N-terminal truncations (which was difficult to analyze since the antiserum against Vti1p did not recognize the truncated versions) should give clear view of the role played by N-terminus in the localization of Vti1p. On the other hand, the stability of the proteins could give an indirect idea about their localization. The Vti1p is very stable and degraded by the vacuolar proteases whereas vtiQ29RW79Rp is highly unstable and requires polyubiquitination for its degradation. The N-terminus of the Vti1p might be responsible for the protein conformation or binding of the N-terminus with some stabilizing factor might have been disrupted, leading to instability of the mutant Vti1p. The N-terminal domain of Ykt6 forms a folded back conformation which is important for the stability of the protein (Tochio *et al.*, 2001). The reason for the ER localization of *CEN* 2 AA mutant but not genomically integrated mutation, could be because of the slow exit kinetics of *CEN* 2AA mutant or there might be too much protein for the slow residual pathway. In other case, the degradation kinetics of the 2 AA mutant might have an effect on the localization. The N-terminus of Vti1p might have signals for its localization and is required for the stability and proper degradation of Vti1p.

The defect in the maturation of CPY but not ALP in *vti1Q29RW79R* cells demonstrates that the N-terminus of Vti1p is important for its function only in the traffic from the TGN to the prevacuole. Vti1p might interact with some regulatory proteins in the traffic from the TGN to the vacuole, which could be disturbed in the mutants, but this additional protein may not be needed in the ALP pathway. A comparable situation was found in vacuolar fusion, it was shown that the deletion of the N-terminal domain of Vam3p resulted in significantly less vacuolar fusion because the N-terminus was required to recruit the HOPS complex (an essential docking factor) and for coordinated docking (Laage and Ungermann, 2001). Since the N-terminal mutant Vti1p shows defects only in the CPY pathway, it again supports the fact that participation of additional proteins in vesicular targeting is necessary to provide the specificity for SNARE function and SNAREs do not have innate specificity (Dilcher *et al.*, 2001; Fischer von Mollard *et al.*, 1997; Lazar *et al.*, 1997; Lupashin *et al.*, 1997). The onset of the CPY sorting defect in *vti1Q29RW79R* cells is immediate upon shift to restrictive temperature. CPY transport to the vacuole is almost completely blocked in 10 min after shift to the restrictive temperature. Misfolding or mistargeting as fast mechanisms lower affinity with interaction partners. The half life of the mutant protein is longer than 2 h at 37°C. This indicates that the CPY transport defect and the instability of vti1Q29RW79Rp are two different autonomous effects. Thus, the N-terminus of Vti1p may play multiple roles.

4.2 Interaction of ENTH domain with SNARE proteins

A full length ENTH domain protein called as enthoprotin or CLINT or epsinR (Hirst *et al.*, 2003; Kalthoff *et al.*, 2002; Mills *et al.*, 2003; Wasiak *et al.*, 2002) emerged as a potential interaction partner for vti1b. The N-terminus of vti1b interacted with ENTH domain of epsinR and also the interaction was specific that vti1b did not interact with other ENTH domains. So far, only two proteins binding to ENTH domains have been identified. The transcription factor PLZF interacts with ENTH domain of Epsin1 which is present in the nucleus as an additional pool (Hyman *et al.*, 2000). The cytoskeletal protein tubulin interacts with ENTH (epsin1 and epsinR) and ANTH (AP180, HIP1 and Hip1R) domains (Hussain *et al.*, 2003).

4.2.1 Ent3p is a yeast ortholog of epsinR

The further investigation showed that this interaction between a SNARE and an ENTH domain was conserved between mammals and yeast. The N-terminus of Vti1p interacted only with the ENTH domain of Ent3p among eight A/ENTH domain proteins in yeast. The following points indicate that Ent3p could be the yeast homolog of epsinR.

The BLAST searches of yeast protein sequences with ENTH domain of epsinR predicted that Ent3p is more related to it and only Ent3p shares sequence homologies with epsinR that extend even beyond the ENTH domain. Also, both proteins interact with AP-1 and the TGN adaptor proteins of the GGA family and colocalize with the clathrin-coated vesicles in the Golgi area and play a role in clathrin coated vesicle formation at the TGN or the endosomes (Duncan *et al.*, 2003; Hirst *et al.*, 2003; Kalthoff *et al.*, 2002; Mills *et al.*, 2003; Wasiak *et al.*, 2002). ENTH domain of Ent3p is required for its membrane localization (Friant *et al.*, 2003) like that of epsinR (Hirst *et al.*, 2003). By liposome binding assay, I could demonstrate that Ent3p specifically binds PI3P and PI3,5P_2 which are regulators of the traffic from TGN to endosome and multivesicular body formation, respectively (Simonsen *et al.*, 2001). But, Friant *et al*., showed that Ent3p binds only with PI3,5P_2 which could be because of the differences in the fusion protein. I used C-terminal Strep tagged ENTH domain which is better than the N-terminal GST tagged ENTH domain used by Friant group. The GST tag is large and since the tag is in the N-terminus, it might have blocked some binding sites in ENTH domain. The ENTH domain of epsinR interacted strongly with PI4P (Hirst *et al.*, 2003; Kalthoff *et al.*, 2002; Mills *et al.*, 2003). But both PI3P and PI4P are present in the Golgi complex (De Matteis *et al.*, 2002) which may substitute for each other to recruit Ent3p or epsinR to the same organelle. This difference in the phosphoinositide binding was predicted by the structural modeling of tertiary structure of the ENTH domains of Ent3p and epsinR with epsin1 ENTH. It showed that the phosphoinositide binding pocket of epsinR and Ent3p is different between each other (Duncan and Payne, 2003). From my study, it has been shown that Ent3p and Vti1p are involved in the TGN to endosome trafficking in yeast (Chidambaram *et al.*, 2004). It is unclear in mammalian cells which SNAREs are involved in this pathway. The binding of vti1b with epsinR specifies that vti1b might be required for this route, supported by the finding that GGAs function in TGN to endosome traffic in mammalian cells (Hinners and Tooze, 2003) with which epsinR interacts. The deletion of

ent3 in other mutant combinations leads to distorted vacuolar transport pathways, (Chidambaram *et al.*, 2004; Duncan and Payne, 2003) parallel to the Cathepsin D processing phenotype observed in epsinR overexpressing mammalian cells (Mills *et al.*, 2003).

4.2.2 Role of Ent proteins in the TGN-endosome trafficking

The overexpression of the C-terminus of the ENTH domain protein Epsin1 has a dominant negative effect on endocytosis in mammalian cells (Itoh *et al.*, 2001). But overexpression of neither C-terminus of Ent3p nor the full length Ent3p demonstrated dominant negative effect in yeast cells. The defect in the CPY transport in *ent3*Δ, *ent3*Δ*ent4*Δ and especially the synthetic defect in *ent3*Δ*ent5*Δ cells showed that Ent3p is involved in CPY traffic and Ent3p and Ent5p are redundant proteins in this pathway. 83 % of CPY reached the vacuole even in *ent3*Δ*ent5*Δ cells indicating that other proteins can almost compensate for their loss. The synthetic defect of *ENT3* in *vti1-1* cells and of *vti1-2* cells demonstrates that *VTI1* and *ENT3* function together in TGN to endosome trafficking. This is in accord with the interaction between Gga2p and Ent3p (Black and Pelham, 2000) and the requirement for GGA proteins in traffic from the TGN to the prevacuole (Costaguta *et al.*, 2001). Absence of Ent3p in *vti1Q29RW79R* cells also shows a synthetic defect in CPY pathway. ALP pathway is not affected in the single *ent* mutants but *ent3*Δ*ent5*Δ cells showed a marginal delay in ALP transport (Duncan *et al.*, 2003). Slightly less mature ALP was found in the absence of Ent5p but not of Ent3p in *vti1-2* cells. *vti1-2ent3*Δ and *vti1-2ent5*Δ cells displayed a synthetic growth defect at 37°C. Temperature sensitive growth defects have been observed in the absence of proteins involved in different post Golgi transport steps. The synthetic defect in the CPY pathway may be the reason for the synthetic growth defect of *vti1-2ent3*Δ cells. In *vti1-2ent5*Δ, the synthetic growth defect might be due to a small synthetic defect in the ALP pathway. *ent3*Δ*ent5*Δ cells secrete α-factor precursor (Duncan *et al.*, 2003). This processing of α-factor precursor requires Kex2p in the TGN which might be lost in *ent3*Δ*ent5*Δ cells. The Kex2p recycles between the TGN and endosomes and the retrograde traffic to the TGN may be defective in *ent3*Δ*ent5*Δ cells. Hence it is likely that Ent5p might be required for the retrograde traffic to the TGN. This may be another reason for the growth defect in *vti1-2ent5*Δ cells. Recent study support this speculation by showing that epsinR is

involved in the retrograde transport of exogenous Shiga toxin and two endogenous proteins TGN38/46 and mannose 6-phosphate receptors from early endosomes to the TGN (Saint-Pol *et al.*, 2004). In contrary to this, the retrograde transport of A-ALP and Vps10p is not affected in *ent3*Δ, *ent5*Δ and *ent3*Δ*ent5*Δ cells, stating that Ent proteins are not involved in the retrograde transport of at least these proteins in yeast. But still Ent5p might have cargo specificity for retrograde transport which has not been analyzed thoroughly or maybe Ent5p is involved in an unidentified pathway.

In addition to epsinR, there are a number of alternative adaptors on the AP-1 pathway whose role should be explored, like the γ ear binding partners γ-synergin, p200 and aftiphilin which all form a complex and facilitate AP-1 function but additional roles await further investigation (Hirst *et al.*, 2005). The same is true for the yeast AP-1 pathway adaptors Ent3p and especially Ent5p. Though Ent3p and Ent5p are redundant, different synthetic transport defects in *vti1* mutant backgrounds indicate that Ent3p and Ent5p have slightly different functions. The function of epsinR might be apportioned between Ent3p and Ent5p.

4.2.3 Consequences of the interaction between ENTH domains and SNAREs

The interaction between the ENTH domains of Ent3p/epsinR and SNAREs Vti1p/vti1b may be required for the sorting and recruitment of the SNAREs into budding vesicles. I could not substantiate this hypothesis by co-immunoprecipitating Ent3p with Vti1p or epsinR with vti1b, even after overexpressing the proteins. But it is common that interactions between adaptor proteins and cargo are often of low affinity and have to be very dynamic because the complexes have to dissociate after vesicle formation. Consequently, the binding between adaptor protein complexes and membrane receptors are hardly ever demonstrable by co-immunoprecipitations and have been studied almost exclusively using *in vitro* binding and yeast two-hybrid assays (Bonifacino and Dell'Angelica, 1999). An analogous adaptor-cargo interaction of UNC-11, a homolog of the ANTH protein AP180, with R-SNARE synaptobrevin was required for proper localization of synaptobrevin in *Caenorhabditis elegans* (Nonet *et al.*, 1999). UNC-11 may directly recruit synaptobrevin into clathrin coated vesicles during endocytosis. It has been shown that SNAREs bind other components of the budding machinery like COPII coat proteins in ER to Golgi transport (Springer and Schekman, 1998) and adaptor

complexes which couple cargo selection to clathrin recruitment. The mammalian R-SNARE VAMP-4 interacts with AP-1 at the TGN (Peden *et al.*, 2001). In yeast, the vacuolar syntaxin Vam3p binds AP-3 in transport from the TGN to the vacuole (Darsow *et al.*, 1998). A complex of mammalian AP-3 and synaptobrevin mediates formation of synaptic vesicles from endosomes (Salem *et al.*, 1998) indicating that incorporation of a SNARE can regulate vesicle budding. In ENTH proteins only the ubiquitin interaction motif has been implicated in cargo binding (Polo *et al.*, 2002; Shih *et al.*, 2002). This UIM motif is located outside of the ENTH domain in epsin family proteins and is absent from epsinR and Ent3p. From our data, we suggested that cargo sorting may be a novel function of the ENTH domain (Chidambaram *et al.*, 2004). The findings are summarized in the Fig.48.

Recently, our hypothesis has been endorsed by the finding that epsinR is a cargo specific adaptor for vti1b (Hirst *et al.*, 2004). Less vti1b was recruited into the clathrin coated vesicles isolated from epsinR (siRNA treated) depleted cells whereas vti1a recruitment was unaffected. The depletion of epsinR caused redistribution of vti1b from the Golgi region to the cell periphery. Given the role of epsinR in the retrograde transport, it was proposed that epsinR might be required for the recycling of vti1b. But in my study, an alteration of the localization of Vti1p was not observed in the absence of Ent3p or Ent5p and the vice versa. In fact, it is certainly difficult to assess a small change in the distribution of Vti1p. In yeast, Golgi, TGN, early and late endosomal structures cannot be distinguished by their morphology. Vti1p is localized to all of these compartments. Vti1p uses the retrograde transport to achieve its proper steady-state localization. Loss of Pep12p should alter the localization of Vti1p but it could not be shown clearly because of the diffuse and punctuate localization of Vti1p (Gerrard *et al.*, 2000a). Ent3p and Ent5p are shown to be important for ubiquitin dependent protein sorting into multivesicular body along with Vps27p (Eugster *et al.*, 2004). This shows that Ent3p and Ent5p could do two different functions like transport from the TGN to the endosomes and sorting in the MVB.

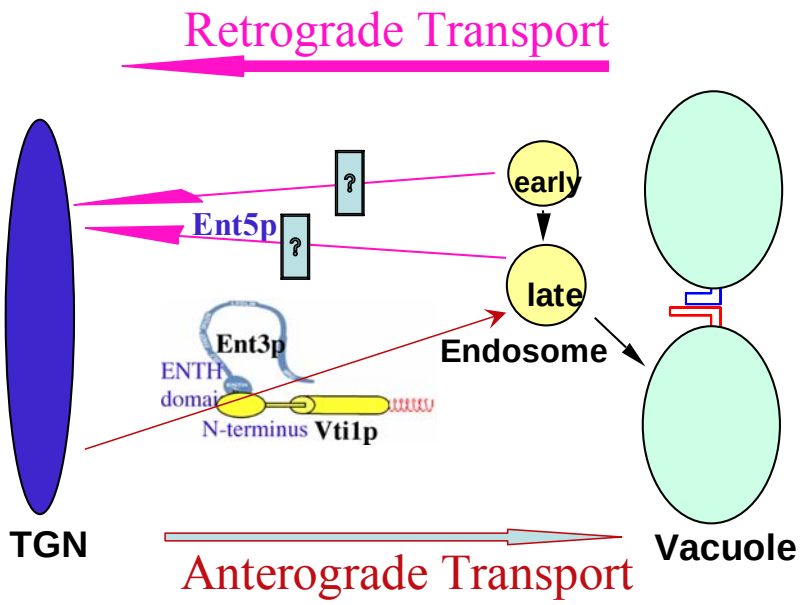

Fig.48. The ENTH domain of Ent3p and the N-terminus of Vti1p interact in the anterograde transport from the TGN to the late endosome. Ent5p may play a role in the retrograde transport from the endosome to the TGN.

4.2.4 Characterization of *ent* mutants

Subcellular fractionation and fluorescence microscopy studies in wt cells showed that Ent3p is a cytosolic protein with barely detectable association with small membrane structures and Ent5p is cytosolic with localization to punctuate structures, which was observed also by other groups (Eugster *et al.*, 2004; Friant *et al.*, 2003). The subcellular fractionation experiment underestimates the membrane pool and may dissociate during procedure. Interestingly, the membrane associated Ent5p was found predominantly in P200 while Ent3p was more prominent in P13 even though both proteins were largely cytosolic, indicating that Ent3p and Ent5p are localized to different compartments. The localization of Ent3p and Ent5p was not affected in *vti1* mutants. Vacuolar morphology and internalization of FM4-64 in *ent3*Δ, *ent5*Δ and *ent3*Δ*ent5*Δ cells are not affected. But Eugster et al, observed fragmented vacuolar morphology in *ent3*Δ*ent5*Δ (Eugster *et al.*, 2004). This dissimilarity might be because of different yeast strain background.

The yeast cell wall consists of a complex structure of cross-linked chitin, β-(1, 3)-d-glucan, β-(1, 6)-d-glucan and mannoproteins. Chitin and β-(1, 3)-d-glucan are synthesiszed by enzymatic complexes at the cell membrane and extruded into the

periplasmic space, mannoproteins are synthesized along the yeast secretory pathway and the site of β-(1, 6)-d-glucan synthesis is still unknown (Raclavsky, 1998). Among them, β-(1, 3)-d-glucan is the main component responsible for the rigidity of yeast cells. β-(1, 3)-d-glucan synthase (GS) is responsible for synthesizing a major structural component of cell wall having Fks1p/Fks2p as its subunits and Rho1p is required as an activator (Douglas *et al.*, 1994; Drgonova *et al.*, 1996). Chitin is mostly concentrated in the septal region although some is dispersed throughout the cell wall. Despite its small quantity, chitin is essential for yeast survival (Shaw *et al.*, 1991). The primary and secondary septa are formed by the deposition of chitin on a chitin ring at the basis of an emerging bud. The daughter and the mother cells are separated by the action of a chitinase that partially hydrolyzes the primary septum. The three chitin synthases, CSI, CSII and CSIII have been identified in yeast (Cabib *et al.*, 1996; Cid *et al.*, 1995). Chs3p is the main player to synthesis chitin at the septum. Chs3p is synthesized at ER and Chs7p is required for its exit out from ER (Trilla *et al.*, 1997). At the Golgi, Chs3p is associated with Chs5p (Santos *et al.*, 1997). Chs5p and Chs6p (Ziman *et al.*, 1998) are necessary for its transfer to the vesicles (chitosomes) that will carry Chs3p to the plasma membrane (Chuang and Schekman, 1996; Ziman *et al.*, 1998). Chs3p may be retained in a ring like area at the base of an emerging bud with the putative activator Chs4p (DeMarini *et al.*, 1997). The major chitin synthase, Chs3p clearly recycles through the TGN. It has been well established that this protein is recovered from the cell surface and dwells in an endocytic compartment before being delivered to the bud neck at the appropriate stage of the cell cycle (Chuang and Schekman, 1996; Ziman *et al.*, 1998). The syntaxin SNARE, Tlg1p is necessary for the correct localization of Chs3p (Holthuis *et al.*, 1998).

The *ent3*Δ*ent5*Δ cells showed abnormal cell shapes with branched cell morphology. But this effect was restricted only to 12.8 % of cells at 30°C and 20 % of cells at 18°C. The abnormal cells have irregular chitin deposition and abnormal actin assembly, though nearly 80% of the cells are normal. But, the *ent3-1*^{ts} mutant cells have an actin organization defect at the restrictive temperature and no defect at the permissive temperature (Friant *et al.*, 2003) which could not be seen with *ent3*Δ. This indicates that the *ent3-1*^{ts} has a dominant negative defect. Since the SNARE Tlg1p is required for the transport of Chs3p, we suspected that Ent3p or Ent5p might interact with Tlg1p for the proper localization of Chs3p which might be distorted in the *ent3*Δ*ent5*Δ cells and so the

septum might have not formed well, subsequently forming elongated and branched cell morphology. But no interaction was found in the two hybrid test between Ent3p and Ent5p with Tlg1p. Also, an effect on the localization of Chs3p was not observed in the mutants. This may be due to technical problems because the Chs3p-GFP localization was very heterogeneous. The β-(1, 3)-d-glucan layer did not look different in the mutants stained with aniline blue. The defects in chitin and actin localization are interdependent. The actin cytoskeleton and polarity establishment proteins also participate in the organization of chitin in the cell wall. The mutants defective in actin display an altered pattern of chitin deposition in which chitin is present over the whole cell surface and is no longer restricted to the bud neck (Novick and Botstein, 1985). There is a correlation between actin delocalization and altered chitin deposition in polarity and bud emergence mutants like *cdc24* (Sloat *et al.*, 1981), *cdc42* and *cdc43* (Adams *et al.*, 1990). The heterogeneous aberration of cell shape in *ent3*Δ*ent5*Δ cells may not be a direct effect of loss of Ent proteins. The general defect by *ent3*Δ*ent5*Δ in the intracellular transport may lead to loss of some components necessary for the biosynthesis of cell wall. For example, it has been shown that the loss of phosphatidic acid phosphatases in yeast caused abnormal cell shapes, aggregation and abnormal phenotypes in cell growth (Katagiri and Shinozaki, 1998). But a very clear defect in the cell wall of *ent3*Δ*ent5*Δ cells is revealed by its sensitivity to many cell wall perturbing agents like NaCl, SDS, calcofluor and zymolyase, demonstrating that the structure of the cell wall is altered. The combinations of *ent3*Δ are very sensitive to NaCl, SDS and calcofluor whereas *ent5*Δ is more resistant to zymolyase, indicating that Ent proteins may have different roles on assembly of the cell wall. Although, Ent proteins show an obvious link with the defects in the organization of the cell wall, these observations are more difficult to explain.

4.2.5 Ent3p is required for the anterograde transport of Pep12p and vti1-2p

Apart from the interaction of Ent3p with Vti1p, it binds also with other endosomal Q-SNAREs Pep12p and Syn8p (to the N-terminus) which are present in the same SNARE complex. A two hybrid interaction was not observed between Ent3p and the R-SNARE Ykt6p in the complex. The N-terminus of Ykt6p is different from that of the other Q-SNAREs which explains for the absence of interaction. Crystal structure of the N-terminus of Ykt6p revealed five β-sheet strands, which are sandwiched by one α-helix on

one side and two α-helices on the other side (Tochio *et al.*, 2001). These interactions with three SNAREs of the same complex are very remarkable, suggesting that Ent3p may interact with individual SNAREs to recruit them into the vesicles or may help them in tethering. Otherwise, it may interact with the self assembled SNARE complex to regulate the core complex formation. The N-terminal domains of SNARE proteins are likely to be involved in controlling the rate of the complex formation and fusion (Antonin *et al.*, 2002a; Dulubova *et al.*, 2001; Misura *et al.*, 2002; Tochio *et al.*, 2001). In this respect, additional regulatory proteins may contribute to influence the effect of the N-terminal domains of SNAREs (Paumet *et al.*, 2004).

The degree of co-immunoprecipitation between the endosomal SNAREs Pep12p and Vti1p is not altered in *ent3*Δ*ent5*Δ cells. The localization of Pep12p is not changed in the *ent* mutants. The localization of Ent3p should be checked in *pep12*Δ cells. By contrast to synthetic defects in *vti1-2ent5*Δ cells, a genetic interaction between *PEP12* and *ENT5* was not observed. Similar to *vti1-2ent3*Δ cells (Chidambaram *et al.*, 2004), the *pep12*Δ*ent3*Δ and *pep12*Δ*ent3*Δ*ent5*Δ cells show synthetic growth defect at 37°C, establishing the genetic interaction between *ENT3* and *PEP12*. In addition, these cells were sensitive to high salt, relating them to the cell wall defects. Intriguingly, Pep12p is stabilized in the absence of Ent3p. In the absence of Ent3p and Ent5p, the stabilization is moderate, may be because of the epistatic effect of Ent5p. Ent3p might be required for the forward transport of Pep12p from the TGN to the endosome. In the absence of Ent3p, the anterograde transport of Pep12p might be blocked and it may get accumulated in the TGN which causes the increased stability (Fig.49).

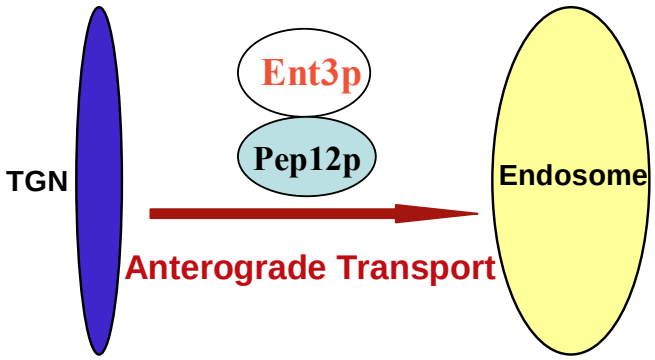

Fig.49. Ent3p is required for the anterograde transport of Pep12p from the TGN to the endosome.

The same effect was observed for vti1-2p in the absence of Ent3p and in turn, vti1-2p was destabilized in the lack of Ent5p. This gives rise to a model that Ent3p may be important for the anterograde transport of vti1-2p and a block in this transport caused increased stability of vti1-2p by accumulating it in the TGN. When the retrograde transport of vti1-2p mediated by Ent5p is interrupted, it is destabilized by degradatative vacuolar proteases when it gets accumulated in the endosome. As the stability of Vti1p was not altered by the Ent proteins, this hypothesis could not be proved for Vti1p. In *vti1-2* cells, general protein transport is impaired which might exert some secondary effects on the stability of vti1-2p. But still the stability and the instability of vti1-2p are very specific to the loss of Ent3p and Ent5p respectively. Unless there is some role played by the Ent proteins, this effect could not be so specific. It may be that it is a complex or combined effect and could not be observed only in the absence of Ent proteins, but needs to down regulate the function of Vti1p also. Ent3p and Ent5p are not essential for the transport of Vti1p. On the other hand, the Ent proteins may be involved in the transport of Vti1p but the loss can be compensated by other proteins. But in the case of vti1-2p, it may not be able to bind the compensatory proteins in the absence of Ent proteins.

4.2.6 Role of Ent proteins in processing of pApe1p

The *ent3*Δ cells are defective in CVT pathway which accumulated more pro aminopeptidase I in the log phase whereas *ent3*Δ*ent5*Δ cells show a rescue effect. Autophagy is not affected in *ent* mutants. It could be that the absence of Ent3p may prevent the fusion of Cvt vesicles with vacuoles through Vti1p. An indirect effect due to a delay or defect in vacuolar processing may also show a defect in the maturation of Ape1p. Some *vps* mutants are essentially wild type for Ape1p processing while others are strongly blocked showing a secondary effect (Klionsky *et al.*, 1992; Scott and Klionsky, 1995). One more possibility is that a putative lipase Cvt17/Aut5p is essential for intravacuolar lysis of autophagic bodies. The transport of Aut5p from the TGN to the endosome could be affected in the *ent3*Δ cells. Aut5p is targeted via the multivesicular body pathway to intravacuolar MVB vesicles by ubiquitin independent manner (Epple *et al.*, 2003). Ent3p is required for the ubiquitin dependent internalization of cargo into MVB, though it could not interact directly with ubiquitin (Friant *et al.*, 2003). Ent3p might be required for the internalization of Aut5p to process the pApe1p inside the

vacuole. Ape1p is recruited onto Cvt membrane and the Cvt vesicle is formed by homotypic membrane fusion which depends on the SNARE Tlg2p and Vps45p (Abeliovich *et al.*, 1999). Ent3p could be needed for this step.

4.3 Outlook

The 2 AA mutations and the N-terminal truncations of Vti1p are helpful tools to study the function of N-terminus. Further studies should be done to find out whether the kinetics of assembly and the amounts of the SNARE complex are altered *in vivo* by the N-terminus of Vti1p and its mammalian homologs. It should be thoroughly investigated if the N-terminus contains some targeting signal. The ALP pathway in the truncations and their localization should be studied. It would be interesting to study if ERAD (ER associated degradation) machinery is involved in the degradation of vtiQ29RW79Rp.

It would be exciting to study whether the ENTH domain binding to the phophoinositides or Vti1p is competitive, cooperative or independent of each other by BIACORE analysis. The budding pattern and the localization of Bud proteins in the *ent3*Δ*ent5*Δ cells could be analyzed. It would be interesting to study the rescue factors for Ape1p processing in *ent3*Δ*ent5*Δ cells. The presence of Ent3p on autophagosomes could be checked to show if the defect is a direct or a secondary effect.

5 Summary

The main aim of the study was to elucidate the function and to find out the interaction partners of the N-terminus of Vti1p.

Immunofluorescence studies localized the mutant Vti1p to the ER pointing out that the N-terminus might have some targeting signal. Pulse chase immunoprecipitations showed that the N-terminus was required for the function of Vti1p in the traffic from the TGN to the endosome and was essential for the stability of the protein as well. The mutant Vti1p was not degraded by the vacuolar proteases. Degradation of mutant Vti1p necessitates the addition of polyubiquitin whereas the wild type Vti1p was degraded by the vacuolar degradation pathway. All these data indicate that the N-terminus could play multiple roles in the targeting, stability and the function of Vti1p.

A yeast two-hybrid screen was done to discover interaction partners of the N-terminus of vti1b. The N-terminus of vti1b interacted specifically with the ENTH domain of enthoprotin/CLINT/epsinR. Further analysis showed that this interaction between a SNARE and an ENTH domain was conserved between mammals and yeast. Yeast Vti1p interacted with the ENTH domain of Ent3p. The studies demonstrated that Ent3p could be the yeast homolog of epsinR. Liposome binding assays showed that the ENTH domain of Ent3p specifically binds with PI3P and PI3,5P_2. Ent3p was involved in the CPY transport and was redundant with Ent5p. The Genetic interactions between *VTI1* and *ENT3* were investigated by pulse chase analyses. Synthetic defects suggested that Vti1p and Ent3p cooperate in transport from the TGN to the prevacuolar endosome.

Subcellular localization and fluorescence studies showed that Ent3p was more cytosolic and less associated with small membranes and Ent5p was localized to the cytosol and to small membranes. The localization of Ent proteins were not affected in the *vti1* mutants and vice versa. The overexpression of Ent3p did not show a dominant negative effect.

About 20 % of the *ent3*Δ*ent5*Δ cells showed abnormal cell shape, disturbed actin assembly and irregular distribution of chitin. A mislocalization of chitin synthase III was not observed. Staining of the β-(1, 3)-glucan layer was also not altered in the mutants. The *ent3*Δ and *ent5*Δ mutants exhibited different cell wall defects demonstrating that Ent3p and Ent5p may have different role on the assembly of the cell wall.

The study was extended to identify Pep12p and Syn8p as further SNARE partners of Ent3p. Synthetic growth defects demonstrated the genetic interaction between Ent3p and Pep12p. Studies on stability of Pep12p inferred that Ent3p is required for the anterograde transport of Pep12p from the TGN to the endosome. For the recycling of vti1-2p, Ent3p and Ent5p were required. The retrograde transport of Vps10p and A-ALP from the endosomes to the TGN was not affected in the *ent* deletions. Also the amount of Pep12p and Vti1p which could be coimmunoprecipitated in the *ent3*Δ*ent5*Δ cells was not altered. Further analysis showed that Ent3p may have a role in the CVT pathway.

This study identified the first cytoplasmic protein binding to a specific ENTH domain. The results revealed a novel function of the ENTH domain and a connection between proteins which function either in vesicle formation or in vesicle fusion.

6 Bibliography

Abeliovich, H., T. Darsow and S. D. Emr (1999). "Cytoplasm to vacuole trafficking of aminopeptidase I requires a t-SNARE-Sec1p complex composed of Tlg2p and Vps45p." EMBO J. **18**(21): 6005-6016.

Adams, A. E., D. I. Johnson, R. M. Longnecker, B. F. Sloat and J. R. Pringle (1990). "CDC42 and CDC43, two additional genes involved in budding and the establishment of cell polarity in the yeast Saccharomyces cerevisiae." J Cell Biol **111**(1): 131-42.

Aguilar, R. C., H. A. Watson and B. Wendland (2003). "The yeast Epsin Ent1 is recruited to membranes through multiple independent interactions." J Biol Chem **278**(12): 10737-43.

Antonin, W., I. Dulubova, D. Arac, S. Pabst, J. Plitzner, J. Rizo and R. Jahn (2002a). "The N-terminal Domains of Syntaxin 7 and vti1b Form Three-helix Bundles That Differ in Their Ability to Regulate SNARE Complex Assembly." J. Biol. Chem. **277**(39): 36449-36456.

Antonin, W., D. Fasshauer, S. Becker, R. Jahn and T. R. Schneider (2002b). "Crystal structure of the endosomal SNARE complex reveals common structural principles of all SNAREs." Nat Struct Biol **9**(2): 107-11.

Antonin, W., C. Holroyd, D. Fasshauer, S. Pabst, G. F. Von Mollard and R. Jahn (2000a). "A SNARE complex mediating fusion of late endosomes defines conserved properties of SNARE structure and function." Embo J **19**(23): 6453-64.

Antonin, W., C. Holroyd, R. Tikkanen, S. Honing and R. Jahn (2000b). "The R-SNARE endobrevin/VAMP-8 mediates homotypic fusion of early endosomes and late endosomes." Mol Biol Cell **11**(10): 3289-98.

Antonin, W., D. Riedel and G. F. von Mollard (2000c). "The SNARE Vti1a-beta is localized to small synaptic vesicles and participates in a novel SNARE complex." J Neurosci **20**(15): 5724-32.

Atlashkin, V., V. Kreykenbohm, E. L. Eskelinen, D. Wenzel, A. Fayyazi and G. Fischer von Mollard (2003). "Deletion of the SNARE vti1b in mice results in the loss of a single SNARE partner, syntaxin 8." Mol Cell Biol **23**(15): 5198-207.

Baba, M., M. Osumi, S. V. Scott, D. J. Klionsky and Y. Ohsumi (1997). "Two distinct pathways for targeting proteins from the cytoplasm to the vacuole/lysosome." J Cell Biol **139**(7): 1687-95.

Barlowe, C. (1997). "Coupled ER to Golgi transport reconstituted with purified cytosolic proteins." J Cell Biol **139**(5): 1097-108.

Barlowe, C., L. Orci, T. Yeung, M. Hosobuchi, S. Hamamoto, N. Salama, M. F. Rexach, M. Ravazzola, M. Amherdt and R. Schekman (1994). "COPII: a membrane coat formed by Sec proteins that drive vesicle budding from the endoplasmic reticulum." Cell **77**(6): 895-907.

Becherer, K. A., S. E. Rieder, S. D. Emr and E. W. Jones (1996). "Novel syntaxin homologue, Pep12p, required for the sorting of lumenal hydrolases to the lysosome-like vacuole in yeast." Mol Biol Cell **7**(4): 579-94.

Black, M. W. and H. R. Pelham (2000). "A selective transport route from Golgi to late endosomes that requires the yeast GGA proteins." J Cell Biol **151**(3): 587-600.

Blobel, G. (1980). "Intracellular protein topogenesis." Proc Natl Acad Sci U S A **77**(3): 1496-500.

Bock, J. B., H. T. Matern, A. A. Peden and R. H. Scheller (2001). "A genomic perspective on membrane compartment organization." Nature **409**(6822): 839-41.

Boehm, M. and J. S. Bonifacino (2001). "Adaptins: the final recount." Mol Biol Cell **12**(10): 2907-20.

Boehm, M. and J. S. Bonifacino (2002). "Genetic analyses of adaptin function from yeast to mammals." Gene **286**(2): 175-86.

Boman, A. L., C. Zhang, X. Zhu and R. A. Kahn (2000). "A family of ADP-ribosylation factor effectors that can alter membrane transport through the trans-Golgi." Mol Biol Cell **11**(4): 1241-55.

Bonifacino, J. S. and E. C. Dell'Angelica (1999). "Molecular bases for the recognition of tyrosine-based sorting signals." J Cell Biol **145**(5): 923-6.

Bonifacino, J. S. and A. M. Weissman (1998). "Ubiquitin and the control of protein fate in the secretory and endocytic pathways." Annu Rev Cell Dev Biol **14**: 19-57.

Brickner, J. H., J. M. Blanchette, G. Sipos and R. S. Fuller (2001). "The Tlg SNARE complex is required for TGN homotypic fusion." J. Cell Biol. **155**(6): 969-978.

Bryant, N. J. and T. H. Stevens (1998). "Vacuole biogenesis in Saccharomyces cerevisiae: protein transport pathways to the yeast vacuole." Microbiol Mol Biol Rev **62**(1): 230-47.

Burri, L. and T. Lithgow (2004). "A complete set of SNAREs in yeast." Traffic **5**(1): 45-52.

Cabib, E., J. A. Shaw, P. C. Mol, B. Bowers and W. Choi (1996). The mycota **Vol III**: 243-267.

Cao, X., N. Ballew and C. Barlowe (1998). "Initial docking of ER-derived vesicles requires Uso1p and Ypt1p but is independent of SNARE proteins." Embo J **17**(8): 2156-65.

Cereghino, J. L., E. G. Marcusson and S. D. Emr (1995). "The cytoplasmic tail domain of the vacuolar protein sorting receptor Vps10p and a subset of VPS gene products regulate receptor stability, function, and localization." Mol Biol Cell **6**(9): 1089-102.

Chapman, E. R., S. An, N. Barton and R. Jahn (1994). "SNAP-25, a t-SNARE which binds to both syntaxin and synaptobrevin via domains that may form coiled coils." J Biol Chem **269**(44): 27427-32.

Cheever, M. L., T. K. Sato, T. de Beer, T. G. Kutateladze, S. D. Emr and M. Overduin (2001). "Phox domain interaction with PtdIns(3)P targets the Vam7 t-SNARE to vacuole membranes." Nat Cell Biol **3**(7): 613-8.

Chen, H., S. Fre, V. I. Slepnev, M. R. Capua, K. Takei, M. H. Butler, P. P. Di Fiore and P. De Camilli (1998). "Epsin is an EH-domain-binding protein implicated in clathrin-mediated endocytosis." Nature **394**(6695): 793-7.

Chen, Y. A. and R. H. Scheller (2001). "SNARE-mediated membrane fusion." Nat Rev Mol Cell Biol **2**(2): 98-106.

Chidambaram, S., N. Mullers, K. Wiederhold, V. Haucke and G. F. von Mollard (2004). "Specific interaction between SNAREs and epsin N-terminal homology (ENTH) domains of epsin-related proteins in trans-Golgi network to endosome transport." J Biol Chem **279**(6): 4175-9.

Chuang, J. S. and R. W. Schekman (1996). "Differential trafficking and timed localization of two chitin synthase proteins, Chs2p and Chs3p." J Cell Biol **135**(3): 597-610.

Cid, V., A. Duran, d. R. F., M. Snyder, C. Nombela and M. Sanchez (1995). "Molecular basis of cell integrity and morphogenesis in *Saccharomyces cerevisiae*." Microbiol Rev. **59**(3): 345-86.

Clague, M. J. (1999). "Membrane transport: Take your fusion partners." Curr Biol **9**(7): R258-60.

Conibear, E. and T. H. Stevens (1998). "Multiple sorting pathways between the late Golgi and the vacuole in yeast." Biochim Biophys Acta **1404**(1-2): 211-30.

Cooper, A. A. and T. H. Stevens (1996). "Vps10p cycles between the late-Golgi and prevacuolar compartments in its function as the sorting receptor for multiple yeast vacuolar hydrolases." J Cell Biol **133**(3): 529-41.

Costaguta, G., C. J. Stefan, E. S. Bensen, S. D. Emr and G. S. Payne (2001). "Yeast Gga coat proteins function with clathrin in Golgi to endosome transport." Mol Biol Cell **12**(6): 1885-96.

Coux, O., K. Tanaka and A. L. Goldberg (1996). "Structure and functions of the 20S and 26S proteasomes." Annu Rev Biochem **65**: 801-47.

Cowles, C. R., G. Odorizzi, G. S. Payne and S. D. Emr (1997a). "The AP-3 adaptor complex is essential for cargo-selective transport to the yeast vacuole." Cell **91**(1): 109-18.

Cowles, C. R., W. B. Snyder, C. G. Burd and S. D. Emr (1997b). "Novel Golgi to vacuole delivery pathway in yeast: identification of a sorting determinant and required transport component." Embo J **16**(10): 2769-82.

Cremona (1999). "Essential role of phosphoinositide metabolism in synaptic vesicle recycling." Cell **99**(2): 179-88.

Darsow, T., C. G. Burd and S. D. Emr (1998). "Acidic di-leucine motif essential for AP-3-dependent sorting and restriction of the functional specificity of the Vam3p vacuolar t-SNARE." J Cell Biol **142**(4): 913-22.

Darsow, T., S. E. Rieder and S. D. Emr (1997). "A multispecificity syntaxin homologue, Vam3p, essential for autophagic and biosynthetic protein transport to the vacuole." J Cell Biol **138**(3): 517-29.

de Camili, P., H. Chen, J. Hyman, E. Panepucci, A. Bateman and A. Brunger (2002). "The ENTH domain." FEBS Lett **513**(1): 11-8.

De Matteis, M., A. Godi and D. Corda (2002). "Phosphoinositides and the Golgi complex." Curr Opin Cell Biol **14**(4): 434-47.

De Nobel, J. G., F. M. Klis, A. Ram, H. Van Unen, J. Priem, T. Munnik and H. Van Den Ende (1991). "Cyclic variations in the permeability of the cell wall of *Saccharomyces cerevisiae*." Yeast **7**(6): 589-98.

Dell'Angelica, E. C., J. Klumperman, W. Stoorvogel and J. S. Bonifacino (1998). "Association of the AP-3 adaptor complex with clathrin." Science **280**(5362): 431-4.

Dell'Angelica, E. C., C. Mullins and J. S. Bonifacino (1999). "AP-4, a novel protein complex related to clathrin adaptors." J Biol Chem **274**(11): 7278-85.

Dell'Angelica, E. C., R. Puertollano, C. Mullins, R. C. Aguilar, J. D. Vargas, L. M. Hartnell and J. S. Bonifacino (2000). "GGAs: a family of ADP ribosylation factor-binding proteins related to adaptors and associated with the Golgi complex." J Cell Biol **149**(1): 81-94.

DeMarini, D. J., A. E. Adams, H. Fares, C. De Virgilio, G. Valle, J. S. Chuang and J. R. Pringle (1997). "A septin-based hierarchy of proteins required for localized deposition of chitin in the Saccharomyces cerevisiae cell wall." J Cell Biol **139**(1): 75-93.

Dilcher, M., B. Kohler and G. F. von Mollard (2001). "Genetic interactions with the yeast Q-SNARE VTI1 reveal novel functions for the R-SNARE YKT6." J Biol Chem **276**(37): 34537-44.

Douglas, C. M., F. Foor, J. A. Marrinan, N. Morin, J. B. Nielsen, A. M. Dahl, P. Mazur, W. Baginsky, W. Li, M. el-Sherbeini and et al. (1994). "The Saccharomyces cerevisiae FKS1 (ETG1) gene encodes an integral membrane protein which is a subunit of 1,3-beta-D-glucan synthase." Proc Natl Acad Sci U S A **91**(26): 12907-11.

Drake, M. T. and L. M. Traub (2001). "Interaction of two structurally distinct sequence types with the clathrin terminal domain beta-propeller." J Biol Chem **276**(31): 28700-9.

Drgonova, J., T. Drgon, K. Tanaka, R. Kollar, G. C. Chen, R. A. Ford, C. S. Chan, Y. Takai and E. Cabib (1996). "Rho1p, a yeast protein at the interface between cell polarization and morphogenesis." Science **272**(5259): 277-9.

Dulubova, I., S. Sugita, S. Hill, M. Hosaka, I. Fernandez, T. C. Sudhof and J. Rizo (1999). "A conformational switch in syntaxin during exocytosis: role of munc18." Embo J **18**(16): 4372-82.

Dulubova, I., T. Yamaguchi, Y. Wang, T. C. Sudhof and J. Rizo (2001). "Vam3p structure reveals conserved and divergent properties of syntaxins." Nat Struct Biol **8**(3): 258-64.

Dumas, J. J., E. Merithew, E. Sudharshan, D. Rajamani, S. Hayes, D. Lawe, S. Corvera and D. G. Lambright (2001). "Multivalent endosome targeting by homodimeric EEA1." Mol Cell **8**(5): 947-58.

Duncan, M. C., G. Costaguta and G. S. Payne (2003). "Yeast epsin-related proteins required for Golgi-endosome traffic define a gamma-adaptin ear-binding motif." Nat Cell Biol **5**(1): 77-81.

Duncan, M. C. and G. S. Payne (2003). "ENTH/ANTH domains expand to the Golgi." Trends Cell Biol **13**(5): 211-5.

Elorza, M. V., H. Rico and R. Sentandreu (1983). "Calcofluor white alters the assembly of chitin fibrils in Saccharomyces cerevisiae and Candida albicans cells." J Gen Microbiol **129**(5): 1577-82.

Epple, U. D., E. L. Eskelinen and M. Thumm (2003). "Intravacuolar membrane lysis in Saccharomyces cerevisiae. Does vacuolar targeting of Cvt17/Aut5p affect its function?" J Biol Chem **278**(10): 7810-21.

Eugster, A., E. I. Pecheur, F. Michel, B. Winsor, F. Letourneur and S. Friant (2004). "Ent5p is required with Ent3p and Vps27p for ubiquitin-dependent protein sorting into the multivesicular body." Mol Biol Cell **15**(7): 3031-41.

Fasshauer, D., W. Antonin, M. Margittai, S. Pabst and R. Jahn (1999). "Mixed and non-cognate SNARE complexes. Characterization of assembly and biophysical properties." J Biol Chem **274**(22): 15440-6.

Fasshauer, D., R. B. Sutton, A. T. Brunger and R. Jahn (1998). "Conserved structural features of the synaptic fusion complex: SNARE proteins reclassified as Q- and R-SNAREs." Proc Natl Acad Sci U S A **95**(26): 15781-6.

Fischer von Mollard, G., S. F. Nothwehr and T. H. Stevens (1997). "The yeast v-SNARE Vti1p mediates two vesicle transport pathways through interactions with the t-SNAREs Sed5p and Pep12p." Journal of Cell Biology **137**(7): 1511-1524.

Fischer von Mollard, G. and T. H. Stevens (1998). "A human homolog can functionally replace the yeast vesicle-associated SNARE Vti1p in two vesicle transport pathways." J Biol Chem **273**(5): 2624-30.

Fischer von Mollard, G. and T. H. Stevens (1999). "The Saccharomyces cerevisiae v-SNARE Vti1p is required for multiple membrane transport pathways to the vacuole." Mol Biol Cell **10**(6): 1719-32.

Ford, M. G., I. G. Mills, B. J. Peter, Y. Vallis, G. J. Praefcke, P. R. Evans and H. T. McMahon (2002). "Curvature of clathrin-coated pits driven by epsin." Nature **419**(6905): 361-6.

Ford, M. G., B. M. Pearse, M. K. Higgins, Y. Vallis, D. J. Owen, A. Gibson, C. R. Hopkins, P. R. Evans and H. T. McMahon (2001). "Simultaneous binding of PtdIns(4,5)P2 and clathrin by AP180 in the nucleation of clathrin lattices on membranes." Science **291**(5506): 1051-5.

Friant, S., E. I. Pecheur, A. Eugster, F. Michel, Y. Lefkir, D. Nourrisson and F. Letourneur (2003). "Ent3p Is a PtdIns(3,5)P2 effector required for protein sorting to the multivesicular body." Dev Cell **5**(3): 499-511.

Fukuda, R., J. A. McNew, T. Weber, F. Parlati, T. Engel, W. Nickel, J. E. Rothman and T. H. Sollner (2000). "Functional architecture of an intracellular membrane t-SNARE." Nature **407**(6801): 198-202.

Gerrard, S. R., B. P. Levi and T. H. Stevens (2000a). "Pep12p is a multifunctional yeast syntaxin that controls entry of biosynthetic, endocytic and retrograde traffic into the prevacuolar compartment." Traffic **1**(3): 259-69.

Gerrard, S. R., A. B. Mecklem and T. H. Stevens (2000b). "The Yeast Endosomal t-SNARE, Pep12p, Functions in the Absence of its Transmembrane Domain." Traffic **1**(1): 45-55.

Gerst, J. E. (1997). "Conserved alpha-helical segments on yeast homologs of the synaptobrevin/VAMP family of v-SNAREs mediate exocytic function." J Biol Chem **272**(26): 16591-8.

Gonzalo, S., W. K. Greentree and M. E. Linder (1999). "SNAP-25 is targeted to the plasma membrane through a novel membrane-binding domain." J Biol Chem **274**(30): 21313-8.

Götte, M. and G. F. von Mollard (1998). "A new beat for the SNARE drum." Trends Cell Biol **8**(6): 215-8.

Gruenberg, J. and K. E. Howell (1989). "Membrane traffic in endocytosis: insights from cell-free assays." Annu Rev Cell Biol **5**: 453-81.

Hanson, P. I., R. Roth, H. Morisaki, R. Jahn and J. E. Heuser (1997). "Structure and conformational changes in NSF and its membrane receptor complexes visualized by quick-freeze/deep-etch electron microscopy." Cell **90**(3): 523-35.

Hasegawa, H., S. Zinsser, Y. Rhee, E. O. Vik-Mo, S. Davanger and J. C. Hay (2003). "Mammalian ykt6 is a neuronal SNARE targeted to a specialized compartment by its profilin-like amino terminal domain." Mol Biol Cell **14**(2): 698-720.

Hess, D. T., T. M. Slater, M. C. Wilson and J. H. Skene (1992). "The 25 kDa synaptosomal-associated protein SNAP-25 is the major methionine-rich polypeptide in rapid axonal transport and a major substrate for palmitoylation in adult CNS." J Neurosci **12**(12): 4634-41.

Hinners, I. and S. A. Tooze (2003). "Changing directions: clathrin-mediated transport between the Golgi and endosomes." J Cell Sci **116**(5): 763-771.

Hinshaw, J. E. and S. L. Schmid (1995). "Dynamin self-assembles into rings suggesting a mechanism for coated vesicle budding." Nature **374**(6518): 190-2.

Hirst, J., G. H. Borner, M. Harbour and M. S. Robinson (2005). "The Aftiphilin/p200/{gamma}-Synergin Complex." Mol Biol Cell **16**(5): 2554-65.

Hirst, J., M. R. Lindsay and M. S. Robinson (2001). "GGAs: roles of the different domains and comparison with AP-1 and clathrin." Mol Biol Cell **12**(11): 3573-88.

Hirst, J., W. W. Lui, N. A. Bright, N. Totty, M. N. Seaman and M. S. Robinson (2000). "A family of proteins with gamma-adaptin and VHS domains that facilitate trafficking between the trans-Golgi network and the vacuole/lysosome." J Cell Biol **149**(1): 67-80.

Hirst, J., S. E. Miller, M. J. Taylor, G. F. von Mollard and M. S. Robinson (2004). "EpsinR is an adaptor for the SNARE protein Vti1b." Mol Biol Cell **15**(12): 5593-602.

Hirst, J., A. Motley, K. Harasaki, S. Y. Peak Chew and M. S. Robinson (2003). "EpsinR: an ENTH Domain-containing Protein that Interacts with AP-1." Mol. Biol. Cell **14**(2): 625-641.

Holthuis, J. C., B. J. Nichols, S. Dhruvakumar and H. R. Pelham (1998). "Two syntaxin homologues in the TGN/endosomal system of yeast." Embo J **17**(1): 113-26.

Huang, W. P. and D. J. Klionsky (2002). "Autophagy in yeast: a review of the molecular machinery." Cell Struct Funct **27**(6): 409-20.

Hughson, F. M. (1997). "Enveloped viruses: a common mode of membrane fusion?" Curr Biol **7**(9): R565-9.

Hurley, J. H. and B. Wendland (2002). "Endocytosis: driving membranes around the bend." Cell **111**(2): 143-6.

Hussain, N. K., M. Yamabhai, A. L. Bhakar, M. Metzler, S. S. G. Ferguson, M. R. Hayden, P. S. McPherson and B. K. Kay (2003). "A Role for Epsin N-terminal Homology/AP180 N-terminal Homology (ENTH/ANTH) Domains in Tubulin Binding." J. Biol. Chem. **278**(31): 28823-28830.

Hussain, N. K., M. Yamabhai, A. R. Ramjaun, A. M. Guy, D. Baranes, J. P. O'Bryan, C. J. Der, B. K. Kay and P. S. McPherson (1999). "Splice variants of intersectin are components of the endocytic machinery in neurons and nonneuronal cells." J Biol Chem **274**(22): 15671-7.

Hyman, J., H. Chen, P. P. Di Fiore, P. De Camilli and A. T. Brunger (2000). "Epsin 1 undergoes nucleocytosolic shuttling and its eps15 interactor NH(2)-terminal homology (ENTH) domain, structurally similar to Armadillo and HEAT repeats, interacts with the transcription factor promyelocytic leukemia Zn(2)+ finger protein (PLZF)." J Cell Biol **149**(3): 537-46.

Itoh, T., S. Koshiba, T. Kigawa, A. Kikuchi, S. Yokoyama and T. Takenawa (2001). "Role of the ENTH domain in phosphatidylinositol-4,5-bisphosphate binding and endocytosis." Science **291**(5506): 1047-51.

Jahn, R., T. Lang and T. C. Sudhof (2003). "Membrane fusion." Cell **112**(4): 519-33.

Jahn, R. and H. Niemann (1994). "Molecular mechanisms of clostridial neurotoxins." Ann N Y Acad Sci **733**: 245-55.

Jahn, R. and T. C. Sudhof (1999). "Membrane fusion and exocytosis." Annu Rev Biochem **68**: 863-911.

Kalthoff, C., S. Groos, R. Kohl, S. Mahrhold and E. J. Ungewickell (2002). "Clint: a novel clathrin-binding ENTH-domain protein at the Golgi." Mol Biol Cell **13**(11): 4060-73.

Kamada, Y., T. Funakoshi, T. Shintani, K. Nagano, M. Ohsumi and Y. Ohsumi (2000). "Tor-mediated induction of autophagy via an Apg1 protein kinase complex." J Cell Biol **150**(6): 1507-13.

Katagiri, T. and K. Shinozaki (1998). "Disruption of a gene encoding phosphatidic acid phosphatase causes abnormal phenotypes in cell growth and abnormal cytokinesis in Saccharomyces cerevisiae." Biochem Biophys Res Commun **248**(1): 87-92.

Kay, B. K., M. Yamabhai, B. Wendland and S. D. Emr (1999). "Identification of a novel domain shared by putative components of the endocytic and cytoskeletal machinery." Protein Sci **8**(2): 435-8.

Kihara, A., T. Noda, N. Ishihara and Y. Ohsumi (2001). "Two distinct Vps34 phosphatidylinositol 3-kinase complexes function in autophagy and carboxypeptidase Y sorting in Saccharomyces cerevisiae." J Cell Biol **152**(3): 519-30.

Kim, J., S. V. Scott, M. N. Oda and D. J. Klionsky (1997). "Transport of a large oligomeric protein by the cytoplasm to vacuole protein targeting pathway." J Cell Biol **137**(3): 609-18.

Kirchhausen, T. (1999). "Adaptors for clathrin-mediated traffic." Annu Rev Cell Dev Biol **15**: 705-32.

Klionsky, D. J., R. Cueva and D. S. Yaver (1992). "Aminopeptidase I of Saccharomyces cerevisiae is localized to the vacuole independent of the secretory pathway." J Cell Biol **119**(2): 287-99.

Klionsky, D. J. and S. D. Emr (2000). "Autophagy as a regulated pathway of cellular degradation." Science **290**(5497): 1717-21.

Kornfeld, S. and I. Mellman (1989). "The biogenesis of lysosomes." Annu Rev Cell Biol **5**: 483-525.

Kreykenbohm, V., D. Wenzel, W. Antonin, V. Atlachkine and G. F. von Mollard (2002). "The SNAREs vti1a and vti1b have distinct localization and SNARE complex partners." Eur J Cell Biol **81**(5): 273-80.

Kucharczyk, R., S. Dupre, S. Avaro, R. Haguenauer-Tsapis, P. P. Slonimski and J. Rytka (2000). "The novel protein Ccz1p required for vacuolar assembly in Saccharomyces cerevisiae functions in the same transport pathway as Ypt7p." J Cell Sci **113 Pt 23**: 4301-11.

Laage, R. and C. Ungermann (2001). "The N-terminal domain of the t-SNARE Vam3p coordinates priming and docking in yeast vacuole fusion." Mol Biol Cell **12**(11): 3375-85.

Lazar, T., M. Gotte and D. Gallwitz (1997). "Vesicular transport: how many Ypt/Rab-GTPases make a eukaryotic cell?" Trends Biochem Sci **22**(12): 468-72.

Le Borgne, R. and B. Hoflack (1998). "Protein transport from the secretory to the endocytic pathway in mammalian cells." Biochimica et Biophysica Acta **1404**: 195-209.

Legendre-Guillemin, V., S. Wasiak, N. K. Hussain, A. Angers and P. S. McPherson (2004). "ENTH/ANTH proteins and clathrin-mediated membrane budding." J Cell Sci **117**(1): 9-18.

Letourneur, F., E. C. Gaynor, S. Hennecke, C. Demolliere, R. Duden, S. D. Emr, H. Riezman and P. Cosson (1994). "Coatomer is essential for retrieval of dilysine-tagged proteins to the endoplasmic reticulum." Cell **79**(7): 1199-207.

Levine, B. and D. J. Klionsky (2004). "Development by self-digestion: molecular mechanisms and biological functions of autophagy." Dev Cell **6**(4): 463-77.

Lewis, M. J. and H. R. B. Pelham (2002). "A New Yeast Endosomal SNARE Related to Mammalian Syntaxin 8." Traffic **3**(12): 922-929.

Lin, R. C. and R. H. Scheller (1997). "Structural organization of the synaptic exocytosis core complex." Neuron **19**(5): 1087-94.

Lippincott-Schwartz, J., T. H. Roberts and K. Hirschberg (2000). "Secretory protein trafficking and organelle dynamics in living cells." Annu Rev Cell Dev Biol **16**: 557-89.

Lohi, O., A. Poussu, Y. Mao, F. Quiocho and V. P. Lehto (2002). "VHS domain -- a longshoreman of vesicle lines." FEBS Lett **513**(1): 19-23.

Loranger, S. S. and M. E. Linder (2002). "SNAP-25 traffics to the plasma membrane by a syntaxin-independent mechanism." J Biol Chem **277**(37): 34303-9.

Lu, J., J. Garcia, I. Dulubova, T. C. Sudhof and J. Rizo (2002). "Solution structure of the Vam7p PX domain." Biochemistry **41**(19): 5956-62.

Lupashin, V. V., I. D. Pokrovskaya, J. A. McNew and M. G. Waters (1997). "Characterization of a novel yeast SNARE protein implicated in Golgi retrograde traffic." Mol Biol Cell **8**(12): 2659-76.

Mallard, F., B. L. Tang, T. Galli, D. Tenza, A. Saint-Pol, X. Yue, C. Antony, W. Hong, B. Goud and L. Johannes (2002). "Early/recycling endosomes-to-TGN transport involves two SNARE complexes and a Rab6 isoform." J Cell Biol **156**(4): 653-64.

Marcusson, E. G., B. F. Horazdovsky, J. L. Cereghino, E. Gharakhanian and S. D. Emr (1994). "The sorting receptor for yeast vacuolar carboxypeptidase Y is encoded by the VPS10 gene." Cell **77**(4): 579-86.

Mellman, I. (1996). "Endocytosis and molecular sorting." Annu Rev Cell Dev Biol **12**: 575-625.

Miller, G. J., R. Mattera, J. S. Bonifacino and J. H. Hurley (2003). "Recognition of accessory protein motifs by the gamma-adaptin ear domain of GGA3." Nat Struct Biol **10**(8): 599-606.

Mills, I. G., G. J. Praefcke, Y. Vallis, B. J. Peter, L. E. Olesen, J. L. Gallop, P. J. Butler, P. R. Evans and H. T. McMahon (2003). "EpsinR: an AP1/clathrin interacting protein involved in vesicle trafficking." J Cell Biol **160**(2): 213-22.

Misura, K. M., J. B. Bock, L. C. Gonzalez, Jr., R. H. Scheller and W. I. Weis (2002). "Three-dimensional structure of the amino-terminal domain of syntaxin 6, a SNAP-25 C homolog." Proc Natl Acad Sci U S A **99**(14): 9184-9.

Misura, K. M., R. H. Scheller and W. I. Weis (2000). "Three-dimensional structure of the neuronal-Sec1-syntaxin 1a complex." Nature **404**(6776): 355-62.

Montecucco, C. and G. Schiavo (1995). "Structure and function of tetanus and botulinum neurotoxins." Q Rev Biophys **28**(4): 423-72.

Morgan, J. R., K. Prasad, W. Hao, G. J. Augustine and E. M. Lafer (2000). "A Conserved Clathrin Assembly Motif Essential for Synaptic Vesicle Endocytosis." J. Neurosci. **20**(23): 8667-8676.

Mukherjee, S., R. N. Ghosh and F. R. Maxfield (1997). "Endocytosis." Physiol Rev **77**(3): 759-803.

Munson, M., X. Chen, A. E. Cocina, S. M. Schultz and F. M. Hughson (2000). "Interactions within the yeast t-SNARE Sso1p that control SNARE complex assembly." Nat Struct Biol **7**(10): 894-902.

Murgui, A., M. V. Elorza and R. Sentandreu (1985). "Effect of papulacandin B and calcofluor white on the incorporation of mannoproteins in the wall of Candida albicans blastospores." Biochim Biophys Acta **841**(2): 215-22.

Murray, R. Z., F. G. Wylie, T. Khromykh, D. A. Hume and J. L. Stow (2005). "Syntaxin 6 and Vti1b form a novel SNARE complex, which is up-regulated in activated macrophages to facilitate exocytosis of tumor necrosis Factor-alpha." J Biol Chem **280**(11): 10478-83.

Nice, D. C., T. K. Sato, P. E. Stromhaug, S. D. Emr and D. J. Klionsky (2002). "Cooperative binding of the cytoplasm to vacuole targeting pathway proteins, Cvt13 and Cvt20, to phosphatidylinositol 3-phosphate at the pre-autophagosomal structure is required for selective autophagy." J Biol Chem **277**(33): 30198-207.

Nichols, B. J. and H. R. Pelham (1998). "SNAREs and membrane fusion in the Golgi apparatus." Biochim Biophys Acta **1404**(1-2): 9-31.

Nicholson, K. L., M. Munson, R. B. Miller, T. J. Filip, R. Fairman and F. M. Hughson (1998). "Regulation of SNARE complex assembly by an N-terminal domain of the t- SNARE Sso1p." Nat Struct Biol **5**(9): 793-802.

Noda, T., K. Suzuki and Y. Ohsumi (2002). "Yeast autophagosomes: de novo formation of a membrane structure." Trends Cell Biol **12**(5): 231-5.

Nonet, M. L., A. M. Holgado, F. Brewer, C. J. Serpe, B. A. Norbeck, J. Holleran, L. Wei, E. Hartwieg, E. M. Jorgensen and A. Alfonso (1999). "UNC-11, a Caenorhabditis elegans AP180 homologue, regulates the size and protein composition of synaptic vesicles." Mol Biol Cell **10**(7): 2343-60.

Novick, P. and D. Botstein (1985). "Phenotypic analysis of temperature-sensitive yeast actin mutants." Cell **40**(2): 405-16.

Novick, P., S. Ferro and R. Schekman (1981). "Order of events in the yeast secretory pathway." Cell **25**(2): 461-9.

Orci, L., M. Stamnes, M. Ravazzola, M. Amherdt, A. Perrelet, T. H. Sollner and J. E. Rothman (1997). "Bidirectional transport by distinct populations of COPI-coated vesicles." Cell **90**(2): 335-49.

Ovalle, R., S. T. Lim, B. Holder, C. K. Jue, C. W. Moore and P. N. Lipke (1998). "A spheroplast rate assay for determination of cell wall integrity in yeast." Yeast **14**(13): 1159-66.

Overstreet, E., X. Chen, B. Wendland and J. A. Fischer (2003). "Either part of a Drosophila epsin protein, divided after the ENTH domain, functions in endocytosis of delta in the developing eye." Curr Biol **13**(10): 854-60.

Owen, D. J. (1999). "A structrual explanation for the binding of multiple ligands by the alpha-adaptin appendage domain." Cell **97**(6): 805-15.

Owen, D. J., P. Wigge, Y. Vallis, J. D. Moore, P. R. Evans and H. T. McMahon (1998). "Crystal structure of the amphiphysin-2 SH3 domain and its role in the prevention of dynamin ring formation." Embo J **17**(18): 5273-85.

Palade, G. (1975). "Intracellular aspects of the process of protein synthesis." Science **189**(4200): 347-58.

Paumet, F., V. Rahimian, M. Di Liberto and J. E. Rothman (2005). "Concerted auto-regulation in yeast endosomal t-SNAREs." J Biol Chem.

Paumet, F., V. Rahimian and J. E. Rothman (2004). "The specificity of SNARE-dependent fusion is encoded in the SNARE motif." Proc Natl Acad Sci U S A **101**(10): 3376-80.

Peden, A. A., G. Y. Park and R. H. Scheller (2001). "The Di-leucine Motif of Vesicle-associated Membrane Protein 4 Is Required for Its Localization and AP-1 Binding." J. Biol. Chem. **276**(52): 49183-49187.

Pelham, H. R. (2001). "SNAREs and the specificity of membrane fusion." Trends Cell Biol **11**(3): 99-101.

Peters, C., P. D. Andrews, M. J. Stark, S. Cesaro-Tadic, A. Glatz, A. Podtelejnikov, M. Mann and A. Mayer (1999). "Control of the terminal step of intracellular membrane fusion by protein phosphatase 1." Science **285**(5430): 1084-7.

Piper, R. C., N. J. Bryant and T. H. Stevens (1997). "The membrane protein alkaline phosphatase is delivered to the vacuole by a route that is distinct from the VPS-dependent pathway." J Cell Biol **138**(3): 531-45.

Piper, R. C., A. A. Cooper, H. Yang and T. H. Stevens (1995). "VPS27 controls vacuolar and endocytic traffic through a prevacuolar compartment in Saccharomyces cerevisiae." J Cell Biol **131**(3): 603-17.

Polo, S., S. Sigismund, M. Faretta, M. Guidi, M. R. Capua, G. Bossi, H. Chen, P. de Camili and P. P. Di Fiore (2002). "A single motif responsible for ubiquitin recognition and monoubiquitination in endocytic proteins." Nature **416**: 451-55.

Pruyne, D. and A. Bretscher (2000). "Polarization of cell growth in yeast." J Cell Sci **113 (Pt 4)**: 571-85.

Raclavsky, V. (1998). "Signalling towards cell wall synthesis in budding yeast." Acta Univ Palacki Olomuc Fac Med **141**: 7-16.

Ram, A. F., A. Wolters, R. Ten Hoopen and F. M. Klis (1994). "A new approach for isolating cell wall mutants in Saccharomyces cerevisiae by screening for hypersensitivity to calcofluor white." Yeast **10**(8): 1019-30.

Reggiori, F., M. W. Black and H. R. Pelham (2000). "Polar transmembrane domains target proteins to the interior of the yeast vacuole." Mol Biol Cell **11**(11): 3737-49.

Rice, L. M., P. Brennwald and A. T. Brunger (1997). "Formation of a yeast SNARE complex is accompanied by significant structural changes." FEBS Lett **415**(1): 49-55.

Rieder, S. E. and S. D. Emr (1997). "A novel RING finger protein complex essential for a late step in protein transport to the yeast vacuole." Mol Biol Cell **8**(11): 2307-27.

Riezman, H., P. G. Woodman, G. van Meer and M. Marsh (1997). "Molecular mechanisms of endocytosis." Cell **91**(6): 731-8.

Robinson, J. S., D. J. Klionsky, L. M. Banta and S. D. Emr (1988). "Protein sorting in Saccharomyces cerevisiae: isolation of mutants defective in the delivery and processing of multiple vacuolar hydrolases." Mol Cell Biol **8**(11): 4936-48.

Robinson, M. S. and J. S. Bonifacino (2001). "Adaptor-related proteins." Curr Opin Cell Biol **13**(4): 444-53.

Rosenthal, J. A., H. Chen, V. I. Slepnev, L. Pellegrini, A. E. Salcini, P. P. Di Fiore and P. De Camilli (1999). "The epsins define a family of proteins that interact with components of the clathrin coat and contain a new protein module." J Biol Chem **274**(48): 33959-65.

Rossi, G., A. Salminen, L. M. Rice, A. T. Brunger and P. Brennwald (1997). "Analysis of a yeast SNARE complex reveals remarkable similarity to the neuronal SNARE complex and a novel function for the C terminus of the SNAP-25 homolog, Sec9." J Biol Chem **272**(26): 16610-7.

Rothman, J. E. (1994). "Mechanisms of intracellular protein transport." Nature **372**(6501): 55-63.

Rothman, J. E. and L. Orci (1996). "Budding vesicles in living cells." Sci Am **274**(3): 70-5.

Rothman, J. E. and F. T. Wieland (1996). "Protein sorting by transport vesicles." Science **272**(5259): 227-34.

Saint-Pol, A., B. Yelamos, M. Amessou, I. G. Mills, M. Dugast, D. Tenza, P. Schu, C. Antony, H. T. McMahon, C. Lamaze and L. Johannes (2004). "Clathrin adaptor epsinR is required for retrograde sorting on early endosomal membranes." Dev Cell **6**(4): 525-38.

Sakamoto, C., C. Kawamoto, K. Takeuchi, I. Miyamoto and H. Shuntoh (2004). "Fission yeast epsin, Ent1p is required for endocytosis and involved in actin organization." Kobe J Med Sci **50**(1-2): 47-57.

Salem, N., V. Faundez, J. Horng and R. Kelly (1998). "A v-SNARE participates in synaptic vesicle formation mediated by the AP3 adaptor complex." Nat Neurosci. **1**(7): 551-6.

Sanderfoot, A. A., F. F. Assaad and N. V. Raikhel (2000). "The Arabidopsis genome. An abundance of soluble N-ethylmaleimide- sensitive factor adaptor protein receptors." Plant Physiol **124**(4): 1558-69.

Sanderfoot, A. A. and N. V. Raikhel (1999). "The Specificity of Vesicle Trafficking: Coat Proteins and SNAREs." Plant Cell **11**(4): 629-642.

Santos, B., A. Duran and M. H. Valdivieso (1997). "CHS5, a gene involved in chitin synthesis and mating in Saccharomyces cerevisiae." Mol Cell Biol **17**(5): 2485-96.

Schekman, R. and L. Orci (1996). "Coat proteins and vesicle budding." Science **271**(5255): 1526-33.

Schmid, S. L. (1997). "Clathrin-coated vesicle formation and protein sorting: an integrated process." Annu Rev Biochem **66**: 511-48.

Scott, S. and D. Klionsky (1995). "In vitro reconstitution of cytoplasm to vacuole protein targeting in yeast." J. Cell Biol. **131**(6): 1727-1735.

Segui-Real, B., M. Martinez and I. V. Sandoval (1995). "Yeast aminopeptidase I is post-translationally sorted from the cytosol to the vacuole by a mechanism mediated by its bipartite N-terminal extension." Embo J **14**(22): 5476-84.

Semenza, J., K. G. Hardwick, N. Dean and H. R. Pelham (1990). "ERD2, a yeast gene required for the receptor-mediated retrieval of luminal ER proteins from the secretory pathway." Cell **61**(7): 1349-57.

Senetar, M., S. Foster and R. McCann (2004). "Intrasteric inhibition mediates the interactionof the I/LWEQ module proteins Talin1, Talin2, Hip1, and Hip12 with actin." Biochemistry **43**(49): 15418-28.

Shaw, J. A., P. C. Mol, B. Bowers, S. J. Silverman, M. H. Valdivieso, A. Duran and E. Cabib (1991). "The function of chitin synthases 2 and 3 in the Saccharomyces cerevisiae cell cycle." J Cell Biol **114**(1): 111-23.

Shih, S. C., D. J. Katzmann, J. D. Schnell, M. Sutanto, S. D. Emr and L. Hicke (2002). "Epsins and Vps27p/Hrs contain ubiquitin-binding domains that function in receptor endocytosis." Nat Cell Biol **4**(5): 389-93.

Simmen, T., S. Honing, A. Icking, R. Tikkanen and W. Hunziker (2002). "AP-4 binds basolateral signals and participates in basolateral sorting in epithelial MDCK cells." Nat Cell Biol **4**(2): 154-9.

Simonsen, A., A. E. Wurmser, S. D. Emr and H. Stenmark (2001). "The role of phosphoinositides in membrane transport." Curr Opin Cell Biol **13**(4): 485-92.

Skehel, J. J. and D. C. Wiley (1998). "Coiled coils in both intracellular vesicle and viral membrane fusion." Cell **95**(7): 871-4.

Sloat, B. F., A. Adams and J. R. Pringle (1981). "Roles of the CDC24 gene product in cellular morphogenesis during the Saccharomyces cerevisiae cell cycle." J Cell Biol **89**(3): 395-405.

Söllner, T., S. W. Whiteheart, M. Brunner, H. Erdjument-Bromage, S. Geromanos, P. Tempst and J. E. Rothman (1993). "SNAP receptors implicated in vesicle targeting and fusion." Nature **362**(6418): 318-24.

Springer, S. and R. Schekman (1998). "Nucleation of COPII vesicular coat complex by endoplasmic reticulum to Golgi vesicle SNAREs." Science **281**(5377): 698-700.

Stahelin, R. V., A. Burian, K. S. Bruzik, D. Murray and W. Cho (2003a). "Membrane binding mechanisms of the PX domains of NADPH oxidase p40phox and p47phox." J Biol Chem **278**(16): 14469-79.

Stahelin, R. V., F. Long, K. Diraviyam, K. S. Bruzik, D. Murray and W. Cho (2002). "Phosphatidylinositol 3-phosphate induces the membrane penetration of the FYVE domains of Vps27p and Hrs." J Biol Chem **277**(29): 26379-88.

Stahelin, R. V., F. Long, B. J. Peter, D. Murray, P. De Camilli, H. T. McMahon and W. Cho (2003b). "Contrasting Membrane Interaction Mechanisms of AP180 N-terminal Homology (ANTH) and Epsin N-terminal Homology (ENTH) Domains." J. Biol. Chem. **278**(31): 28993-28999.

Stahl, B., J. H. Chou, C. Li, T. C. Sudhof and R. Jahn (1996). "Rab3 reversibly recruits rabphilin to synaptic vesicles by a mechanism analogous to raf recruitment by ras." Embo J **15**(8): 1799-809.

Stepp, J. D., A. Pellicena-Palle, S. Hamilton, T. Kirchhausen and S. K. Lemmon (1995). "A late Golgi sorting function for Saccharomyces cerevisiae Apm1p, but not for Apm2p, a second yeast clathrin AP medium chain-related protein." Mol Biol Cell **6**(1): 41-58.

Storrie, B., R. Pepperkok and T. Nilsson (2000). "Breaking the COPI monopoly on Golgi recycling." Trends Cell Biol **10**(9): 385-91.

Sutton, R. B., D. Fasshauer, R. Jahn and A. T. Brunger (1998). "Crystal structure of a SNARE complex involved in synaptic exocytosis at 2.4 A resolution." Nature **395**(6700): 347-53.

Sweet, D. J. and H. R. Pelham (1993). "The TIP1 gene of Saccharomyces cerevisiae encodes an 80 kDa cytoplasmic protein that interacts with the cytoplasmic domain of Sec20p." Embo J **12**(7): 2831-40.

Terrian, D. M. and M. K. White (1997). "Phylogenetic analysis of membrane trafficking proteins: a family reunion and secondary structure predictions." Eur J Cell Biol **73**(3): 198-204.

Tochio, H., M. M. Tsui, D. K. Banfield and M. Zhang (2001). "An autoinhibitory mechanism for nonsyntaxin SNARE proteins revealed by the structure of Ykt6p." Science **293**(5530): 698-702.

Traub, L. M., M. A. Downs, J. L. Westrich and D. H. Fremont (1999). "Crystal structure of the alpha appendage of AP-2 reveals a recruitment platform for clathrin-coat assembly." Proc Natl Acad Sci U S A **96**(16): 8907-12.

Traub, L. M. and S. Kornfeld (1997). "The trans-Golgi network: a late secretory sorting station." Curr Opin Cell Biol **9**(4): 527-33.

Trilla, J., T. Cos, A. Duran and C. Roncero (1997). "Characterization of *CHS4* (*CAL2*), a gene of Saccharomyces cerevisiae involved in chitin biosynthesis and allelic to *SKT5* and *CSD4*." Yeast **13**: 795-807.

Uemura, T., M. H. Sato and K. Takeyasu (2005). "The longin domain regulates subcellular targeting of VAMP7 in Arabidopsis thaliana." FEBS Lett.

Ungermann, C., G. F. von Mollard, O. N. Jensen, N. Margolis, T. H. Stevens and W. Wickner (1999). "Three v-SNAREs and two t-SNAREs, present in a pentameric cis-SNARE complex on isolated vacuoles, are essential for homotypic fusion." J Cell Biol **145**(7): 1435-42.

Wasiak, S., A. Y. Denisov, Z. Han, P. A. Leventis, E. de Heuvel, G. L. Boulianne, B. K. Kay, K. Gehring and P. S. McPherson (2003). "Characterization of a gamma-adaptin ear-binding motif in enthoprotin." FEBS Lett **555**(3): 437-42.

Wasiak, S., V. Legendre-Guillemin, R. Puertollano, F. Blondeau, M. Girard, E. de Heuvel, D. Boismenu, A. W. Bell, J. S. Bonifacino and P. S. McPherson (2002). "Enthoprotin: a novel clathrin-associated protein identified through subcellular proteomics." J Cell Biol **158**(5): 855-62.

Weimbs, T., S. H. Low, S. J. Chapin, K. E. Mostov, P. Bucher and K. Hofmann (1997). "A conserved domain is present in different families of vesicular fusion proteins: a new superfamily." Proc Natl Acad Sci U S A **94**(7): 3046-51.

Weimbs, T., K. Mostov, S. H. Low and K. Hofmann (1998). "A model for structural similarity between different SNARE complexes based on sequence relationships." Trends Cell Biol **8**(7): 260-2.

Wendland, B., K. E. Steece and S. D. Emr (1999). "Yeast epsins contain an essential N-terminal ENTH domain, bind clathrin and are required for endocytosis." Embo J **18**(16): 4383-93.

Whyte, J. R. C. and S. Munro (2002). "Vesicle tethering complexes in membrane traffic." J Cell Sci **115**(13): 2627-2637.

Yamaguchi, T., I. Dulubova, S. W. Min, X. Chen, J. Rizo and T. C. Sudhof (2002). "Sly1 binds to Golgi and ER syntaxins via a conserved N-terminal peptide motif." Dev Cell **2**(3): 295-305.

Zeng, Q., T. T. Tran, H. X. Tan and W. Hong (2003). "The cytoplasmic domain of Vamp4 and Vamp5 is responsible for their correct subcellular targeting: the N-terminal extenSion of VAMP4 contains a dominant autonomous targeting signal for the trans-Golgi network." J Biol Chem **278**(25): 23046-54.

Zheng, H., G. F. von Mollard, V. Kovaleva, T. H. Stevens and N. V. Raikhel (1999). "The plant vesicle-associated SNARE AtVTI1a likely mediates vesicle transport from the trans-Golgi network to the prevacuolar compartment." Mol Biol Cell **10**(7): 2251-64.

Ziman, M., J. S. Chuang, M. Tsung, S. Hamamoto and R. Schekman (1998). "Chs6p-dependent anterograde transport of Chs3p from the chitosome to the plasma membrane in Saccharomyces cerevisiae." Mol Biol Cell **9**(6): 1565-76.

Publications

Subbulakshmi Chidambaram, Nina Müllers, Katrin Wiederhold, Volker Haucke, and Gabriele Fischer von Mollard (2004). Specific interaction between SNAREs and epsin N-terminal homology (ENTH) domains of epsin-related proteins in trans-Golgi network to endosome transport. **J. Biol. Chem**. 6;279(6):4175-9.

Meik Dilcher, Beate Veith, **Subbulakshmi Chidambaram**, Enno Hartmann, Hans Dieter Schmitt and Gabriele Fischer von Mollard (2003). Use1p is a yeast SNARE protein required for the traffic from the Golgi to the ER .**EMBO J,** 22:14, 3664-3674.

Meik Dilcher, **Subbulakshmi Chidambaram**, Beate Veith, Enno Hartmann, Hans Dieter Schmitt and Gabriele Fischer von Mollard (2003). Use1p is a yeast SNARE protein required for the traffic from the Golgi to the ER. **Yeast,** 20(S1), S34:1-19.

Acknowledgement

I thank Prof. Dr. Dr. h. c. Kurt von Figura for being my main examiner.

I give my special thanks to PD Dr. Stefan Irniger for his critical reading of my thesis as a co-referee.

My sincere and warm thanks go to my supervisor Professor Dr. Gabriele Fischer von Mollard who kindly took me in as a part of her group and always provided me with excellent supervision and facilities to do my thesis work. I also want to thank her for training me to think and write scientifically.

I would like to thank Prof. Dr. Detlef Doenecke, the speaker of the Graduiertenkolleg 521 for arranging scientific meetings and motivating to attend the practical courses & seminars.

I thank my 'Thesis Committee' members, Prof. Dr. Reinhard Jahn, Prof. Dr. Volker Hauke and Prof. Dr. Micheal Thumm for their constructive and helpful comments on my thesis.

My thanks to PD Dr. Peter Schu, Prof. Dr. Thomas Dierks, Prof. Dr. Stefan Höning and Dr. Jobst Landgrebe who were always helpful and provided detailed technical advice and reagents.

I greatly appreciate my colleagues Dr. Vadim Atlachkine, Dr. Meik Dilcher, Dr. Vera Kreykenbohm, Nina müllers, Beate Veith and Namitha Kanwar for their technical support and for creating a lovely and pleasant environment in the lab. I am indebted to Dr. Meik Dilcher, an affectionate and caring friend who is always empathetic and helped me in all possible ways. I extend my thanks to Dr. Constanze Riel and Dr. Anna Boulankina for their help and kind interactions in and outside of the lab.

I thank Prof. Thumm's group members and especially Dr. Ulrike Epple for fruitful discussions.

I should thank Dr. P.N. Rekha, Malaiyalam Mariappan, Karthikeyan Radhakrishnan, Premkumar Sinha and Santhoshlakshmi Kante for creating a home out of home feeling.

My warm thanks to one of my brothers Dr. T.E.V. Balaji, for his invaluable moral support. I would not fail to mention Sreedhar Kilaru, for his good friendship.

Finally, I owe my deepest and loving thanks to my fiancè Pandian Arunachalam. Without his continuous love and warm support the making of this thesis would have been much more difficult. It is my great pleasure to dedicate this thesis to him.

Curriculum Vitae

I was born on 10th June 1978 as the first child of Chidambaram Kuthalampillai and Thangamani Chidambaram in Dharmapuri, Tamil Nadu, India. From 1983 till 1988, I had my elementary education in a Government school in Karimangalam, Dharmapuri, India. In 1988, I joined a high school in Karimangalam and successfully completed in 1993 with a secondary school-leaving certificate. In 1993, I started studying higher secondary in St.Annes Girl's Higher Secondary School, Trichy, India and successfully compeleted in 1995.

During 1995-1998, I studied Biochemistry in Annai Sandhya Women's College, Krishnagiri affiliated to Madras University, India, to obtain my Bachelor's degree.

At Madurai Kamaraj University, I specialized my Master's degree in Integrated Biology with a dissertation entitled 'Diurnal variations in visual response from the retina of the bat *Cynopterus sphinx* 1791 (*vahl*) to white light pulses', during 1998-2000.

In 2001, I obtained a Summer Research Fellowship from Indian Academy of Sciences and joined the department of Microbiology and Cell biology in Indian Institute of Sciences, Bangalore, India and carried out a project entitled 'An unexpected absence of queuosine modification in the tRNAs of an *E. coli* B strain'.

In June 2002, I had started my Ph.D thesis presented here with the title 'Characterization of ENTH domain proteins and their interaction with SNAREs in *S. cerevisiae'* in the department of Biochemistry II, Georg-August Universität Göttingen, Germany under the guidance of Prof. Dr. Gabriele Fischer von Mollard.